LYMPHOCYTES IN HEMOCHROMATOSIS:

A GENOMIC AND FUNCTIONAL APPROACH

MÓNICA ISABEL ENCARNAÇÂO COSTA
TESE DE DOUTORAMENTO APRESENTADA
À FACULDADE DE MEDICINA DA UNIVERSIDADE DO PORTO
PROGRAMA DOUTORAL EM BIOMEDICINA

Porto, Julho 2015

MÓNICA ISABEL ENCARNAÇÃO COSTA

LYMPHOCYTES IN HEMOCHROMATOSIS:
A GENOMIC AND FUNCTIONAL APPROACH

Orientador: Doutor Idílio Jorge Matias Pereira Pinto, PhD
Categoria: Investigador
Afiliação: Instituto de Biologia Molecular e Celular do Porto - Basic Clinical Research on Iron Biology. Instituto de Ciências Biomédicas Abel Salazar da Universidade do Porto.

Co-Orientador: Professora Maria da Graça Beça Gonçalves Porto, PhD, MD
Categoria: Professor Catedrático Convidado
Afiliação: Instituto de Ciências Biomédicas Abel Salazar da Universidade do Porto. Hospital Geral de Santo António Centro Hospital do Porto. Instituto de Biologia Molecular e Celular do Porto - Basic Clinical Research on Iron Biology.

U.PORTO
FMUP FACULDADE DE MEDICINA
UNIVERSIDADE DO PORTO

Dissertação de candidatura ao grau de Doutor em Biomedicina submetida à Faculdade de Medicina da Universidade do Porto

Porto, Julho 2015

Júri das provas de doutoramento

Presidente Doutora Maria Leonor Martins Soares David
Diretora da Faculdade de Medicina (por delegação reitoral)

Vogais

Doutora Manuela Morgadinho Faustino Monteiro dos Santos
Professora da Université de Montréal, Canada

Doutora Luísa Maria de Sousa Mesquita Pereira
Investigadora Principal do Instituto de Patologia e Imunologia Molecular da Universidade do Porto.

Doutora Ana Espada de Sousa
Professora Catedrática da Faculdade de Medicina da Universidade de Lisboa

Doutor José Eduardo Torres Eckenroth Guimarães
Professor Catedrático da Faculdade de Medicina da Universidade do Porto

Doutora Maria da Graça Beça Gonçalves Porto
Professora Catedrática do Instituto de Ciências Biornédicas Abel Salazar da Universidade do Porto

Declaration

The results included in this thesis constitute research work of scientific articles published in international journals.

Ao abrigo do Art. 8º do Decreto-Lei nº 388/70 fazem parte integrante desta dissertação os seguintes trabalhos publicados e submetidos em revistas internacionais. Em cumprimento com o disposto no referido Decreto-Lei, declaro que participei ativamente na recolha e estudo do material incluído em todos os trabalhos.

Scientific papers:

Costa M, Cruz E, Barton JC, Thorstensen K, Morais S, et al. (2013) Effects of Highly Conserved Major Histocompatibility Complex (MHC) Extended Haplotypes on Iron and Low CD8+ T Lymphocyte Phenotypes in HFE C282Y Homozygous Hemochromatosis Patients from Three Geographically Distant Areas. PLoS ONE 8(11): e79990

Costa M, Cruz E, Oliveira S, Benes V, Ivacevic T, et al. (2015) Lymphocyte gene expression signatures from patients and mouse models of hereditary hemochromatosis reveal a function of HFE as a negative regulator of CD8+ T-lymphocyte activation and differentiation in vivo. PLoS One 10: e0124246

Author´s contribution in other publications:

Arezes J, Costa M, Vieira I, Dias V, Kong XL, et al. (2013) Non-transferrin-bound iron (NTBI) uptake by T lymphocytes: evidence for the selective acquisition of oligomeric ferric citrate species. PLoS One 8: e79870.

Pinto JP, Arezes J, Dias V, Oliveira S, Vieira I, Costa M et al. (2014) Physiological implications of NTBI uptake by T lymphocytes. Front Pharmacol 5: 24.

Financiamento

Acknowledgments

Agradecimentos

Em primeiro lugar gostaria de agradecer à Professora Graça Porto, por ter sido a minha mentora e me ter ensinado muito acerca da hemocromatose e da genética dos linfócitos mas principalmente por ter sido um exemplo extraordinário de dedicação e trabalho. É inspirador trabalhar consigo, obrigada por me orientar nos meus pensamentos e ter-me incentivado sempre a pensar melhor.

Agradeço ao meu orientador Jorge Pinto, por ter acreditado em mim e me ter dado a oportunidade de iniciar esta viagem.

Agradeço aos responsáveis do Programa Doutoral em Biomedicina por me terem aceitado como estudante, condição fundamental para poder realizar o meu doutoramento.

Gostaria de agradecer à professora Filipa Carvalho, por todo o apoio que me deu e por toda a disponibilidade com que me recebia.

Quero agradecer ao grupo BCRIB (original e actual): Susana Oliveira, Vera Dias, Inês Vieira, Emerência Teixeira, João Arezes, Joana Tomás, Susana Almeida e mais recentemente Tiago Duarte, Sílvia Chambel, Andreia Gonçalves e Ana Gomes. Proporcionaram-me um ambiente fantástico de companheirismo e de amizade. Quero agradecer em particular à Inês Vieira por todas as horas partilhadas no biotério e no laboratório, adorei a tua companhia nesta jornada e gostaria de manter esta amizade. Um agradecimento especial à Doutora Eugénia, pelas longas horas de trabalho e pela amizade partilhada nessas horas.

Deixo uma palavra de amizade aos nossos grupos vizinhos (III e Molecular Parasitology): João Neves, Miguel Ramos, Tânia Cruz, Sandra Carvalho, Filipa Teixeira, Georgina Alves e Márcia Lamy (adorei partilhar o espaço e as horas convosco).

Agradeço aos antigos membros do Grupo de Evolução Molecular: Bruno Aguiar e ao Ramiro Hojas e Helder Rocha com quem criei laços de amizade. Agradeço a orientação do Doutor Jorge Vieira e da Doutora Cristina Vieira durante o meu percurso inicial pelo grupo.

Agradeço a disponibilidade da Catarina Leitão do serviço de Citometria do IBMC pelas horas extraordinárias, pelo apoio técnico e pela amizade.

Agradeço à Paula Magalhães do serviço CCGEN, por todos os momentos de cumplicidade e motivação, pelo apoio técnico com muita simpatia sempre à mistura, ficas no meu coração.

Ao serviço do Biotério do IBMC e em especial à tratadora Isabel Duarte e à veterinária Sofia Lamas por todo o apoio e assistência nas mais variadas "urgências".

Ao serviço de Hematologia Clínica do Hospital Santo António em particular ao Sr Francisco Dias, incansável e sempre prestável. Um agradecimento especial à Enfermeira Graça Melo por toda a ajuda e disponibilidade na recolha de amostras.

A todos os doentes seguidos na consulta de Hemocromatose no Hospital Santo António obrigada pela colaboração, sem vocês este estudo não seria possível.

Aos estagiários, Anaísa Valido e Fábio Ferreira um obrigada pelas perguntas difíceis.

A todos os colaboradores presentes nas publicações integrantes nesta tese. Obrigada, este trabalho é vosso também e as conclusões são o fruto de um longo trabalho de equipa.

A special thanks to Martina Muckentaller, for being so available to discuss our work and also for receiving me at Heidelberg and guiding me in the part of the Affymetrix analysis work. Also would like to thank to the GeneCore group at EMBL, especially to Tomy Ivacevic for helping me with the software analysis.

Às minhas "irmãs adoptivas" Carla Oliveira e Liliana Andrade por todos os momentos de descompressão.

O meu agradecimento mais especial é dirigido à minha família. Aos meus pais por serem as pessoas que estão sempre presentes, por me apoiarem incondicionalmente e acreditarem em mim. Agradeço ao Micael e ao Gonçalo por todo o amor e motivação.

Obrigada!

Abstract

Hereditary hemochromatosis (HH) is the most common genetic iron-overload disease among Caucasians, classically associated with the p.C282Y mutation in the *HFE* gene, localized at the Major Histocompatibility Complex (MHC) region in chromosome 6. Immunological abnormalities have been consistently observed in HH patients, namely a phenotype of low CD8$^+$ T-lymphocyte numbers associated with a more severe iron-overload. The genetic transmission of this low CD8 trait was first associated with the inheritance of certain HLA alleles markers and more recently, with a SNP microhaplotype named A-A-T, in the context of a strong linkage disequilibrium in the region between *HLA* and *HFE*. The physiological mechanism how CD8$^+$ T lymphocytes can act as clinical modifiers of disease susceptibility in HH was still unsolved.

The main objectives of this thesis were: i) to study the genetic contribution of the MHC-class I region to the setting of CD8$^+$ T- lymphocyte numbers and ii) to perform a functional approach by addressing the iron handling ability of these cells and the involvement of other lymphocyte proteins in cellular/systemic iron homeostasis.

We first tested the predictive value of MHC markers on CD8 and iron phenotypes with studies of genotype/phenotype associations in different geographically distant HH populations (Porto, Portugal; Alabama, USA and Nord- Trøndelag, Norway). This study revealed that the microhaplotype A-A-T cannot be used as a universal predictive marker neither for the iron phenotype nor for the low CD8 phenotype. Moreover, the most common HLA haplotypes A*01-B*08 or A*03-B*07 showed different conservation patterns among the three populations revealing different recombination histories which reflect on the different genotype-phenotype associations. Because HH patients from Porto displayed the strongest genotype association with the low CD8 trait, this population was chosen to further characterize the haplotype structure in HH. Results from a high density mapping covering 63 markers along the *HLA-HFE* region revealed the existence of two major haplotype groups (AA and CG group haplotypes) with distinct conservation patterns in both HH patients and controls, suggesting a selective stronger recombination suppression in AA haplotype group, which, in the case of HH associated chromosomes, includes the classical ancestral HLA A*03-B*07 haplotype. The inheritance of the HH ancestral haplotype in homozygosity seemed to be most strongly associated with the low CD8 phenotype supporting the hypothesis of a still unidentified major quantitative trait locus for that particular phenotype in this region.

Regarding the mechanisms how CD8$^+$ T cells may modify systemic iron levels, we evaluated the *in vitro* response of lymphocytes to changes in ferric-citrate (as non-transferrin-

bound iron, NTBI) and the NTBI retention ability of peripheral blood mononuclear cells (PBMCs) isolated from HH patients and from normal controls. We were able to prove that peripheral T lymphocytes take up and retain high levels of NTBI, preferentially the Fe_3Cit_3 oligomeric species. In HH patients, the retention capacity of PBMCs was significantly correlated with the iron re-accumulation patterns after intensive treatment. In terms of CD8$^+$ T cell gene expression, results obtained in both animal and human models of HH support a direct effect of HFE on the transcriptional profile of CD8$^+$ T lymphocytes. Results from the transcriptional profile of CD8$^+$ T lymphocytes in HH patients suggest that the *HFE* defect affects the homeostatic equilibrium of central and effector memory cells. In the animal model, HFE deficiency induced the up-regulation of several genes clustered in the functional categories of lymphocytes activation/differentiation pathways. The most significant result was obtained with the higher expression of calgranulin S100a9, a result further confirmed in HH patients at the gene and protein levels.

In summary, the results obtained in the context of this thesis constitute an important step forward in the characterization of lymphocyte abnormalities in HH. At the genomic level, they reveal novel aspects of haplotype conservation that may help explain differences among distinct populations regarding the impact on CD8 and iron phenotypes. At the functional level, not only they reveal novel aspects of disease heterogeneity possibly explained by different NTBI retention capacity of PBMCs, but also bring into light the importance of S100a9 as a new molecular player interacting with HFE in CD8 lymphocyte function.

Resumo

A Hemocromatose Hereditária (HH) é a doença genética de sobrecarga de ferro mais comum na população caucasiana, classicamente associada à mutação p.C282Y no gene *HFE*, localizado no cromossoma 6 na região do Complexo Principal de Histocompatibilidade. Os doentes com HH apresentam frequentemente várias anomalias imunológicas, tais como um fenótipo de baixo número de linfócitos CD8$^+$ T no sangue associado a uma maior sobrecarga sistémica de ferro. A transmissão genética deste fenótipo (baixo número de linfócitos CD8$^+$ T) foi inicialmente associado à heritabilidade de certos alelos HLA e mais recentemente de um outro marcador genético muito conservado na região entre os genes *HLA* e *HFE*, composto por 3 SNP e denominado como microhaplótipo A-A-T. O mecanismo pelo qual os linfócitos CD8$^+$ T actuam como modificadores clínicos de susceptibilidade à doença na HH ainda estava por decifrar.

Os principais objectivos desta tese foram os seguintes: i) estudar a contribuição genética da região do MHC classe I para a definição do números de linfócitos CD8$^+$ T e ii) realizar uma abordagem mais funcional testando a capacidade de aquisição e modulação do ferro pelos linfócitos CD8$^+$T assim como a identificação de outras proteínas expressas por estas células envolvidas na homeostasia do ferro a nível celular e sistémico.

No campo da genética dos linfócitos, testámos o valor preditivo dos marcadores do MHC associados ao número de linfócitos e à sobrecarga sistémica de ferro através de estudos de associação genótipo/fenótipo em diferentes populações de doentes HH geograficamente distantes (Porto, Portugal; Alabama, EUA e Nord-Trøndelag, Noruega). Este estudo revelou que o microhaplótipo A-A-T não pode ser usado como um marcador preditivo universal nem para o fenótipo de ferro nem para o fenótipo de número baixo de linfócitos CD8$^+$ T. Observámos que os haplótipos mais frequentes HLA-A*01-B*08 ou HLA-A*03-B*07 apresentaram diferentes padrões de conservação entre as três populações, revelando diferentes histórias de recombinação que se refletem em diferentes associações genótipo-fenótipo. A população de doentes de HH da região do Porto conserva uma maior associação dos marcadores genéticos ao fenótipo de números baixos de linfócitos e por este motivo a sua estrutura haplotípica foi caracterizada de forma mais pormenorizada. O mapeamento genético de 63 marcadores ao longo da região HLA-HFE revelou a existência de dois grandes grupos de haplótipos (definidos por AA e GC) com padrões de conservação diferentes, tanto nos doentes com HH como nos controlos, sugerindo uma supressão de recombinação selectiva mais forte no grupo AA que inclui o haplótipo clássico ancestral da HH, o HLA A*03-B*07. A herança do haplótipo ancestral HH em homozigotia revela uma forte associação com o fenótipo de baixo número de CD8$^+$ T apoiando a hipótese de que um locus responsável pela transmissão quantitativa desse fenótipo se encontra nesta região.

Relativamente ao estudo funcional no qual se pretendeu elucidar a forma como as células CD8$^+$ T podem modificar os níveis de sistémicos de ferro, foi avaliada a resposta *in vitro* destas células à incubação com citrato de ferro (como fonte de ferro não-ligado à transferrina- NTBI) e a capacidade de retenção desta forma de NTBI pelas células mononucleares de sangue periférico (PBMCs) isoladas a partir de doentes com HH e de controlos. Os resultados provaram que os linfócitos T periféricos são capazes de captar e reter elevados níveis de NTBI, e identificámos a espécie oligomérica Fe_3Cit_3 como a molécula que os linfócitos internalizam preferencialmente. Em doentes com HH, a capacidade de retenção dos PBMC foi significativamente correlacionada com o perfil de re-acumulação de ferro após o tratamento intensivo. Os resultados da análise da expressão génica nas células CD8$^+$ T por microarray, em modelos animais e humanos de HH, suporta um efeito directo do HFE sobre o perfil de transcrição dos linfócitos CD8$^{+.}$T. Os resultados da análise da expressão génica dos linfócitos CD8$^+$ T de doentes com HH sugerem que a deficiência no HFE afecta o equilíbrio homeostático das células de memória central e efetoras. No modelo animal, a ausência de *HFE* resultou numa expressão diferencial de vários genes funcionalmente agrupados em vias de activação/ diferenciação de linfócitos. O gene com maior diferença na expressão entre os animais deficientes no *HFE* em relação aos controlos foi a calgranulina *S100A9*, que se encontrou sobre-expressa na ausência de *HFE*, um resultado confirmado nos doentes com HH ao nível do mRNA e da proteína.

Em resumo, os resultados obtidos no contexto desta tese fornecem informações relevantes na exposição das anomalias nos linfócitos em doentes com HH. No campo da genética, foram relevados novos aspectos relativos à conservação dos haplótipos ancestrais que podem ajudar a explicar as diferenças encontradas na associação ao fenótipo de número baixo de linfócitos CD8$^+$ T e sobrecarga de ferro entre as diferentes populações. Os estudos funcionais proporcionaram avanços no conhecimento da interacção dos linfócitos com o NTBI, revelaram a existência de diferenças na capacidade de retenção de NTBI pelos PBMC dos doentes com HH que podem explicar alguma da heterogeneidade clínica, e encontrámos uma ligação nova entre a molécula S100A9 e o HFE com potencial interacção na modelação da função dos linfócitos CD8$^+$ T.

List of Abbreviations

ACTN1	Actinin, alpha 1
APC	Allophycocyanin
BMP	Bone morphogenic protein
CCR7	Chemokine (C-C motif) receptor 7
CD	Cluster of differentiation
cDNA	Complementary deoxyribonucleic acid
DAMPs	Damage-associated molecular pattern molecules
DAP12	TYRO Protein Tyrosine Kinase Binding gene
DAVID	Database for Annotation, Visualization and Integrated Discovery
Dcytb	Duodenal cytochrome b
DFO	Desferrioxamine
DMT1	Divalent metal transporter 1
DNA	Deoxyribonucleic acid
ER	Endoplasmatic Reticulum
FACS	Fluorescence activated cell sorting
FCS	Fetal calf serum
FSC	Forward-scattered light
Fe	Iron
Fe(II)	Ferrous iron
Fe(III)	Ferric iron
FeCit	Iron-citrate
FITC	Fluorescein isothiocyanate
FOSL2	FOS-like antigen 2
FPN1	Ferroportin 1
GAPDH	Glyceraldehyde 3-phosphate dehydrogenase
GO	Gene Ontology
HAMP	Hepcidin gene
HFE	Hemochromatosis gene
HH	Hereditary Hemochromatosis
HJV	Hemojuvelin
HLA	Human leukocyte antigen
HMW-NTBI	High-molecular-weight NTBI

IFN	Interferon
IgG	Immunoglobulin G
IL	Interleukin
IRE	Iron responsive element
IRP1	Iron regulatory protein 1
IRP2	Iron regulatory protein 2
KEGG	Kyoto Encyclopedia of Genes and Genomes
KS	Kolmogorov–Smirnov
Lcn2	Lipocalin 2
LEF1	Lymphoid Enhancer-Binding Factor 1
LIP	Labile iron pool
LMW-NTBI	Low molecular weight - NTBI
LPS	Lipopolysaccharide
mAB	mouse antibody
MACS	Magnetic-activated Cell sorting
MCP-1	Monocyte chemoattractant protein-1
MFI	Medean fluorescence intensity
MHC	Major histocompatibility complex
MIP-1α	Macrophage Inflammatory proteins 1α
mRNA	Messenger RNA
NAA50	N(alpha)-acetyltransferase 50
NR4A2	Nuclear Receptor Subfamily 4, Group A, Member 2
NRAMP1	Natural resistance-associated macrophage protein one
NTA	Nitrilotriacetate
NTBI	Non-transferrin-bound iron
P2RY8	Purinergic Receptor P2Y, G-Protein Coupled, 8
PBMCs	Peripheral blood mononuclear cells
PBS	Phosphate buffered saline
PCR	Polymerase chain reaction
PE	R-Phycoerythrin
PerCP	Peridinin-chlorophyll proteins
PGBD1	PiggyBac Transposable Element Derived 1
QTL	Quantitative trait locus
RAG	recombination-activating genes
ROS	Reactive oxygen species

RPMI	Roswell Park Memorial Institute Medium
RT-PCR	Reverse transcriptase PCR
S100A8	S100 calcium-binding protein A8 (Calgranulin A)
S100a9	S100 calcium-binding protein A9 (Calgranulin B)
SF	Serum ferritin
SLC40A1	Solute carrier family 40 (iron-regulated transporter), member 1
SSC	Side-scattered light
TBIS	Total body iron stores
T_{CM}	Central memory T cell
T_{EM}	Effector memory T cell
Tf	Transferrin
TfR1	Transferrin receptor 1
TfR2	Transferrin receptor 2
TfSat	Transferrin saturation
TLR	Toll-like receptor
TNF-α	Tumor necrosis factor α
Tyrobp	Tyrosine kinase binding protein
UPR	Unfolded protein response
UTR	Untranslated region
ZNF	Zinc finger

Table of contents

Chapter 1

General Introduction

Iron and the immune system: hanging hands through history

"Neither prevailing nor emerging dogmas see the circulation of the blood or the metabolism of iron as a motivating force for the development of a complex system of surveillance. While searching for evidence for this view, I came to be interested in iron as a target of surveillance by the immune system"

Maria de Sousa, 1989 [1]

Introductory remarks on the growth of knowledge of a subject are usually good opportunities to trace paths and highlight hallmarks considered most important for the field advance in a determined perspective. The interest on the relationship between iron and the immune system traces back to the seventies, last century (de Sousa, 1978) [2, 3], and since then it evolved encompassing the growing knowledge on the cellular and molecular players involved in iron homeostasis, in particular in the clinical model of Hereditary Hemochromatosis. The strong link between iron metabolism and the immune system has been the subject of several reviews devoted to this topic [4-7] but it is generally forgotten in historical reviews within the iron biology field [8, 9]. In this context, the first chapter of this thesis revisits a recent review on relevant historical marks in the iron biology field [8] adding and highlighting the concurrent hallmarks which brought together the iron biology and the immunology fields. A chronologic list of the selected major historical achievements is given in Table 1, where hemochromatosis hallmarks are highlighted in grey, and more specific immune related contributions are highlighted in green.

The first description of an iron related disease, although not recognised as such, was made by Lange in 1554, when he described a frequent disease among young woman who to him appeared to be "sadly pallid". The disease phenotype was a pale appearance and a disturbed mental state that he believed to be caused by the "filthy blood of the menses" that was being absorbed and moved to the head and so the patient become foolish and delirious [10]. In 1615 this condition was called by Jean Varandal as "chlorosis" due to the "greenish-yellow" colour of the skin [11] but it was only identified as an iron deficient hipochromic anemia in 1936 [12], a long time lapse after the first measurements of iron in the blood in

1713 [13], or the introduction of the first red cell count in 1852 and the first haemoglobinometer devise in 1876 [14].

The term "hemochromatosis" ("hemo" for blood, "chromate" for color and "osis" for disease) was first used by the German pathologist Friedrich Daniel Von Recklinghausen in a short report published in 1889 where he reported a case of "bronze stain" in organs such as liver, pancreas and skin at an autopsy [15]. This term hemochromatosis was later applied to all cases of iron overload associated with organ damage, and assumed to be the case of the disease syndrome of "bronze cirrhosis and diabetes" previously described by Trousseau back in 1865 [16]. In 1935, Joseph Sheldon suggested that the multi-visceral nature of the iron overload syndrome resulted from an inherited metabolic defect [17]. In 1950 the iron-overload patients started to be treated through phlebotomies (bloodletting) [18]. A huge advance on the identification of the putative gene for Hereditary Hemochromatosis (HH) was achieved in 1975 when Marcel Simon linked the HH syndrome with particular HLA-A and B alleles, placing the major histocompatibility complex region at chromosome 6 as a hotspot to look for the disease causing gene [19]. This link of an iron related disease with the genetic region involved in the immune system regulation constituted a good argument to suspect that the disease could be somehow immune related. At the same time, and based on her studies of lymphoid cell positioning demonstrating that lymphocytes migrate to areas of iron accumulation [2], De Sousa advanced in 1978 the postulate that the immunological system should have a role in monitoring tissue iron toxicity [3]. The impact of iron on the immune system also started at this time to be a subject of great interest after the demonstration of the immuno-suppressive effect of blood transfusions [20]. Altogether, evidences for this cross-talk between iron and the cells of the immune system and the association of HH with the MHC, all led to concentrate efforts on the search for immunological abnormalities in HH patients. The first description by Reimão et al in 1991 [21] of abnormalities in the relative proportions of T lymphocyte subsets in HH patients related to the severity of iron overload, and the following demonstration that this disproportion was specifically due to defects in the CD8$^+$ T cell pool [22], constituted the starting point to approach the reverse question, i.e., to look for iron metabolism abnormalities in experimental models of primary T lymphocyte immune deficiencies. As a result, the first experimental model of hemochromatosis was described by De Sousa and co-workers in 1994 with the study of mice depleted of the the β2 microglobulin gene (*β2m* $^{(-/-)}$) which were shown to develop a severe liver iron overload mimicking the human HH disease [23, 24]. Because it codes for an anchor protein essential for MHC-Class I expression at the cell membrane, *β2m* ablation leads to an almost complete depletion of CD8$^+$ T cells [25, 26]. As extrapolated from the human model, CD8$^+$ depletion could be therefore the cause for the induced iron overload. Two years later, in 1996, Feder et al. cloned the *HFE* gene (originally designated as HLA-H) where a single mutation (p.C282Y)

was found in the vast majority of HH patients [27]. This finding naturally removed the impact of the *β2m*[(-/-)] model as a proof of concept for the involvement of CD8^{+} T cells as modifiers of iron overload, because HFE, as a non-classical MHC Class I protein, also requires the presence of *β2m* to be expressed at the cell surface. This question was clarified, however, when Santos et al. demonstrated that mice deficient for both *β2m* and *Rag1* (a recombinase activator gene required for normal B and T development) had an even more severe phenotype of iron overload with heart fibrosis [28]. For the following years CD8^{+} T lymphocyte abnormalities in HH were consistently found and characterized in the peripheral blood [22, 29-32] and in the liver [33], where low numbers were associated with a higher hepatic damage [33], and novel mouse models were generated with selective immune deficiencies to confirm the impact of lymphocytes as modifiers of iron overload [28, 34, 35].

The discovery of HFE was perhaps, the single research event that most significantly contributed to initiate the "molecular era" of hemochromatosis. From that time on, discoveries of novel molecular players came to explain many other rare forms of HH providing substantial new knowledge on the complex regulation of systemic iron homeostasis [36]. These findings turned the beginning of the XXI century a very exciting time for the history of iron biology. In 2000 the liver-expressed antimicrobial protein called hepcidin was discovered [37] and it was found to be downregulated in the *Hfe* knockout mice (*Hfe*^{-/-}) [38]. After the description of the ferroportin and its involvement in cellular iron export, the functional regulation of ferroportin expression by hepcidin was established in 2005 by Nemeth and Kaplan [39]. Hepcidin is now generally recognised as the master regulator of systemic iron levels through regulation of cellular iron export. The more recent demonstration that *in vitro* activated T cells also express hepcidin in response to the exposure to transferrin-bound and non-transferrin bound iron support, for the first time, a functional role for T lymphocytes in response to iron [40].

A great contribution in the immuno-genetic perspective was the demonstration, in studies performed in HH families, that a low CD8 phenotype is genetically transmitted in linkage with other MHC genes namely HLA suggesting, for the first time, the existence of a putative genetic trait located at the MHC region implicated in the transmission of CD8 numbers in linkage with the p.C282Y mutation [41-44]. Moving from the genetic associations to the functional interactions between HFE and MHC Class I proteins, an important study was performed by Almeida et al in 2005 first advancing the hypothesis that the mutated HFE interfered with the classical MHC class I presentation route [45].

Although HH offers the best model to address the complex interactions between iron metabolism and the immune system, in many other immune related conditions iron has been placed at the centre namely infection [46], inflammation [47] and cancer [48]. A long way track is still needed, however, to fully understand all the mechanisms involved in the

regulation of local and systemic iron homeostasis in these conditions as well as the clinical implications of iron homeostasis disturbances in those disorders. Most strikingly, the putative role of HFE in immune related conditions beyond iron overload has been remarkably neglected.

Table 1 Time of the most important achievements in the hemochromatosis and iron metabolism

Year	Discovery	Researchers
1554	First description of "chlorosis"	Lange [10]
1713	Human blood show to contain iron	Lemery & Geolfroy [13]
1865	A case of "bronze diabetes and cirrhosis" is described	Trousseau [16]
1871/1882	Hypertrophic pigmentary cirrhosis and diabetes	Troisier-Hanot & Chauffard [49]
1889	The term "hemochromatosis" is created to describe bronze-colored organs and tissues at autopsy	Von Recklinghausen [15]
1935	Hemochromatosis is hypothesized to be hereditary and related to iron metabolism	Sheldon [17]
1937	The first iron protein (ferritin) is identified and crystalized	Laufberger [50]
1937	First study on the role of intestinal absorption in iron metabolism	Widdowson & McCance [51]
1939	Effect of iron in inflammatory joint disease	Hiyeda [47]
1946	An iron-binding protein (transferrin) is identified in human plasma	Schade & Caroline [52]
1950	Bloodletting reported as a treatment for hemochromatosis	Davis&Arrowsmith [18]
1950	Liver biopsy reported as a tool for diagnosing hemochromatosis	Davids & Laurens [53]
1951	First report of juvenile hemochromatosis	Plattner, Nussbaumer & Rywlin [54]
1951	Radioiron studies of intestinal absorption in hemochromatosis	Alper & Bothwell [55]
1955	First comprehension review on hemochromatosis	Finch & Finch [56]
1961	Hemochromatosis as a variant of alcoholic cirrhosis and nutritional siderosis	MacDonald [57]
1963	Intestinal iron absorption shown to be regulated at the enterocyte/blood interface	Crosby [58]
1969	Phlebotomy reported to improve survival in hemochromatosis	Williams & Sherlock [59]
1975	Hemochromatosis is shown to be a hereditary autosomal recessive HLA-linked disease	Simon [19]
1976	First description of the transcriptional control of ferritin	Zahringer & Munro [60]
1978	Iron binding proteins add a role in the control of lymphoid cell migration	De Sousa [2]
1978	Postulated role for the Immunological system in the surveillance of tissue iron toxicity	De Sousa [3]
1978	Demonstration of the immuno-suppressive effect of blood transfusions	Keown & Deschamps [20]

Year	Description	Reference
1978	Iron as a determining factor for microbial cell growth	Weinberg [46]
1980	Iron & cancer: transformed cells acquire the capacity to bind iron through the expression of surface transferrin receptors	Faulk [48]
1983	First description and characterization of iron-mediated oxidative damage in hemochromatosis	Bacon & Recknagel [61]
1985	Survival and causes of death reported in a large series of hemochromatosis patients	Niederau & Strohmeyer [62]
1987	"Iron responsive elements" are found in the mRNA of ferritin	Aziz & Munro - Hentze & Klausner [63, 64]
1988	First large population screening study using blood iron measures in HLA-linked hemochromatosis	Edwards & Kushner [65]
1989	Defective iron retention by reticuloendothelial macrophages is described in hemochromatosis	Fillet [66]
1989	Generation of the immunological deficient mice model (β2-microglobulin knockout) that lack peripheral CD8 T cells	Koller and Zijlstra [25, 26]
1991	Increased iron absorption in hemochromatosis linked to increased mucosal iron transfer to the plasma	McLaren [67]
1991	Immunological abnormalities in HH patients: decrease CD4/CD8 rations of circulating T lymphocytes	Reimão [21]
1994	A novel correlation between CD8$^+$ lymphocytes and iron overload	Porto [23]
1994	CD8$^+$ T-cell deficient mice (β2-microglobulin knockout mice) develop a severe hepatic iron overload: the first mouse model of Hereditary Hemochromatosis	De Sousa & Santos [23, 24]
1996	Identification of the gene mutated in HLA-linked hemochromatosis : **HFE** (a non.classical MHC Class I protein)	Feder & Wolf [27]
1997	Divalent metal transporter 1 (DMT1)- the first mammalian transmembrane iron transporter is identified	Fleming & Andrews-Gunshin & Hedlger [68, 69]
1999	Description of non-HFE related hemochromatosis in adults (later identified as ferroportin disease)	Pietrangelo [36]
1999	Identification of transferrin-receptor 2 (TfR2) gene	Kawabata [70]
2000	Description of TfR2-associated hemochromatosis	Camaschella & Gasparini [71]
2000	Description of liver-expressed antimicrobial protein (hepcidin) in human	Krause & Adermann [37]
2000	Description of ferroportin1 (MTP-1; IREG-1) gene	Abboud & Hailie-Donovan & Zon [72-74]
2001	Description of ferroportin-associated iron overload ("ferroportin disease")	Montosi & Pietrangelo [75]
2001	Hepcidin expression in the liver is linked to iron	Pigeon & Loreal [76]
2002	Decreased hepcidin levels in HFE null mice	Ahmad & Fleming [38]
2000-06	Documentation of the penetrance of HFE-associated hemochromatosis	Kushner-Beutler-Olynyk-Powell [77-80]
2003	Description of hepcidin-associated hemochromatosis	Roetto & Camaschella [81]
2003	Decreased hepcidin expression documented in human HFE-related hemochromatosis	Bridle & Andreson-Gehrke & Stremmel [82, 83]
2004	HJV gene isolated and HJV-related hemochromatosis reported	Papanikolaou [84]
2004	Genetic transmission of Low CD8 numbers phenotype is associated with HLA-HFE haplotype	Cruz [41]
2005	C282Y mutation of HFE influences MHC class I presentation pathway	Almeida [45]
2005	Hepcidin is shown to cause FPN1 degradation in vitro: a model for regulation of iron homeostasis in vivo	Nemeth & Kaplan [85]

2004-06	Low progression rate of HFE-related hemochromatosis is documented	Olynyk-Anderson & Nordestgaard-Allen [86-88]
2006	HJV/BMP signaling shown to regulate hepcidin and iron metabolism	Babbit &Lin [89]
2006	A model for iron sensing based on HFE/TfR2 is proposed	Goswami & Andrews [90]
2009	ER stress controls hepcidin expression and iron metabolism in vivo	Vecchi & Pietrangelo [91]
2009	BMP6 shown to be the key endogenous regulator of iron metabolism	Andriopoulos, Corrandi, Xia & Babitt-Meynard &Roth [92, 93]
2009	BMP6 signalling shown to be impaired in HFE null mice	Corradini &Babitt-Kautz &Roth [94, 95]
2010	Activated T lymphocytes express hepcidin in response to transferrin-bound iron and non-transferrin bound iron	Pinto [40]

Adapted from Pietrangelo *et al* 2010 [8]

Normal Iron Homeostasis

A healthy adult normally keeps in his body a total of 3 to 4g of iron. Since there is no excretory mechanism for iron, daily losses are mostly due to sweat and epithelial desquamation of skin, intestine and genitourinary track. In men these iron losses are of approximately of 1mg, but in women, due to menstruation, pregnancy and lactation, these losses may reach up to 2mg a day. In order to compensate for these physiological iron losses, 1-2mg of iron is absorbed from a normal diet which may contain 15mg of iron [96].

In general, the systemic iron homeostasis in humans can be monitored by the transferrin saturation levels. Plasma transferrin is normally about 30% saturated with iron. A transferrin saturation <16% indicates iron deficiency, whereas a saturation >50% can be a sign of iron overload. Under constant rates of transferrin production and catabolism, the transferrin saturation is influenced by: i) the amount of iron absorbed from the diet, ii) the amount of iron utilized by the bone marrow (mostly for erythropoiesis) and other tissues, and iii) and the amount of iron recycled and released by splenic macrophages [97].

The major players and mechanisms regulating systemic iron homeostasis classically consider four major compartments (involving particular cell types): the <u>uptake</u> compartment (enterocytes), the <u>functional</u> compartment (erythroid precursors and other proliferating cell pools), the <u>recycling</u> compartment (spleen macrophages) and the <u>storage</u> compartment (hepatocytes and macrophages) (Fig.1).

The uptake of iron from the diet is mostly performed at the brush border of duodenal enterocytes. There are two sources of dietary iron: heme and non-heme iron, the first being absorbed more efficiently. Heme iron is estimated to contribute to 10–15% of total iron intake in meat-eating populations but because heme iron is much more efficiently absorbed, it could contribute to up 40% of total absorbed iron [98, 99]. Inorganic iron is less well absorbed than heme iron and is affected by both body iron status and by dietary enhancers (such as ascorbic acid) and inhibitors (for example: phytic acid, tannic and chlorogenic acids and soy protein) [98, 99]. Inorganic iron, mostly Fe(III), is very insoluble so in order to move across the enterocyte brush border membrane through the iron transporter divalent metal-ion transporter 1 (DMT1) it has to be reduced to Fe(II) by the duodenal cytochrome B (Dcytb) reductase and possibly by others reductases. Enterocyte iron is exported to the blood via ferroportin 1 (FPN1), also known as solute carrier family 40 member 1 (SLC40A1) which is the only known iron exporter in mammals. With expression on the basolateral membrane of enterocyte, FPN1 acts in partnership with the ferroxidase hephaestin that oxidizes exported ferrous iron to Fe(III) for binding to plasma transferrin [100]. After being exported by the enterocytes, iron circulates in plasma bound to the glycoprotein transferrin which has two high-affinity binding sites for Fe(III). Transferrin-binding maintains Fe(III) in a safe soluble

form, and is the major source of iron to cells that express the membrane receptor (transferrin receptor, TfR1) whose complex is internalized by endocytosis in order to fulfil cellular iron needs [97]. Non-transferrin-bound iron (NTBI) species begins to be present in the circulation and to be accumulated in parenchymal cells leading to organ damage even before transferrin becomes fully saturated [101, 102]. NTBI is bonded with low molecular weight ligands such as ATP, AMP, citrate, phosphate, lactate, acetate, carbohydrates and amino acids as well as albumin [102-104].

The functional compartment involves mainly the erythroid precursors that use 75% of the systemic iron fraction to incorporate the heme group, responsible for oxygen transport. These cells acquire transferrin-bound iron via TfR1, but it is also proposed that these cells can take up ferritin that macrophages release in erythroblastic islands [105]. Iron is also an essential nutrient for many cellular functions such as: energy production in the mitochondria, DNA synthesis and the production of myoglobin in the muscles. It is also a co-factor of several iron-requiring metalloenzymes such as catalase, hydrogenase or aconitase [106]. The majority of the iron found inside the cell (95-97%) is bound to transferrin and ferritin [107]. However, a free labile iron pool (LIP) fraction that corresponds to 3-5% of total iron content can also be found inside the cells. This LIP is mostly low–molecular weight chelatable iron, either Fe(II) or Fe(III), associated with a variety of ligands such as: citrate, phosphate, carbohydrates, nucleotides and nucleosides among others. This labile iron pool is the major source of oxidative stress by participating in the Haber-Weis-Fenton's reactions that originates free radicals that cause damage to all macromolecules (lipids, proteins and DNA) [108]. The amount of iron that is not used can be either stored inside ferritin, or can be exported by FPN1 [109].

The recycling compartment is composed by the reticuloendothelial system (spleen and liver macrophages) that recycle every day 20–25 mg of iron from the turnover of senescent erythrocytes. This recycled fraction of iron is the main source for functional iron needs. Senescent red blood cells are phagocytosed and iron is transported from the phagocytic vesicles to the cytosol by NRAMP1 (natural resistance-associated macrophages protein 1) that is a DMT1 homolog transporter [110]. Export of ferrous iron from macrophages occurs via FPN1 which interacts with ceruloplasmin (a multicopper oxidase) which oxidases Fe(II) to Fe(III) for loading onto transferrin [97]. Since the amount of plasma iron is just over 10% of the amount used daily, this implicates that plasma iron is turned over many times each day. Under normal conditions, 80%–90% of the recycled iron is reused for hemoglobin synthesis [111]. The remaining 10%–20% of the recycled iron is stored inside the macrophage as ferritin.

Like the reticuloendothelial cells, hepatocytes are also an important site of iron storage in the form of ferritin. Hepatocytes are the major storage compartment for iron; they

become particularly important when the iron-binding capacity of plasma transferrin is exceeded as they can rapidly clear the NTBI species formed from circulation. The identity of the hepatocyte NTBI uptake system is not known, DMT1 was pointed as important NTBI transporter [112, 113] however, hepatocytes can accumulate iron in the absence of DMT1 [114]. Therefore, other potential candidates include: the L-type voltage-dependent Ca2+ channels [115, 116], and the already identified for their ability to transport other metal ions, the Zip-14 [117]. Most importantly, hepatocytes play a central role in iron homeostasis as the site of regulated production of the hormone hepcidin. Hepcidin is the master regulator of systemic iron levels. It orchestrates systemic iron fluxes and controls plasma iron levels by binding to FPN1 on the surface of iron-releasing cells, triggering its internalization and degradation and therefore reducing iron transfer to transferrin [85]. Systemic hepcidin levels regulate the amount of iron that is exported into circulation by the enterocytes, therefore its expression gives feedback of systemic iron status for regulation of dietary iron absorption.
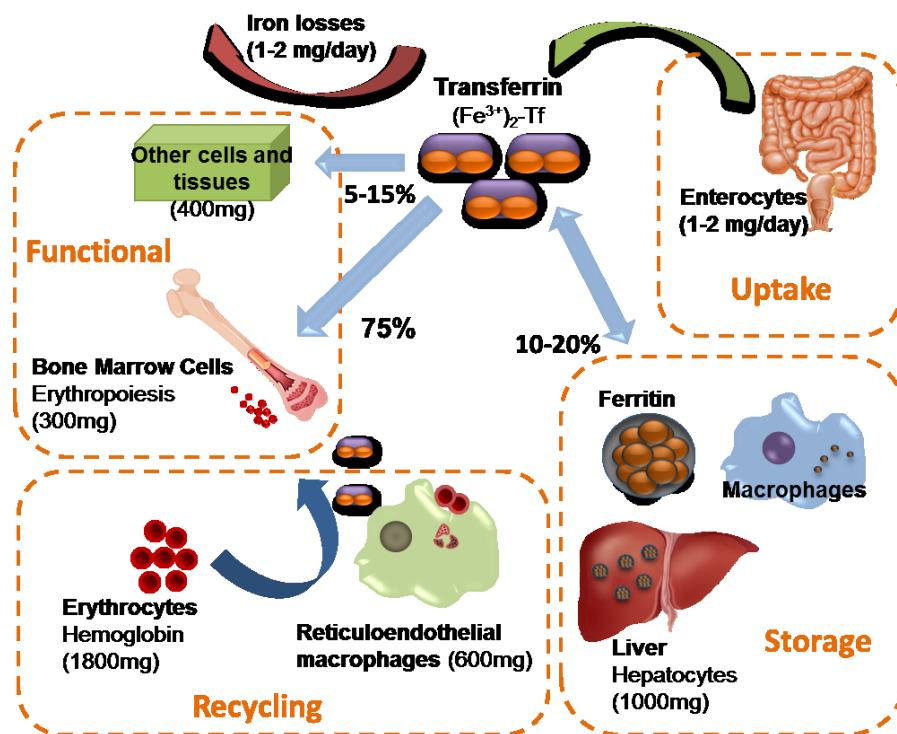
Fig. 1 Iron distribution in the adult human body and the four major compartments involved in the processes of iron uptake, storage, recycling and functional involved in iron homeostasis with the principal cellular players.

In terms of cellular iron homeostasis, the uptake and storage of cellular iron is regulated by a post-transcriptional mechanism involving mRNA-protein interactions – the IRE/IRP system. Iron responsive elements (IRE) are 30 nucleotide cis-regulatory structures present in the 3' or 5' untranslated region (UTR) of mRNAs, that code for iron metabolism proteins. Iron regulatory proteins 1 and 2 (IRP1 and IRP2) are cytoplasmatic and belong to

the protein family of Fe-S cluster isomerases. The IRE-IRP regulatory system is based in the ability of cytosolic IRP to affect the stability of a previously synthesized mRNA, or to alter the efficiency with which a given transcript is translated [118-121].
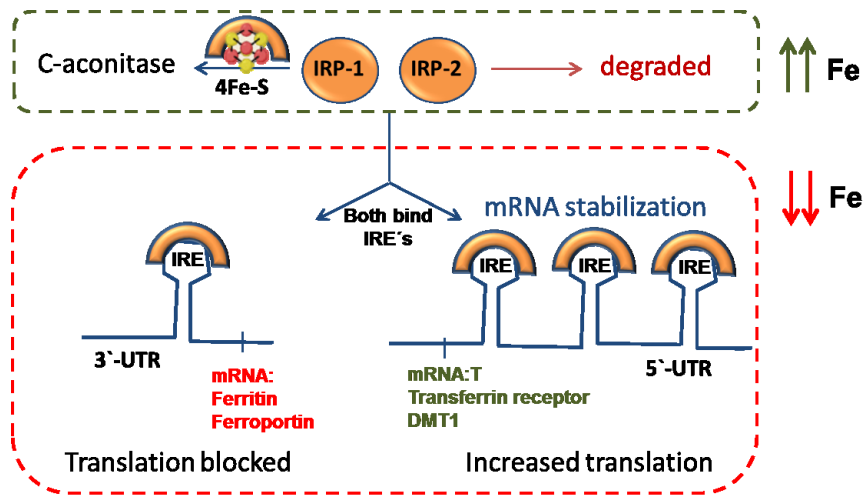
Fig.2 Regulation of cellular iron metabolism: the IRE/IRP system.

Under iron-deficient conditions, IRP1 is free to bind to IREs. If IRP-1 binds to the 5′ UTRs of target mRNAs it inhibits their translation (such as ferritin and ferroportin mRNAs), whereas IRP interaction with multiple 3′ UTR IREs results in increased mRNA stability (such of the TfR1). As a consequence, TfR1-mediated iron uptake increases and the iron storage in ferritin and export via ferroportin decrease, thus LIP content increases in order to fulfil the cell iron needs [97]. Under iron-loaded conditions, IRP1 is inactivated by assembling 4Fe/S cluster at the IRE-binding site that confers aconitase activity to the holoprotein. IRP1 and IRP2 are then signalled by the FBXL5 iron-sensing F-box protein and recruits the SKP1-CUL1 E3 ligase complex that promotes IRP ubiquitination and degradation by the proteasome (Fig.2).

Hereditary hemochromatosis: an iron-overload disorder

Hereditary hemochromatosis (HH), classically associated with the p.C282Y mutation in HFE, is an autosomal recessive disease that predisposes patients to an increased intestinal iron absorption and iron export from macrophages, resulting in progressive tissue iron overload which leads to irreversible organ damage if not treated timely. The pancreas, skin, joints and mostly the liver are the main target sites for iron deposition which leads to organ failure through production of oxidant species. Early symptoms are non-specific such as fatigue, arthralgia, malaise, abdominal pain, etc. The principal severe clinical manifestations associated with iron overload are: liver cirrhosis, hepatocellular carcinoma, diabetes and arthritis. These consequences can be avoided if HH patients are early detected and start a therapeutic phlebotomy treatment. Early diagnosis, i.e., before the onset of irreversible organ damage, and prompt initiation of iron-depletion therapy prevents irreversible organ damage, and increases the survival of patients with hemochromatosis [122]. A proper follow-up of circulating iron parameters, such the serum ferritin levels (that reflect the iron stores) and the transferrin saturation (that indicates the amount of potential NTBI in circulation), aimed at keeping them at normal levels, offers these patients a life expectancy similar to that of a normal population.

An early diagnosis of HH may be difficult if only based on its clinical context, without any familiar related history. To confirm an iron-overload condition, measures of some biochemical blood parameters are highly informative although not 100% specific. Transferrin saturation above 50% in females or 60% in males is abnormal and suggestive of HH, although other liver pathologies have to be discarded such as alcohol or viral liver disease. The serum ferritin concentration is usually a good marker of body iron stores although increased levels are also observed in inflammatory conditions and in hepatocellular necrosis. Once there is a strong suspicion of HH, i.e., in the presence of suggestive biochemical abnormalities not explained by other conditions, a genetic diagnosis should be done, based on the detection of the p.C282Y mutation in *HFE*.

HFE: the gene and its mutations

The *HFE* gene codes for a 343 residue type I transmembrane glycoprotein homologous to Class I MHC molecules (it shares 37% of sequence identity with the HLA-A2). *HFE* has three extracellular domains analogous of α1, α2 and α3 domains of a MHC-I immunoglobulin (Fig.3). In contrast with the classic MHC-class I molecules, the α1 and α2 domains are not-polymorphic and too narrow to accommodate a short peptide. Given this structural limitation, HFE is believed not to present antigens to T-lymphocytes. As with any

other MHC-I classical protein, HFE folding occurs in the endoplasmatic reticulum (ER), where its α3 domain interacts with the Class I light chain β2-microglobulin (β2m). The correctly folded protein leaves the ER and is presented at the cell membrane. HFE is predominantly expressed at duodenum, liver, pancreas, placenta, kidney, reticulo-macrophagic system and ovary, while in colon, leukocytes, brain and lung the expression is low. Two common missense mutations were originally described by Feder et al, in the *HFE* gene; the p.C282Y and the p.H63D. The p.C282Y mutation is a single-base substitution of a guanidine to an adenine at nucleotide 845, resulting to the substitution of a tyrosine for a cysteine at amino-acid 282. This mutation provokes the disruption of the α3 domain intrachain disulfide bond with β2m (Fig.3) and so the molecule cannot migrate to cell surface and stays trapped in the ER following proteasomal degradation. The p.H63D mutation is a substitution of a cytosine to a guanidine at nucleotide 187, resulting in a substitution of an aspartate for a histidine at amino-acid 63. This mutation occurs in α1 domain and does not affect the ER folding, migration and presentation of the protein at cell membrane although it can slightly change the affinity of transferrin to its receptor [27]. According to the most recent clinical guidelines (EASL 2010), only the p.C282Y mutation in homozygosity confirms the diagnosis of HFE related HH [123]. The role of p.H63D as a risk factor for iron overload is still debated [124, 125].
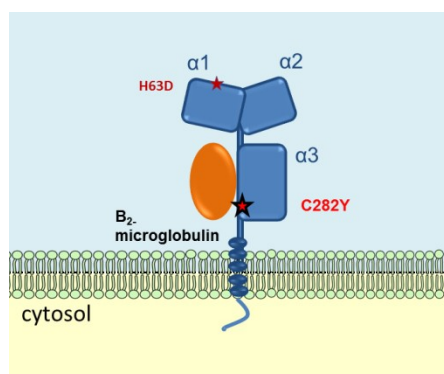
Fig. 3 HFE molecular structure (non-classical MHC Class I molecule) with the HH associated mutations represented in red.

HFE: the molecular functions in iron homeostasis

Hepcidin expression is normally up-regulated by dietary or parenteral iron loading [76], in order to systemically feedback the enterocytes to limit intestinal iron absorption. In HH, this mechanism fails. In some patients the hepcidin levels may be at normal levels but they are still inadequately low for the amount of iron load [126, 127] and they do not respond, with increasing hepcidin levels, after an acute oral iron challenges [126]. Because this expected up-regulation of hepcidin in response to iron loading is impaired in patients with HH, HFE is expected to be involved in the regulation of hepcidin expression.

HFE has been suggested be an "iron-sensor" acting by switching between two sensors of the Tf-Fe levels, TfR1, and TfR2, on the plasma membrane of hepatocytes [90]. This model is supported by the following findings: HFE binds to TfR1 competing with Tf-Fe for the receptor binding site. By contrast, TfR2 can bind both HFE and Tf-Fe simultaneously [128]. The HFE–TfR1 functional interaction gained new insight from experimental mouse models generated either to promote or abolish this complex. The results from mice with constitutive expression of HFE-TfR1 complex were very similar to the HFE-deficient mice who show low hepcidin production and systemic iron overload suggesting that the TfR1 sequesters HFE to prevent its participation in hepcidin activation. Conversely, mutations that abolish the HFE-TfR1 interaction or mice with increased HFE levels display iron deficiency due elevated hepcidin expression [129]. Hepcidin activation by holotransferrin requires both HFE and TfR2 [130]. Altogether, the described observations support a model in which high concentrations of Tf-Fe2 displace HFE from TfR1 to promote its interaction with TfR2, which is further stabilized by increased Tf-Fe2 binding to the lower-affinity TfR2. More recently another partner was added to HFE-TfR2complex, the hemojuvelin (HJV). The HJV protein acts as a BMP (Bone morphogenic protein) co-receptor, thereby activating hepcidin transcription via the BMP-SMAD signaling cascade. BMP6, which is activated by increased iron levels, is the endogenous ligand for HJV [92, 93]. Moreover, the BMP/SMAD signaling pathway is impaired in HH as well as in *Hfe*-knockout mice, suggesting a crucial role of HFE in BMP/SMAD signalling [131].

T-Lymphocytes Homeostasis

The ability to maintain T cell homeostasis allowed vertebrate organisms to produce an effective immune response. In order to maintain that immune responsiveness, distinct lymphocytes populations with different immune functions must also be maintained in equilibrium [132]. The lymphocytes TCRαβ are originated from lymphoid progenitor cells, haematopoietic stem cells originating from the bone marrow that home to the thymus. In the thymus a complex process of maturation it will occur which involves the recognition of MHC Class I molecules by the T cell receptors (TCR) and the submission to positive and negative selection which result in the production of CD4$^+$ or CD8$^+$ single-positive T lymphocytes [133]. From the thymus, single positive T lymphocytes migrate in a naïve state to the peripheral organs, where they circulate between the secondary lymphoid organs and the blood [134]. The pool of T-cells that present in the periphery consists of naïve CD4$^+$ and CD8$^+$ T cells, central memory (CM) and effector-memory (EM) subpopulations, each occupying a specific homeostatic niche [135]. CD4$^+$ Treg and TH17 CD4$^+$ effector T cells constitute an independent pool of cells occupying separate homeostatic niches [136, 137].

The peripheral T cell population is conserved at very constant numbers. The numbers of naïve T cells at the periphery is dependent on the stimulation of T cells through their TCRs. When peripheral major histocompatibility complex (MHC) class I or class II expression is absent, T cells are unable to survive due the lack of TCR-mediated T cell stimulation [138]. Also, induction of TCR deletion results in the disappearance of peripheral T cells, showing that T cells need to receive signals through their TCR to support their survival in the periphery [136]. Naïve T lymphocytes travel to T-cell areas of secondary lymphoid organs in search of antigen presented by dendritic cells [139, 140]. Once activated, they start to proliferate and give origin to effector cells that can migrate to B-cell areas or to inflamed tissues [141, 142]. A fraction of primed T lymphocytes persists as circulating memory cells that can confer protection and give, upon secondary challenge, a qualitatively different and quantitatively enhanced response [143, 144].

The differentiation process of T lymphocytes

When peripheral naïve T cells return to lymph nodes, they first roll on high endothelial venules using CD62L (L-Selectin). This allows the chemokine receptor CCR7 to engage its ligand SLC (secondary lymphoid-tissue chemokine), which is displayed by endothelial cells [145]. The CCR7–SLC interaction activates integrins that promote firm adhesion and transmigration of the T cells into the lymph node [146, 147]. In contrast to naïve T cells, memory/effector cells migrate mostly through peripheral tissues [148]. This migration allows

a quicker response and is controlled by the expression of different sets of integrins and chemokine receptors [139, 149]. Some memory T cells must also reach the lymph nodes when they need to trigger a secondary proliferative response. The two types of memory response might depend on subsets of memory T cells produced with distinct homing and effector capacities. Because CCR7 and CD62L are essential for lymphocyte migration to lymph nodes [139, 150], the co-expression of these receptors helps to distinguish a supposed subset of memory T cells that home to lymph nodes. Human naïve and memory T cells can be identified by the reciprocal expression of the CD45RA or CD45R0 isoforms [151]. Staining of peripheral blood T cells with antibodies to CD45RA and CCR7 revealed three subsets of CD4$^+$ and CD8$^+$ cells: one naive CD45RA$^+$CCR7$^+$; and two memory subsets, CD45RA$^-$CCR7$^+$ and CD45RA$^-$CCR7$^-$. Both naïve and CCR7$^+$ memory cells expressed high levels of CD62L, whereas the CCR7$^-$ memory cells expressed CD62L to a lower and variable extent. Within CD8$^+$ T cells, an extra subset of CD45RA$^+$CCR7$^-$ cells can be identified. In addition, the two CCR7$^+$ subsets expressed high levels of CD62L, whereas most of the cells among the two CCR7$^-$ subsets lacked CD62L (Fig.4). The expression of the receptors responsible for lymph-node-homing on a distinct subset of memory CD4$^+$ and CD8$^+$ T cells points out different functions [135].
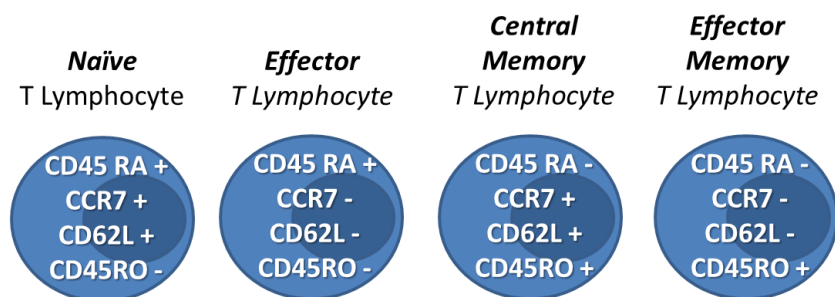
Fig. 4 T-Lymphocyte phenotype (Naïve, Effector, Central memory and Effector memory) with some cell membrane markers expressed accordingly the specific differentiation state.

T cell activation and gene expression profile of activation

Naïve T lymphocytes that survive to the apoptosis process become memory or effector T cells through a differentiation process that involves alteration in expression of membrane receptors and/or intracellular cytokines. After activation, the receptors that are expressed work as differentiation markers such cytokine receptors and growth factors, for example: α chain of IL-2 receptor (CD25), β chain of IL-12 receptor, the transferrin receptor (CD71) and the insulin receptor (CD220). Most of these receptors are involved in the cell cycle control and nutrient transport to fulfil the needs of the cell in its division process. While some of these receptors are immediately expressed after activation (for example, CD69 and CD25) others are expressed days after activation (for example CD71). Some other receptors

decrease or even abolish their expression after activation, an example of these are: CD62L integrin, CCR7⁺ receptor and the ζ TCR chain. During the activation and expansion process, naïve T lymphocytes stop expressing at different stages of the differentiation process the CD62L, CCR7 and CD28 receptors giving rise to effector or memory T cells (Figure 4) [152, 153].

Another very specific and heterogeneous TCRαβ lymphocyte subset of either CD4 or CD8 activated cells is defined by the expression of IL-2 receptor α chain (CD25) and the transcription factor Foxp3 and are called as regulatory or Treg cells. The Treg lymphocytes are able to suppress the immunological response mediated by other T cells and can be divided in two major groups: the natural and the inductive or adaptive Treg. The natural Treg are CD4$^+$CD25$^+$ (characterized by protein expression of CTLA-4 and Glucocorticoid induced TNF receptor, GITR) and are produced in the thymus under specific signals. The adaptive Treg can be CD4$^+$CD25$^+$, CD8$^+$CD25$^+$ or CD8$^+$CD28$^-$ and are produced in the thymus but differentiate at the periphery under certain stimulatory factors such as IL-10 and TGF-β [154].

Final remarks on the homeostatic control of CD8$^+$ T lymphocyte subsets at the periphery

As discussed above, multiple regulatory mechanisms operate for the maintenance of T cell numbers and functions under a strict homeostatic equilibrium. These mechanisms are known to operate in an independent manner for the different subsets of naïve or memory effector T lymphocytes [155]. While naïve T cells persist mainly as long-lived resting cells, memory cell survival depends on their constant self-renewal by triggering and cell division at the periphery [156]. The types of interactions implicated in these processes are naturally complex and differ according to the cell type. Focusing on CD8$^+$ T lymphocytes, the cell population implicated in hereditary hemochromatosis [22, 29-32], it is now well described that they go through successive effector phases, inflammatory and cytotoxic, with potentially different T cell properties [157, 158]. Notably, the survival and expansion of CD8$^+$ T memory cells, in contrast to naïve cells, is not restricted to TCR-MHC-peptide interactions but needs only a nonspecific MHC class I interaction in the absence of antigen [159, 160].

Hereditary hemochromatosis: an immunological disorder

HFE: linkage to other MHC-class I genes

The major histocompatibility complex (MHC) has been studied for more than 60 years, and its early history is well documented [161]. Serological typing revealed associations between the MHC and many interesting immune phenotypes long before the cloning of class I and class II genes and determination of the structures of their encoded proteins. The MHC genetic region was first suggested as a possible region to look for a hereditary hemochromatosis (HH) gene by Simon et al because of the high frequency of HLA-A3 allele found among patients [162]. The most informative data about the genetic transmission of the syndrome was obtained through family studies that allowed to confirm the autosomal recessive disease inheritance in linkage with the HLA region. The disease associated gene should be therefore localized in the short arm of chromosome 6. Linkage analyses with several markers within the MHC region, helped to define a conserved haplotype, the HLA-A*03-B*07, as the most commonly associated with the disease in all populations studied, and this was assumed, as the founder chromosome, in spite of its high conservation, suggesting a very recent age for the p.C282Y mutation. In 1996, Feder et al. sequenced by positional cloning the MHC class I- region between HLA-A and the D6S276 gene marker and, by further linkage-disequilibrium and full haplotype analysis, identified a 250-kilobase region located more than three megabases telomeric from the major histocompatibility complex on chromosome 6 that was identical by descent in 85 percent of HH patients. Because it was a MHC class I related gene, they first named as *HLA-H*. The name of the gene was changed because there was a different pseudogene already named as HLA-H and so the hemochromatosis gene was renamed by the HUGO Genome database Nomenclature Committee as *HFE* that means **H**igh **Fe** (iron) (Fig.5).
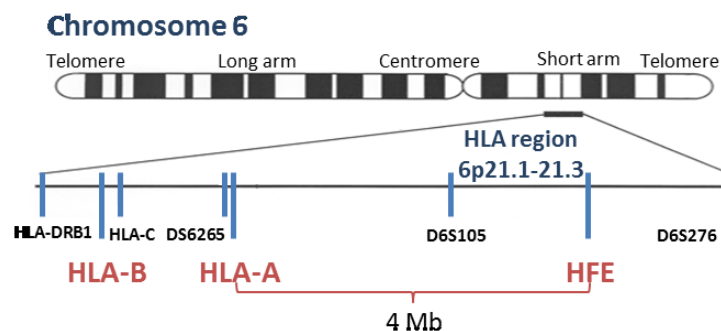
Fig. 5 Physical map of the MHC region with the distance between the *HLA-A* markers and *HFE* gene

After the general and global use of the genetic tests for detection of the most common *HFE* mutations, larger genetic studies were performed and the allele frequencies data of distinct populations became available. It became evident that the p.C282Y mutation is highly common in most European descent populations but it is almost absent in non-Caucasian populations from Africa. Within Europe the p.C282Y allele (Adenine (A)) frequency ranges from 0.013 to 0.140 with a north–south gradient. The highest frequencies are observed in populations from Ireland, United Kingdom and Brittany, and in Scandinavian populations. This high incidence in the northern populations support the proposed origins for the spread of the hemochromatosis mutation, the first by Simon suggesting that it was a unique and recent event originated in a Celtic population with a subsequent spreading by population migration, and the later suggested by Milman where arguing that the Viking conquests and migrations could have played a more significant role in the spread of the mutation [163].

Table 2 Allele frequency of the nucleotide at 845 position of *HFE* gene (Guanine – wild-type or Adenosine - C282Y mutation) and respective genotype in different world populations. Information was obtained from the 1000 Genomes project [164]

Population	Allele frequency (count)	Genotype frequency (count)
1000GENOMES: **ALL**	G: 0.987 (4945) A: 0.013 (63)	G|G: 0.976 (2443) A|A: 0.001 (2) A|G: 0.024 (59)
1000GENOMES: **AFRICAN**	G: 0.998 (1319) A: 0.002 (3)	G|G: 0.995 (658) A|G: 0.005 (3)
1000GENOMES: **AMERICAN**	G: 0.978 (679) A: 0.022 (15)	G|G: 0.960 (333) A|A: 0.003 (1) A|G: 0.037 (13)
1000GENOMES: **EAST ASIAN**	G: 1.000 (1008)	G|G: 1.000 (504)
1000GENOMES: **SOUTH ASIAN**	G: 0.998 (976) A: 0.002 (2)	G|G: 0.996 (487) A|G: 0.004 (2)
1000GENOMES: **EUROPE**	G: 0.957 (963) A: 0.043 (43)	G|G: 0.917 (461) A|A: 0.002 (1) A|G: 0.082 (41)

The recent age for the p.C282Y mutation is supported not only by its restricted ethnic distribution (only European derived populations) but also by the extreme conservation of an ancestral haplotype spanning 4Mb at the MHC region. Initial linkage studies, using several polymorphic markers, estimated that the ancestral mutation may have originated between 62 and 69 generations ago but other estimations based on recombination rates suggested that mutation is older (126 to 250 generations). Such a young age for the p.C282Y mutation contrasts with the very high allele frequency observed among European derived populations,

suggesting an increase in frequency due to a positive selective pressure where the p.C282Y may have conferred some advantage or could have been hitchhiked associated with other advantageous MHC gene alleles, given the strong linkage disequilibrium found in the region [165].

Although the frequency of the p.C282Y mutation in most European derived populations is very high (about 5-200) the proportion of patients with a fully developed phenotype found in clinical practise seems to be very low. Most homozygotes for the p.C282Y mutation of *HFE* show a common biochemical phenotype characterized by high transferrin saturation, as shown in family studies where homozygous relatives displayed this iron overload phenotype, yet they were still asymptomatic. The question remains whether under-diagnosis of HH results from the non-specific nature of early symptoms or incomplete penetrance of p.C282Y mutation. Family screening has proved to be highly effective in early case detection and disease prevention. Large population screening programs, however, revealed that the clinical penetrance of HH is very low. Beutler et al reported that the disease penetrance should be of less than 1% [79], a screening study in an Australian population showed that 50% of detected homozygous had clinical features of hemochromatosis and 25% had hepatic fibrosis or cirrhosis [166]. A population screening in Norway, revealed that only 10% of detected homozygous subjects displayed hepatic fibrosis or cirrhosis [167]. In a multiethnic screening study of Hemochromatosis and iron-overload disorder, 99771 participants collected blood samples and tested for transferrin saturation, serum ferritin, and p.C282Y and p.H63D mutations of the *HFE* gene [168]. The results revealed different prevalences of p.C282Y homozygotes among different populations: non-Hispanic whites (0.44%), Native Americans (0.11%), Hispanics (0.027%), Africans (0.014%), Pacific Islanders (0.012%), or Asians (0.000039%). Among the p.C282Y homozygous participants (227) in whom iron overload condition had not been diagnosed, serum ferritin levels were greater than 300 ng/ml in 78 of 89 (87%) men and greater than 200 ng/ml in 79 of 138 (57%) women. Serum ferritin levels above 1000 ng/ml, which is associated with a high risk of liver fibrosis [169], were detected in 364 participants undiagnosed for iron overload (29 were p.C282Y homozygotes). Among men, p.C282Y homozygotes and compound heterozygotes were more likely to report a history of liver disease than were participants without *HFE* mutations. However, the question of prevalence, penetrance and natural progression of clinical hemochromatosis is difficult to address because of the huge clinical heterogeneity found among HH patients. It can vary from a simple biochemical abnormality to a severe iron-overload with organ damage. The reasons for that heterogeneity are not fully understood. The discovery of novel modifiers of the clinical expression of type I HH may give new insights about the systemic regulation of iron homeostasis and could also explain the different disease susceptibilities among different populations. Among these, immunological

abnormalities have been consistently observed in HH patients, which will be next described in more detail.

Immunological abnormalities in HH

The genetic and biologic context of the hemochromatosis gene, *HFE,* is the MHC complex which is an extended gene cluster of extreme importance by the immunological functions they encode. In fact, HFE was first described as an aberrant MHC Class I like protein, when discovered by Feder et al, in 1996 [27]. The mechanism how could this protein contribute to iron overload was not obvious at all. The first hypothesis advanced at the time was that the protein could interact indirectly through association with components of the immunological system, an idea supported by previous observations by Arosa et al. on the functional interaction between the immunological system and iron metabolism [170].

The postulate that the immunological system could have a role in monitoring tissue iron toxicity, as part of its surveillance function, was first advanced by De Sousa in 1978, based on her observations on lymphocyte traffic and positioning [2]. It was implicit in that postulate that the adaptive system and its circulating components participate in the recognition and binding of metals as a protective device against metal toxicity and the preferential use of indispensable metals such as iron or zinc by bacteria or transformed cells. This motivated a series of studies of lymphocytes expression and function in hemochromatosis patients. Both these and further studies in animal models contributed to support and strengthen the notion of an inextricable link between iron and the immunological system.

The finding of abnormalities in the relative proportions of the two major T lymphocytes populations (CD4$^+$ and CD8$^+$ T cells) in HH patients [21], and the observation of an iron overload similar to HH in the β2m knockout mice lacking MHC class I and CD8 T lymphocytes preceded the discovery of HH gene [23]. Reimão and co-workers had shown that patients with high CD4/CD8 rations (>2.9) display a faster re-entry of iron into the serum transferrin pool after intensive phlebotomy treatment, reaching abnormal transferrin saturation values (>60%) more rapidly than patients with normal CD4/CD8 rations (approximately 1) [21]. A significantly inverse correlation was found with the numbers of CD8$^+$ T cells, and not with CD4$^+$ T cells, and the amount of iron mobilized by phlebotomy treatment [22, 30]. These CD4/CD8 rations and the relative or absolute numbers of CD4$^+$ and CD8$^+$ T-cell populations were not altered by the treatment [22, 32]. In 2001, those low numbers of peripheral CD8$^+$ T cells were also associated with low number of those cells in the liver, being directly associated with the iron hepatic tissue amount [33]. Other groups recapitulated these findings namely the low CD8$^+$ T cell numbers associations with certain

HLA haplotypes and with a more severe iron overload [171]. Functional specific abnormalities have been previously described in CD8^{+} T lymphocytes from HH patients namely, a defective lymphocyte-specific tyrosine kinase (p56lck) activity, decreased cytotoxic activity, an increased number of CD8^{+} T cells lacking CD28 co-stimulatory molecule and an high percentage of cells in an activated state (HLA-DR^{+}) [29, 152, 170]. The reduction of CD8^{+}CD28^{+} expressing cells in HH patients was inversely correlated with transferrin saturation, which does not rule out the role of circulating iron as a modulator of T cell profiling [172]. But the HFE itself could also influence T cell homeostasis by acting over the MHC-I antigen presentation pathway. In 2005, Rohrlich et al described that HFE deletion in mice is associated with a decreased number of T cells expressing αV6 TCRs [173]. Also, by using transgenic mice they observed a direct cytolytic recognition for human HFE by mouse TCR, which occurs independently of HFE-bound peptides. These observations are in agreement with the previous finding that TCR-delta knockout mice develop hepatic iron overload, suggesting that cellular iron status might be transmitted to lymphocytes through HFE engagement with TCR [174]. This p.C282Y mutation is known to prevent HFE association with β2m leading to the accumulation of the misfolded protein in the endothelial reticulum (ER) with consequent induction of an unfold protein response (UPR).This UPR activation results in a significant down-regulation of MHC-I cell surface expression [175]. Moreover, inhibition of the ER stress response in cells expressing the HFE p.C282Y mutant protein leads to the restoration of MHC-I levels [176]. These observations point to an effect of the p.C282Y mutation in the HFE gene beyond the strict iron regulation and suggest the importance of HFE at the interplay between the two systems of iron homeostasis and immune responses.

Iron and lymphocytes: evidence from the immune deficient mouse models

A good insight into the question of the impact of immune cell abnormalities on iron homeostasis is given by animal models. The first hereditary hemochromatosis animal model preceded the discovery of the HH gene. It was described by De Sousa et al. when they demonstrated that *β2m*[(-/-)] deficient mice, that are almost depleted in CD8^{+} T cells due to a severe decrease in the expression of MHC-Class I molecules, develop a severe hepatic iron overload phenotype mainly observed in liver parenchyma cells, without accumulation in kupffer cells [23]. Moreover, *β2m*[(-/-)] mice were not able to reduce intestinal iron absorption in response to an iron overload condition and displayed an abnormally high transferrin saturation values (>80%) recapitulating the human model of HH [24]. After the discovery of the non-classical MHC-class I *HFE* gene, the knockout mouse was generated confirming

that the *Hfe*[(-/-)] mice display liver iron deposition, and increased TfSat mainly due to an increase in iron absorption. The knock in mice for the p.C282Y mutation were shown to display a less severe phenotype liver iron phenotype than the *Hfe*[(-/-)] and even less iron deposition when in compound heterozygosity with the p.H63D mutation [177]. Moreover, the *Hfe*[(-/-)] mice do not show any immunological abnormality in terms of lymphocyte numbers. In order to address the synergistic effect of HFE and MHC-class I dependent lymphocyte defects, the knockout mice for mature lymphocytes was generated by depletion of the recombination activating gene 1 (*Rag1*). Multiple combinations of gene defects provide evidence that, , although the absence of lymphocytes alone does not predispose to an iron overload phenotype [174], the lack of both *Hfe* and lymphocytes (*Hfe*[(-/-)]*Rag*[(-/-)] and *β2m*[(-/-)] *Rag*[(-/-)]), led to a more severe liver iron phenotype with the last model showing a specific deposition of iron in the heart and pancreas [28, 35]. These mice models constituted important support to strengthen earlier clinical observations in HH patients where lymphocytes act as modifiers of the primary iron overload condition.

Chapter 2

Background, aims and outline of the thesis

Background

Hereditary Hemochromatosis (HH) is the most common genetic disorder of iron overload [178]. Most HH patients are homozygous for the p.C282Y mutation in the HFE protein, encoded by *HFE*, a non-classical MHC-class I gene located at position 6p21.3, near the HLA locus [179]. The exact mechanism underlying the involvement of HFE in HH is still not clarified.

Immunological abnormalities have been consistently described in HH in association with the iron overload phenotype, particularly in the number of peripheral blood CD8+ T lymphocytes [30, 33, 180]. There is presently strong evidence that the numbers of CD8$^+$T lymphocytes are genetically transmitted in association with genes at the MHC-class I region. [41-43, 181]. The question remains if a putative MHC-class I-linked gene involved in the setting of CD8$^+$T lymphocyte numbers is an important modifier of the clinical expression in HH.

The mechanism(s) underlying the participation of lymphocytes in iron homeostasis remain mostly unknown. A recent study using human peripheral blood lymphocytes revealed that these cells are able to sense elemental iron and respond by modulating the expression of the central effector protein in iron metabolism: hepcidin [40]. However, it is not known what is the modifier effect of lymphocytes in systemic iron homeostasis and whether there are abnormalities in lymphocyte gene expression/regulation in HH. Also, a complete lack of information exists on the involvement of other lymphocyte proteins in iron cellular/systemic homeostasis as well as on the iron handling capabilities of these cells.

Aims and outline of the thesis

The general objective of this thesis is to clarify the role of lymphocytes in iron homeostasis, using Hereditary Hemochromatosis (HH) as a model. With this approach it is expected that the work will contribute to elucidate (1) the genetic contribution of the MHC-class I region to the setting of lymphocyte numbers and (2) the mechanisms how lymphocytes may act as modifiers of the clinical expression in HH.

The specific objectives of the thesis are:

1. **To evaluate the predictive value of MHC markers known to be associated with CD8 T cells numbers in Portuguese HH patients**

   The inheritance of certain HLA alleles are known to be associated with the genetic transmission of lower numbers CD8$^+$ T lymphocytes as also a SNP microhaplotype

named A-A-T, was recently found to be associated with a more severe phenotype and also with the "low CD8 phenotype" in HH Portuguese population [44]. We present the results of a genomic approach analysing the MHC genetic region and its association with the CD8$^+$ T-cell phenotype in HH patients. More specifically, in **Chapter 3.1** we aimed to test whether the predictive value of the A-A-T microhaplotype remains in other populations' settings. For that purpose, we analysed HH patients from 3 geographically distant populations (Porto, Portugal; Alabama, USA and Nord-Trøndelag, Norway), where the A-A-T extended haplotypes were determined and the association with CD8$^+$ T-lymphocyte numbers was evaluated.

2. **To refine the genetic region between *HFE* and *HLA-B* in HH patients and controls**
   In **Chapter 3.2** we aimed to better characterize the *HLA-HFE* haplotype structure of the HH Portuguese patients by performing a high density mapping with coverage of 63 SNPs markers within this region. With this approach we were able to gain a better insight into the recombination history and founder effects of HH associated haplotypes in our population, as well as their association with the "low CD8 phenotype".

3. **Evaluate the *in vitro* cellular response of lymphocytes and monocytes to changes in non-transferrin-bound iron (NTBI) in HH patients versus normal healthy blood donors.**
   As one of the major cellular components of peripheral blood, T lymphocytes can be exposed to circulating NTBI and have been for a long time proposed to act as a first physiological barrier against iron-mediated toxicity in situations of systemic iron overload [179]. Until now little was known about the capacity of T lymphocytes to take up NTBI. In **Chapter 3.3** we aimed to address the ability of CD8$^+$ T lymphocytes to store iron acquired as NTBI. For that purpose we performed *in vitro* studies addressing the kinetics of NTBI uptake (Results 1) and export (Results 3) by human CD8$^+$ T lymphocytes after exposure to iron citrate. The hypothesis that CD8$^+$ T cells may act as NTBI "buffers" and modify the disease outcome was tested by comparing NTBI retention ability by CD8$^+$ T cells isolated from peripheral blood of HH patients and normal subjects (blood donors) (Results 4).

4. **Characterize the response of CD8 T lymphocytes to iron overload in terms of gene expression, using a wide-genome Affymetrix microarray approach.**
   In **Chapter 3.4** we aimed to address the transcriptional profile of peripheral CD8$^+$ T cells in the biological context of *Hfe* absence. To avoid the MHC genetic diversity found in patients, we first looked in the HH mouse model (*Hfe*$^{-/-}$) which has a homogenous genetic

background. Using a wide-genome microarray approach, we addressed the transcriptional response of CD8$^+$ T lymphocytes from the HH mouse model and the respective genetic background control (C57BL/6) and compared them either in iron normal conditions and after induce systemic iron overload by an iron-rich diet. The results obtained in the HH mice model, were further tested in the human disease context by analysing the most differently expressed genes found in the *Hfe*$^{-/-}$ context in human CD8$^+$ T cells isolated from HH patients and normal subjects.

Chapter 2

Chapter 3

Results

3.1   **Effects of highly conserved major histocompatibility complex (MHC) extended haplotypes on iron and low CD8$^+$ T lymphocyte phenotypes in HFE C282Y homozygous hemochromatosis patients from three geographically distant areas**

3.2   **High-density mapping of the genomic region between *HFE* and *HLA*-B in Hereditary Hemochromatosis: is there a selective recombination suppression of the classical ancestral?**

3.3   **In vitro response of T lymphocytes to iron and how they may act as modifiers of the clinical expression in HH**

3.4   **Lymphocyte gene expression signatures from patients and mouse models of hereditary hemochromatosis reveal a function of HFE as a negative regulator of CD8$^+$ T-lymphocyte activation and differentiation in vivo**

3.1

Effects of highly conserved major histocompatibility complex (MHC) extended haplotypes on iron and low CD8+ T lymphocyte phenotypes in HFE C282Y homozygous hemochromatosis patients from three geographically distant areas

Content

Abstract

Introduction

Methods

Results

1. **Clinical heterogeneity among the HH populations from Porto, Alabama and Nord-Trøndelag**
2. **Analysis of genetic markers between *HFE* and *HLA-B* in the HH populations from Porto, Alabama and Nord-Trøndelag**
3. **Haplotype conservation in HH patients from Porto, Alabama and Nord-Trøndelag**
4. **Associations of the CD8^{+} T lymphocyte phenotype with MHC markers in HH patients**
5. **Associations of the iron phenotype with MHC markers in HH patients**

Discussion

Concluding remarks

Supplementary data

Abstract

Hereditary Hemochromatosis (HH) is a recessively inherited disorder of iron overload occurring commonly in subjects homozygous for the C282Y mutation in *HFE* gene localized on chromosome 6p21.3 in linkage disequilibrium with the human leukocyte antigen (HLA)-A locus. Although its genetic homogeneity, the phenotypic expression is variable suggesting the presence of modifying factors. One such genetic factor, a SNP microhaplotype named A-A-T, was recently found to be associated with a more severe phenotype and also with low CD8 $^+$T-lymphocyte numbers. The present study aimed to test whether the predictive value of the A-A-T microhaplotype remained in other population settings.

In this study of 304 HH patients from 3 geographically distant populations (Porto, Portugal 65; Alabama, USA 57; Nord-Trøndelag, Norway 182), the extended haplotypes involving A-A-T were studied in 608 chromosomes and the CD8$^+$ T-lymphocyte numbers were determined in all subjects. Patients from Porto had a more severe phenotype than those from other settings. Patients with A-A-T seemed on average to have greater iron stores (p=0.021), but significant differences were not confirmed in the 3 separate populations. Low CD8$^+$ T-lymphocytes were associated with HLA-A*03-A-A-T in Porto and Alabama patients but not in the greater series from Nord-Trøndelag.

Although A-A-T may signal a more severe iron phenotype, this study was unable to prove such an association in all population settings, precluding its use as a universal predictive marker of iron overload in HH. Interestingly, the association between A-A-T and CD8$^+$ T-lymphocytes, which was confirmed in Porto and Alabama patients, was not observed in Nord-Trøndelag patients, showing that common HLA haplotypes like A*01-B*08 or A*03-B*07 segregating with HFE/C282Y in the three populations may carry different messages. These findings further strengthen the relevance of HH as a good disease model to search for novel candidate loci associated with the genetic transmission of CD8$^+$ T-lymphocyte numbers.

Keywords: Hereditary Hemochromatosis, *HFE*, MHC, CD8$^+$ T lymphocytes, Iron, C282Y

Introduction

The major histocompatibility complex (MHC) region on chromosome 6p21.3 constitutes the most dense gene region of the human genome. It has been estimated that 40% of classical MHC genes are expressed in the immune system [182]. These genes are physically clustered, possibly reflecting functional relationships, and are characterized by high polymorphism levels and strong linkage disequilibrium. These characteristics make the MHC region a paradigm in many aspects of genomic research, particularly in disease association studies. Genetic variation in the MHC is associated with more disorders than any other genomic region, the majority of which are immune-related. Nevertheless, fine mapping of those disease associations and the identification of specific functional variants remain difficult. Both structural and regulatory variants are important in disease associations and may operate in tandem [182].

A classic example of disease association with extreme linkage disequilibrium at the MHC region is Hereditary Hemochromatosis (HH), an autosomal recessive disorder of primary iron overload characteristically found in Caucasians and associated with homozygosity for the *HFE* p.Cys282Tyr mutation (C282Y) in the vast majority of cases. *HFE* encodes a non-classical MHC class-I molecule and is localized 4Mb telomeric to *HLA-A* [27], in very strong association with an ancestral haplotype carrying the human leukocyte antigen (HLA) antigens A*03 and B*07 [183, 184]. By applying several types of linkage-disequilibrium calculations to analyze the HH locus, Ajioka and co-workers found very high disequilibrium values over a large region from 150 kb centromeric to 5 Mb telomeric of *HLA-A*, partly due to an unusual low recombination rate of approximately 28% of the expected value [185]. In the same study, a haplotype phylogeny for HH chromosomes suggested that the origin of *HFE* C282Y is recent. These observations also provided a plausible explanation for previous difficulties in localizing the HH gene [186, 187].

Despite the genetic homogeneity at *HFE* among HH patients, their iron phenotypes are highly variable. Consequently, possible environmental and genetic modifiers of iron phenotypes in hemochromatosis have been intensively investigated. Among others, genes within the MHC class I region, inherited in linkage with the ancestral C282Y-containing haplotype, have been implicated in the clinical heterogeneity of *HFE*-associated HH [188]. However, conflicting results obtained by different authors have still not solved this question. Earlier independent studies in geographically different populations have shown that the number of copies of the common ancestral haplotype HLA-A*03-B*07 was associated with the expression of iron phenotypes. Patients with two copies of the ancestral haplotype were shown to have more severe iron overload phenotypes than those with one or no copy of the ancestral haplotype in studies performed in Australia, Italy and Alabama, USA [189-192].

Moreover, Pratiwi *et al*. showed by extended linkage disequilibrium analysis in patients from Australia that there are two distinct peaks of association separated by 2 Mb in the region of *HFE*, a pattern not expected for a single gene disorder [193]. This suggested that a gene modifying the phenotype of C282Y homozygotes could be localized around the area of D6S105. More recent studies did not support the previous observations [194-197]. In a review of the origin and spread of the hemochromatosis mutation, Distante and co-workers [194] reported that although associations of HLA haplotypes with the severity of iron overload were described, no such relationship was found in patients from the UK (R.Raha-Chowdhury, A. Bomford and M. Worwood, unpublished data). In another study of 8 HH families from Britanny, France, Sachot and co-workers analyzed C282Y homozygous relatives with no clinical signs of the iron overload in comparison to the respective probands who had abnormal iron phenotypes. They found no evidence that either *HFE* polymorphisms or variants in 10 microsatellite markers surrounding *HFE* could explain phenotypic variability in the respective kinships [195]. Barton and co-workers extended their study of genotype/phenotype correlations to a population of 141 C282Y homozygous probands from Alabama, USA, and did not reproduce the previous observations that were based on a relatively small number of probands [196]. Finally, in a study of HLA haplotypes of HH patients in a rural population from a former Norwegian province in Central Sweden, Olsson and co-workers could not find an association of the HLA-A*03 with the iron phenotype. Interestingly however, they found that males with double copies of the very common A*01-B*08 haplotype expressed a milder phenotype, supporting again an association of iron overload with the MHC region, but in the setting of a different haplotype [197].

Altogether the above described studies demonstrate that associations between the HH phenotype and the classical HLA markers vary among different cohorts from geographically distinct populations (who naturally diverge due to genetic drift or recombination events) and point to the necessity to look for novel markers at the MHC region that may help explaining the phenotypic variability in HH patients. One such factor could be a new 500 kb microhaplotype localized between *HFE* and the *HLA-A* locus as described by Cruz and co-workers [44]. This haplotype was associated with a more severe phenotype in its carriers and also with low CD8^{+} T lymphocyte numbers, which in previous studies from Portugal have predicted a more severe iron overload [21, 22, 30, 32]. Low lymphocyte numbers were also associated with a more severe phenotype in patients from Alabama in particular those with HLA-A*01-B*08 [171]. However, this same haplotype reported in a former Norwegian province seemed to be associated with a milder phenotype [197]. Unfortunately, no data are available regarding CD8^{+} T lymphocyte numbers in this population from Central Sweden.

In the present study we sought to test whether the predicting value of the microhaplotype described by Cruz *et al.* [44] could be reproduced in other settings, i.e., in different populations from geographically distant regions. In this context, we explored the degree of conservation of the reported HH-associated haplotypes in relation to their effect on the low CD8$^+$ T lymphocyte phenotype or the clinical expression of iron overload. Our data indicate that although the same haplotypes are observed in distant geographical regions, their relative frequencies are variable, which may explain differences in genotype/phenotype associations among different populations.

Methods

Ethics Statement

The study was approved by the Ethical Committees of Centro Hospitalar do Porto, Porto; Institutional Review Board of Brookwood Medical Center, Alabama and The Regional Committee for Medical and Health Research Ethics, REC Central, Trondheim. Written informed consent was obtained from participants according to the Helsinki declaration.

Study Populations & clinical data

Three different populations of Hereditary Hemochromatosis patients from geographically distant regions were included in this study. The only inclusion criteria for the purpose of the study were the confirmation of homozygosity for the C282Y *HFE* mutation and to be an adult, because the CD8$^+$ T lymphocyte phenotype is stable in adults. The first group included 65 unselected, unrelated HH patients from the north of Portugal, mainly from the Porto district area, consecutively identified between 1985 and 2011 in non-screening settings and regularly followed up at the Hemochromatosis Outpatient Clinic of Santo António Hospital, Porto and Predictive and Preventive Genetic Centre, Porto. This group of patients is designated as Porto patients. The second group of patients included 57 unrelated HH patients diagnosed in non-screening settings from central Alabama, USA, diagnosed between 1988 and 2010 and treated at Southern Iron Disorders Center, Birmingham, Alabama. These probands were selected for the present study only because they presented for diagnosis or treatment in a consecutive mode. This group of patients is designated as Alabama patients. The third group of patients included 182 patients from the Nord-Trøndelag County, Norway, who were diagnosed with HH as part of a population screening study (HUNT2) between 1995 and 1997, and were followed up at St. Olav Hospital, Trondheim. This group of patients is designated as Nord-Trøndelag patients. Most of the clinical and laboratory information about all patients were already available and described elsewhere [41, 43, 44, 188, 198-200]. Previously available information included, in all patients, the iron parameters at diagnosis: transferrin saturation (TfSat) and serum ferritin (SF); *HFE* genotype (all homozygous for the C282Y mutation); and *HLA* class I alleles (A and B) as determined by low-resolution DNA-based techniques (PCR/sequence-specific oligonucleotide probes, Dynal RELI™ SSO, Dynal Biotech Ltd, UK). Values of total body iron stores (TBIS) estimated by quantitative phlebotomies were available from 104 patients (34 from Porto, 32 from Alabama and 38 from Nord-Trøndelag).

Immunophenotyping

Blood counts of T-CD8$^+$ lymphocyte subpopulation were available for all study participants. T-lymphocyte subpopulations were determined by FACS analysis using anti-CD3 and anti-CD8 monoclonal antibodies as previously described in detail [41]. We defined as a "low CD8 phenotype" the finding of CD8$^+$ T lymphocyte numbers below the 25% percentile in controls. This value was 310x10^3/ml in Porto and Alabama patients and 319x10^3/ml for Nord-Trøndelag patients. Mean values (± standard deviation) in controls were 433(±168) x10^3/ml in Porto and Alabama and 490(±234) x10^3/ml in Nord-Trøndelag.

Genetic markers at the MHC region

In addition to *HFE* and *HLA* genotyping, genetic information on three single nucleotide polymorphisms (SNPs) localized in the region between *HFE* and *HLA-A* was obtained in all patients included in this study. These SNPs were localized in the genes: piggyBac transposable element derived 1 (*PGBD1, rs1997660*), zinc finger protein 193 (*ZNF193, rs7206*) and zinc finger protein 165 (*ZNF165, rs203878*), and defined a SNP microhaplotype of 500 kilobases (kb). These were the SNP microhaplotypes previously described in Porto patients [44] and were determined "de novo" in patients from Alabama by gene sequencing as described in [44] and in patients from Nord-Trøndelag by hybridization probe melting curve analysis on the LightCycler®, Roche Diagnostics. Details on primer and probe sequences in addition to PCR conditions for SNP analysis can be provided by request.

Generation of phased chromosomes and haplotype construction

HLA A-B haplotypes, and the SNP microhaplotypes defined by the genes *PGBD1, ZNF193* and *ZNF165,* were defined in HH patients by family segregation whenever informative family members were available. Otherwise they were inferred by the PHASE program.

Statistical methods

Associations of *HLA* alleles and haplotypes in chromosomes carrying the C282Y mutation in *HFE* were tested by the Chi-square test by comparison of their frequencies in HH patients from the 3 different regions of Porto, Alabama and Nord-Trøndelag with those of the respective reference normal populations. For the purpose of statistical analysis, only alleles or haplotypes with frequencies respectively higher than 10% and 7% in any of the tested population were considered. Information about HLA allele and haplotype reference frequencies in the normal populations from Porto (north Portugal) was obtained at the "Allele*Frequencies in worldwide populations" database. Frequencies for the Alabama control population were reviewed from the data previously analyzed by Barton and co-

workers [198]. Frequencies in the non-Sami population from Norway were obtained from the data described by Harbo *et al.* 2009 [201], also published at the "Allele*Frequencies in worldwide populations" database [202]. In order to eliminate the artificially lowered frequencies in HH chromosomes of other alleles and haplotypes that were due to the relatively high frequencies of alleles A*03 and B*07 and the haplotype A*03-B*07, we estimated (in patients and respective controls) "corrected" allele and haplotype frequencies by subtracting from the denominator respectively the sum of A*03 and B*07 alleles or the number of A*03-B*07 haplotypes. These corrected frequencies allowed a more meaningful comparison between frequencies in HH and control chromosomes, as originally described by Marcel Simon and co-workers [184]. To analyze the relative strength of HLA allele or haplotype associations, the etiological fraction delta (δ) was calculated as described according to the formula $\delta=(FAD-FAP)/(1-FAP)$ where FAD is the allele frequency in HH chromosomes and FAP the allele frequency in control chromosomes [203-205]. In the case of multiple comparisons we used the Bonferroni correction to test for the significance of differences.

To investigate the association of $CD8^+$ T lymphocyte numbers with particular genotypes, we assigned to each chromosome the value of $CD8^+$ T lymphocytes of the respective carrier. Differences in mean $CD8^+$ T lymphocyte values among groups were tested by the Student's T-test or the One-Way analysis of variance (ANOVA) as appropriate. In addition, patients with $CD8^+$ T lymphocyte numbers below the 25% percentile of the respective controls were selected and their chromosomes assigned as "low CD8 phenotype" cases. Differences in the relative frequencies of "low CD8 phenotype" cases among groups were tested by the Chi-square test.

Quantitative measures of iron parameters were also compared among the 3 populations of HH patients from Porto, Alabama and Nord-Trøndelag. Because of skewness in the distribution of serum ferritin and total body iron stores, for statistical purposes the logarithmic transformation was applied to those values. For representation in table and figure, however, the non-transformed values were used. Differences in means among groups were tested by One-Way analysis of variance (ANOVA) or the Student's T-test as appropriate.

Data were analyzed by Statgraphics software (Statgraphics Graphics System, version 7.0). Values of *P* <0.05 were defined as significant.

Results

1 - Clinical heterogeneity among the HH populations from Porto, Alabama and Nord-Trøndelag

A summary of the iron-related parameters of the HH patients from Porto, Alabama and Nord-Trøndelag is provided in Table 1, where values are given according to gender. Significant differences among the 3 populations of patients were observed in males for TfSat, SF, and TBIS, with P values < 0.00001 in all cases. These differences were explained by a more severe expression in patients from Porto and a milder expression in Nord-Trøndelag patients. In females, SF (P<0.00001) and TBIS (P<0.04) were also significantly different among the 3 populations, with Porto and Nord-Trøndelag patients having respectively the highest and lowest values. The HH cohort from Nord-Trøndelag was the only one in which patients were identified in screening programs. Moreover, previous studies in the same population showed that, in general, Nord-Trøndelag patients have a low prevalence of clinical symptoms and less severe iron overload [199, 200].

Table 1 Iron parameters (at diagnosis) in HH patients from Porto, Alabama and Nord-Trøndelag

	N	TfSat (%)	SF (ng/ml)	TBIS (g)
HH male patients from:				
Porto	43	90 ± 14 (63-123)	1750 ± 295 (163-7685)	7.93 ± 0.78 (2.19-17.40)
Alabama	32	73 ± 17 (41-100)	815 ± 82 (123-2119)	3.66 ± 0.50 (0.40-10.40)
Nord-Trøndelag	103	81 ± 9 (58-100)	541 ± 63 (27-3511)	3.23 ± 0.47 (1.12-15.32)
P value		*<0.00001*	*<0.00001*	*<0.00001*
HH female patients from:				
Porto	22	81 ± 18 (55-111)	543 ± 286 (67-3954)	3.20 ± 1.33 (1.10-13.80)
Alabama	25	74 ± 20 28-100)	433 ± 78 (65-1892)	1.93 ± 0.27 (0.40-5.60)
Nord-Trøndelag	79	73 ± 12 (51-97)	172 ± 27 (16-1151)	1.65 ± 0.30 (0.89-4.32)
P value		*n.s.*	*<0.00001*	*0.040*

Transferrin saturation (TfSat) is presented as arithmetic mean ± standard deviation; serum ferritin (SF) and total body iron stores (TBIS) are presented as geometric mean ± standard error. Minimum-maximum values are in parenthesis. TBIS was available in 34 males from Porto, 32 from Alabama and 38 from Nord-Trøndelag and in 13 females from Porto, 23 from Alabama and 12 from Nord-Trøndelag. Statistically significant differences (*P value indicated*) were tested among groups using One-way Anova.

2 - Analysis of genetic markers between *HFE* and *HLA-B* in the HH populations from Porto, Alabama and Nord-Trøndelag

From the study of 304 HH patients with C282Y homozygosity from three geographically distant regions, namely Porto, Portugal (n=65), Alabama, USA (n=57) and Nord-Trøndelag, Norway (n=182), we obtained respectively 130, 114 and 364 chromosomes carrying *HFE* C282Y. These were genetically characterized with 5 different markers including *HLA-A* alleles, *HLA-B* alleles, and SNPs in the genes *PGBD1, ZNF193* and *ZNF165*. HLA A-B haplotypes and SNP microhaplotypes were assigned by family segregation, or generated by PHASE in patients without available informative family members (see Methods).

HLA-A and HLA-B allele frequencies were first analyzed in HH chromosomes from the three populations. Results are summarized in Table 2 (uncorrected data are shown in Table S1). As expected from all previously published studies of HLA associations in HH, the most common HLA-A and B alleles in chromosomes from all the three HH populations from Porto, Alabama and Nord-Trøndelag were A*03 (respectively 0.408, 0.474 and 0.420) and B*07 (respectively 0.238, 0.307 and 0.288); these frequencies were significantly different from those of the corresponding controls (Table 2). The strength of these significant associations was measured by estimating the etiological fraction delta (see Methods) being similar in all populations (Table 2). After correcting for the strong effect of A*03 and B*07 on other allele frequencies (see Methods), other significantly associated HLA alleles were found in the populations from Porto (A*01, B*08 and B*40) and Nord-Trøndelag (A*11, B*14 and B*44). In Alabama patients, the only additional HLA allele with a statistically significant association was B*14, suggesting that Alabama patients represent a genetically more conserved population.

The most prevalent HLA A-B haplotype in the three populations from Porto, Alabama and Nord-Trøndelag was A*03-B*07, the proportion of its carriers being 0.169, 0.272 and 0.214, respectively (see also Table 2). Although these haplotype frequencies do not differ statistically among the different populations (shown in Supplementary Table 1), the strength of their associations to HH, as measured by the etiological fraction delta, is stronger in Alabama (δ=0.247) than in Nord-Trøndelag (δ=0.164) or Porto (δ=0.158), suggesting a more recent founder effect in Alabama HH patients. This interpretation is also consistent with our observation that the prevalence of HLA-A and -B alleles and haplotypes is less diverse in Alabama patients than in Porto or Nord-Trøndelag patients. After we corrected for the predominance of A*03-B*07 haplotypes on other haplotype frequencies (see Methods), the next most common HLA haplotype found in patients from all populations was A*01-B*08, although the respective frequencies of A*01-B*08 did not differ significantly from those in the respective control populations. The A*03-B*14 haplotype also occurred in hemochromatosis chromosomes from Alabama and Nord-Trøndelag patients. The significance of this

association could be defined only in the Alabama population due to lack of sufficient available information about control subjects in Porto and Nord-Trøndelag. Nevertheless, its significance might be supported by the very low frequencies found in controls from Scandinavia [206]. The haplotype A*02-B*44, a very common haplotype in normal Caucasian populations, was found at similar frequencies in all non-A*03-B*07-carrying chromosomes from the three present populations. These respective frequencies did not differ significantly from those in the respective control subjects.

We next analyzed the SNP microhaplotypes defined by the SNPs in the genes *PGBD1, ZNF193* and *ZNF165* in the three populations (results shown in Table S1). Previous studies in HH patients had revealed that the most conserved of these SNP microhaplotypes was the one designated as A-A-T and that this microhaplotype is also transmitted in association with a more severe iron phenotype of HH [44]. This microhaplotype was the most prevalent in all the populations studied here but its relative frequency differed significantly among them (P=0.0003). Porto patients had the highest A-A-T frequency (0.908) and Nord-Trøndelag patients the lowest (0.765). Among the non-A-A-T SNP microhaplotypes, the most common was G-G-G, the frequency of which also differed significantly among the three populations (P=0.003). G-G-G frequency was highest in Nord-Trøndelag patients (0.160) and lowest in Porto patients (0.062).

In summary, the observation of differences in the relative frequencies of the described HLA and SNP markers among the three geographically distant populations of HH patients support the postulate that evolutionary histories among populations differ due to differences in genetic drift and recombination of the HH founder chromosomes in the respective geographic regions.

Table 2 HLA allele and haplotype associations in *HFE* C282Y carrying chromosomes of HH patients from three populations

HLA-	Porto HH Patients (n=130 chromosomes)	Controls* (n=15874 chromosomes)	P value	δ	Alabama HH Patients (n=114 chromosomes)	Controls* (n=830 chromosomes)	P value	δ	Nord-Trøndelag HH Patients (n=364 chromosomes)	Controls* (n=1152 chromosomes)	P value	δ
	allele frequency		*P value*	*δ*	*allele frequency*		*P value*	*δ*	*allele frequency*		*P value*	*δ*
A*03	0.408	0.101	0.000	0.330	0.474	0.166	0.000	0.369	0.420	0.155	0.000	0.310
B*07	0.238	0.060	0.000	0.180	0.307	0.130	0.000	0.203	0.288	0.148	0.000	0.160
	*corrected allele frequency**				*corrected allele frequency**				*corrected allele frequency**			
A*01	0.208	0.124	0.026	0.096	0.283	0.214	ns		0.223	0.180	ns	
A*02	0.299	0.295	ns		0.300	0.328	ns		0.360	0.406	ns	
A*11	0.052	0.078	ns		0.067	0.068	ns		0.137	0.052	0.000	0.090
A*24	0.065	0.117	ns		0.067	0.082	ns		0.100	0.061	ns	
B*08	0.131	0.079	0.053	0.057	0.165	0.152	ns		0.127	0.143	ns	
B*14	0.051	0.072	ns		0.139	0.040	0.0001	0.103	0.100	0.032	0.000	0.071
B*15	0.020	0.061	ns		0.025	0.005	ns		0.085	0.130	ns	
B*35	0.162	0.126	ns		0.051	0.094	ns		0.077	0.107	ns	
B*40	0.101	0.035	0.000	0.068	0.013	0.014	ns		0.135	0.132	ns	
B*44	0.162	0.162	ns		0.203	0.163	ns		0.228	0.159	0.000	0.082
	haplotype frequency				*haplotype frequency*				*haplotype frequency*			
A*03B*07	0.169	0.013	0.000	0.158	0.272	0.033	0.000	0.247	0.214	0.060	0.000	0.164
	*corrected haplotype frequency**				*corrected haplotype frequency**				*corrected haplotype frequency**			
A*03B*14	0.019	n.a.			0.096	0.009	0.000	0.089	0.077	n.a.	n.a	
A*01B*08	0.065	0.034	ns		0.108	0.069	ns		0.098	0.096	ns	
A*02B*44	0.037	0.038	ns		0.096	0.062	ns		0.080	0.075	ns	

Comparisons between patients and controls were done using the Chi-square test (*P* values indicated) and the strength of the associations was estimated by the etiological fraction delta (**δ**).

* HLA allele and haplotype frequencies in the controls populations from Porto (north Portugal) were obtained at the "Allele Frequencies in worldwide populations" database (Gonzalez-Galarza *et al*.(2011) Nucleic Acids Res 39:913-919), from Alabama were reviewed from previous data reported by Barton et al. (2002) BMC Med Genet 3:9; and from Norway were obtained in the study by Harbo *et al.* (2009) Tissue Antigens 75:207-217.

** Corrected allele and haplotype frequencies (see Methods) were calculated by subtracting from the denominator, respectively, the sum of A*03 and B*07 alleles and the number of A*03B*07 haplotypes.

n.a.=data not available; ns=not significant.

3 - Haplotype conservation in HH patients from Porto, Alabama and Nord-Trøndelag

We analyzed the degree of haplotype conservation as a measure of their proximity from the ancestral HH founder chromosomes by selecting the HH chromosomes carrying the most commonly associated HLA-A alleles (A*01, A*02 and A*03) and calculating the degree of conservation (%) of the most common SNP microhaplotype A-A-T in those chromosomes. Results are shown in Table 3 and Figure 1. In general, a high degree of conservation was observed in cohorts from Porto, Alabama and Nord-Trøndelag for chromosomes carrying A*03 (respectively 94%, 98% and 97%), including the A*03-B*07-carrying chromosomes (respectively 91%, 100% and 99%). In contrast, significant differences occurred among the three populations regarding the conservation of chromosomes carrying A*01 or A*02 alleles (Table 3).
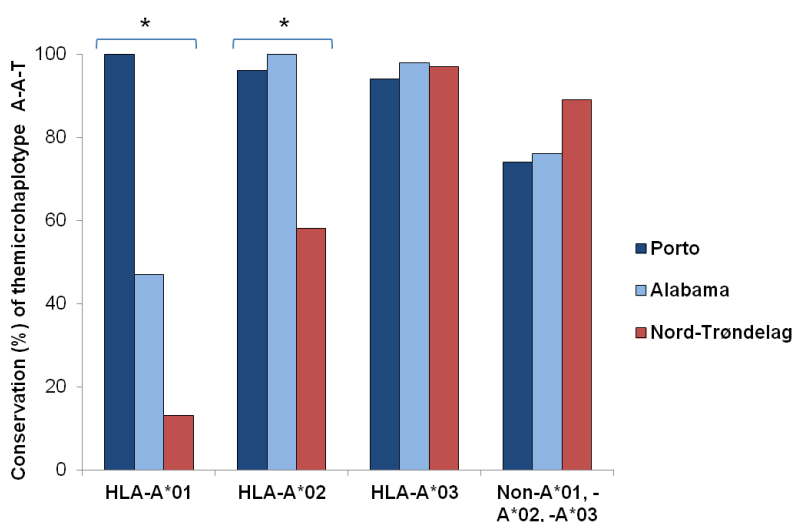
Fig. 1 Conservation (%) of the SNP microhaplotype A-A-T according to HLA-A alleles in chromosomes from HH patients. A comparison of the percent haplotype conservation among the three groups of HH patients from Porto, Alabama and Nord-Trøndelag was done using the Chi-square test and significant results are indicated by a * (P<0.00001)

These differences are illustrated in Figure 1, particularly visible for chromosomes carrying HLA-A*01. In the case of Porto patients, the SNP microhaplotype A-A-T is conserved in all HLA-A*01 carrying chromosomes (16/16), including all HLA-A*01-B*08 carrying chromosomes (7/7). This was not observed in either Alabama or Nord-Trøndelag. In the case of Alabama patients, 53% (9/17) of HLA-A*01-carrying chromosomes (or 56%, 5/9, of A*01-B*08 carrying chromosomes) do not conserve the A-A-T microhaplotype. In Nord-Trøndelag patients, 87% (41/47) of chromosomes carrying HLA-A*01 (or 86%, 25/29, of A*01-B*08 carrying chromosomes) do not conserve the A-A-T microhaplotype. In the Nord-Trøndelag population the A-A-T microhaplotype was not conserved in 42% (32/76) of A*02

carrying chromosomes. In contrast, the percentage of conservation was 96% (22/23) and 100% (18/18) in Porto and Alabama cohorts, respectively.

Table 3 Comparison of the conservation of the SNP microhaplotype A-A-T in chromosomes of HH patients from Porto, Alabama and Nord-Trøndelag

Associated HLA alleles	Associated SNP microhaplotype	Percentage (n) of haplotypes			P^*
		Porto	Alabama	Nord-Trøndelag	
A*01					
	Conserved A-A-T	100% (16)	47% (8)	13% (6)	2.52×10^{-9}
	Non conserved A-A-T	0	53% (9)	87% (41)	
A*02					
	Conserved A-A-T	96% (22)	100% (18)	58% (44)	3.06×10^{-5}
	Non conserved A-A-T	4% (1)	0	42% (32)	
A*03					
	Conserved A-A-T	94% (50)	98% (53)	97% (148)	n.s.
	Non conserved A-A-T	6% (3)	2% (1)	3% (5)	
Non A*01-A*02-A*03					
	Conserved A-A-T	74% (28)	76% (19)	89% (78)	n.s.
	Non conserved A-A-T	26% (10)	24% (6)	11% (10)	

* Relative frequencies of conserved and non-conserved haplotypes among three populations were compared using the Chi-square test (*P values* are indicated).

Taken together, the present results further suggest that the recombination histories or founder effects of the C282Y-carrying HH chromosomes differ in the three hemochromatosis populations studied. This may affect other traits encoded in the same chromosomal region, including determinants of $CD8^+$ T lymphocyte numbers or other putative modifiers of iron overload.

4 - Associations of the $CD8^+$ T lymphocyte phenotype with MHC markers in HH patients

We sought to investigate the association of $CD8^+$ T lymphocyte numbers with particular MHC markers. First, we analyzed the distribution of $CD8^+$ T lymphocyte numbers in the three populations of HH patients, each of whom had C282Y homozygosity. Low $CD8^+$ T lymphocyte numbers were common in patients from each geographic region (Fig. 2), but the distribution of T lymphocyte numbers differed. Patients from Porto and Alabama had a more striking deviation to low numbers than patients from Nord-Trøndelag (Fig. 2).

We then analyzed the associations of the "low CD8 phenotype" with particular extended haplotype combinations among the three different populations. A "low CD8 phenotype" was defined as $CD8^+$ T lymphocyte numbers below the 25% percentile in the respective controls, i.e., $310x10^3$/ml for Porto and Alabama, and $319x10^3$/ml for Nord-Trøndelag (see Methods). The extended haplotype combinations were chosen to reflect the degree of conservation relative to the most common ancestral haplotype, i.e., if the A-A-T microhaplotype was conserved or not and, within A-A-T conserved haplotypes, if HLA-A*03 was conserved or not (Table 4). We estimated the frequencies of "low CD8 phenotype" cases for each haplotype combination. The results, illustrated in Table 4, demonstrate that there are differences among the three populations. The "low CD8 phenotype" was significantly associated with the most conserved haplotypes carrying A-A-T and the HLA-A*03 in the populations from Porto (P=0.045) and Alabama (P=0.012) but not in the population from Nord-Trøndelag. These associations were also reflected on the mean $CD8^+$ T lymphocyte counts. Values in Porto and Alabama patients were significantly lower than the expected values in controls (P=0.0017 and P=0.021, respectively).
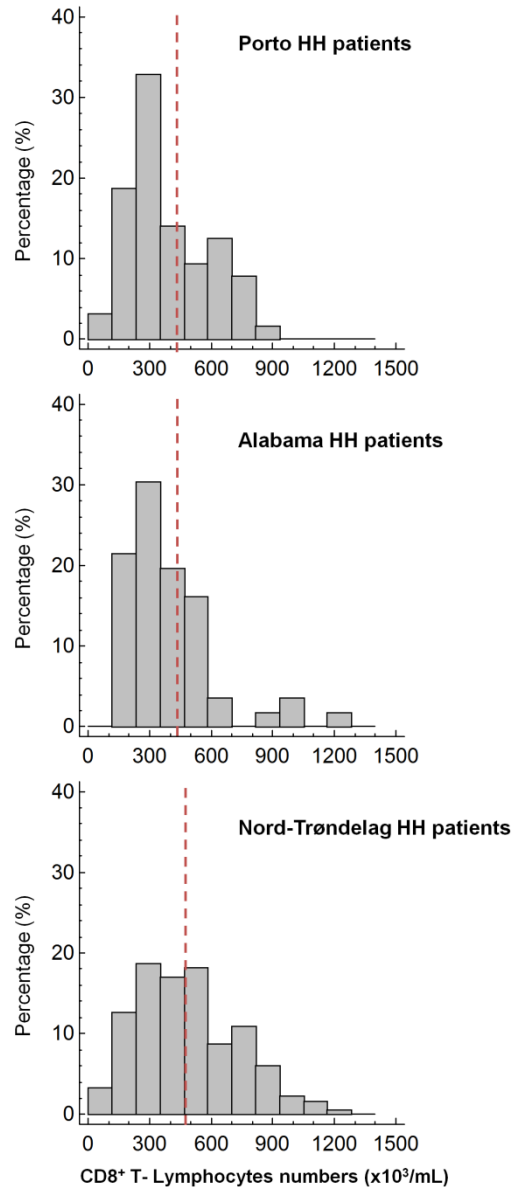

Fig. 2 Distribution of peripheral blood $CD8^+$ T lymphocytes in HH patients from Porto, Alabama and Nord-Trøndelag The dash lines indicate the mean value observed in the respective control populations

Table 4 Correlations between haplotype conservation and the CD8$^+$ T lymphocyte phenotype in chromosomes of HH patients from Porto (n=128), Alabama (n=112) and Nord-Trøndelag (n=362).

Extended haplotype combinations	Relative frequency of the "low CD8 phenotype" in HH patients				Mean (±SD) of CD8+ T lymphocytes(x10^3/ml) in HH patients			
	Porto	**Alabama**	**Nord-Trøndelag**	*P* value	**Porto**	**Alabama**	**Nord-Trøndelag**	*P* value
Conserved-A-A-T With HLA-A*03	44.0% (22/50)*	49.0% (25/51)*	25.7% (38/148)	0.0026	370 ± 179*	369 ± 233*	507 ± 251	0.0001
Conserved-A-A-T Without HLA-A*03	39.4% (26/66)	31.1% (14/45)	38.3% (49/128)**	n.s.	393 ± 194	453 ± 263	458 ± 259	n.s.
Non-conserved-A-A-T	16.7% (2/12)	43.8% (7/16)	31.4% (27/86)	n.s.	540 ± 207	430 ± 331	469 ± 216	n.s.

The percentage (case/total numbers) of patients with CD8$^+$ T lymphocytes below the 25% percentile ("low CD8 phenotype") are indicated followed by the mean (±standard deviation) of CD8$^+$ T lymphocyte counts (x10^3/ml) for each haplotype combination. (*P*) Statistical significant differences among the 3 populations of patients (using the Chi-square test or One-way ANOVA, as appropriate, see M&M). (*) Results significantly lower (p<0.05) than the respective control populations (using the Chi-square test or Student T-test, as appropriate, see M&M). (**) Result significantly lower than the respective control due to a small (n=5) founder group of HLA-A*01 patients. The statistical significance is lost if this group is excluded.

Taken together, the different patterns of association of the "low CD8 phenotype" with particular extended haplotype combinations in the three populations of patients suggest a stronger founder effect in the patients from Porto and Alabama with fewer recombination events between a putative locus marking the "low CD8 phenotype." In patients from Nord-Trøndelag, genotype/phenotype associations were apparently lost.

5 - Associations of the iron phenotype with MHC markers in HH patients

In order to analyze the effect of associated SNP microhaplotypes on the clinical expression of iron overload, HH patients were divided in two groups, according to the presence, in homozygosity, of the ancestral SNP microhaplotype A-A-T. For statistical purposes, males and females were analyzed separately. Results are presented in Table 5 and Figure 3. No significant differences were found in females and no significant differences were found for TfSat in both males and females (Fig.3). In general, the average SF and TBIS values in male patients were significantly higher (respectively *P*=0.027 and *P*=0.021) in those homozygous for the A-A-T microhaplotype than in those carrying one or more non-A-A-T microhaplotype. Even if the average SF and TBIS values in male patients appeared higher in those homozygous for the A-A-T, no significant differences were seen in the 3 separate populations (Table 5).

In conclusion, these results may support a general prediction of a more severe iron phenotypes in patients' populations carrying the conserved A-A-T microhaplotype in

homozygosity, but they also show that, for individual purposes, the microhaplotype A-A-T cannot be used as a universal marker of iron phenotype in HH.
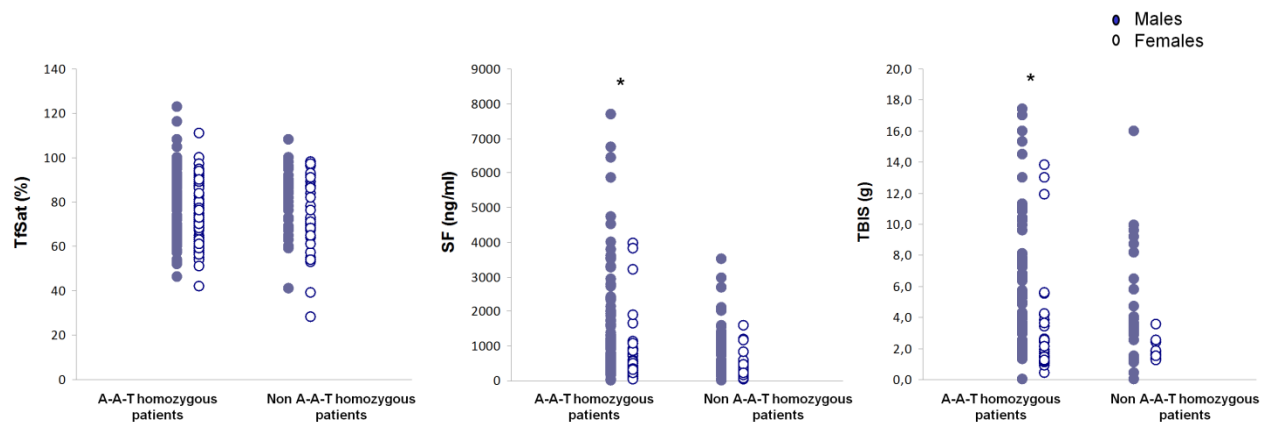
Fig. 3 Effect of the SNP microhaplotypes on the expression of iron overload. Comparisons of the iron parameters: transferrin saturation (TfSat), serum ferritin (SF) and total body iron stores (TBIS) between groups of HH patients divided according to the associated SNP microhaplotypes (A-A-T homozygous or non-A-A-T homozygous). Males are represented by solid circles and females represented by open circles. Significant differences in the mean values (by the Student´s T test) are indicated by an * (P=<0.027).

Table 5 Average values of total body iron stores (TBIS) and serum ferritin (SF) of HH male patients according to the associated SNP microhaplotypes (A-A-T homozygous or non- A-A-T homozygous)

	All HH patients	HH patients from		
		Porto	Alabama	Nord-Trøndelag
Average of TBIS (g) in:				
A-A-T homozygous male patients	**4.98 [4.24-5.85] (n=77)**	8.08 [6.42-10.11] (n=29)	3.83 [3.01-4.88] (n=24)	3.62 [2.75-4.76] (n=24)
Non-A-A-T homozygous male patients	**3.37 [2.43-4.69] (n=27)**	7.11 [3.07-16.48] (n=5)	3.23 [1.34-7.75] (n=8)	2.65[1.87-3.77] (n=14)
*P**	*0.021*	*n.s.*	*n.s.*	*n.s.*
Average of SF (ng/ml) in:				
A-A-T homozygous male patients	**849 [718-1004] (n=124)**	1764 [1296-2400] (n=36)	818 [670-999] (n=24)	571 [461-707] (n=64)
Non-A-A-T homozygous male patients	**602 [470-771] (n=51)**	1652 [576-4737] (n=5)	806 [402-1616] (n=8)	496 [381-646] (n=38)
*P**	*0.027*	*n.s.*	*n.s.*	*n.s.*

TBIS and SF are presented as geometric mean and 95% Confidence Interval for Mean [Lower Bound - Upper Bound]; the numbers of patients in each group (n) are indicated in each case. *(P) Statistical significant differences using the Student´s T- test (with log transformed values, see methods)

Discussion

The question of HLA haplotype conservation in HH has been a focus of scientific interest for a long time, and several interpretations about its role in the recent evolutionary history of chromosomes carrying the C282Y mutation have been largely discussed [183-187, 194, 197, 207, 208]. Besides the well described A*03-B*07 ancestral haplotype [183-187], also the A*01-B*08 haplotype is very long and resistant against recombination, and appears to be derived from a single ancestor [194, 197]. The present study explored the implications of haplotype conservation on HH patient's phenotypes. While not confirming the value of the A-A-T microhaplotype as a universal predictive marker of iron overload in HH, the study revealed important differences in both the genetic composition and the genotype/phenotype correlations among the geographically distant populations which may help explaining differences in phenotype and local penetrance of the disease. The most relevant questions raised by these results were: Why do all A*01-B*08 haplotypes from Porto patients carry the conserved A-A-T microhaplotype, but only 47% in Alabama and 13% in Nord-Trøndelag? Why don't we see an association of the A-A-T microhaplotype with low CD8$^+$ T lymphocytes in the Nord-Trøndelag population, as we observe in Porto and Alabama? Could the selection of "non-conserved" chromosomes in *HFE* C282Y homozygotes may help us in future to identify the individual loci contributing to the "low CD8 phenotype" and/or other novel associated modifiers of iron overload? Could the loss of A-A-T microhaplotype provide the explanation for the mild phenotype of A*01-B*08 carriers in particular populations, such as the one described in a former Norwegian province in Sweden [197]?

In a recent study, Baschal and co-workers analyzed HLA data and genotypes for thousands of SNPs across the MHC complex in a large number of families, demonstrating the occurrence of multiple common "completely" conserved complex SNP haplotypes in the MHC region, several of them influencing disease susceptibility [209]. They suggested that such conservation could also occur in other genomic areas and proposed that this type of analysis of conservation versus sub-conservation of extended haplotypes may be an important tool for further positioning of disease-associated loci. In the present study, we took advantage of the known occurrence of highly conserved MHC-linked haplotypes in patients with HH and its known association with a phenotype of low CD8$^+$ T lymphocyte numbers to study the distribution and composition of the HH-associated chromosomes and explain differences found in genotype/phenotype correlations among three geographically distant populations. Although high frequencies of the low CD8$^+$ T lymphocyte phenotype were found in all HH populations, the pattern of association of this phenotype with particular haplotypes differed among patients from the three geographic regions, possibly reflecting diverse haplotype structures due to different recombination histories or founder effects.

Haplotype heterogeneity among populations

The simple analysis of the distribution of *HLA* associated haplotypes (Table 2), in addition to the degree of conservation of the associated A-A-T SNP microhaplotype (Table 3, Fig. 1) in the three cohorts of patients from Porto, Alabama and Nord-Trøndelag, shows that the strong association of HH with the HLA-A*03-B*07 haplotype is the most consistent observation in all populations studied, confirming the existence of a common ancestral haplotype subsequently modified by recombination and geographical scattering due to migrations [184]. The diversity of associations with other haplotypes reveals differences among populations which agree with the expected differences in the history of their HH-carrying chromosomes, taking into consideration particular founder effects or the time for recombination events. The most stricking differences are observed in chromosomes carrying HLA-A*01 (which include the ancestral HLA-A*01-B*08), in which the SNP microhaplotype A-A-T was conserved in 100% chromosomes of Porto patients, while it was less conserved in patients from Alabama (47%) and much less conserved in or Nord-Trøndelag patients (13%) (see Fig.1), supporting the different founder effects or distinct recombination histories in the respective populations. The highest haplotype diversity observed in the Nord-Trøndelag population is also consistent with the high frequency of *HFE* C282Y in Norwegians [199, 200, 210], possibly related with characteristics of rapid population growth that has occurred in northwestern Europe since the Celtic period [194]. On the contrary, patients from Alabama showed the lowest haplotype diversity, reflecting a more recent founder effect. A previous study showed that aggregate "British Isles" or Scotland indices of ancestry were significantly greater and the proportion of non-British Isles, non-Native American ancestry was significantly lower in Alabama hemochromatosis probands with *HFE* C282Y homozygosity than in population control subjects [211, 212]. These observations suggest that British Isles ancestry likely accounts for the relatively high C282Y allele frequency and association of HLA-A*03-B*07 and *HFE* C282Y in central Alabama whites. Therefore, the evidence of a recent founder effect in Alabama HH patients suggested by the present results agrees with the previous ancestry studies and with the predominance of English people among whites who migrated to and settled the geographic area of the present State of Alabama in the late 18th and early 19th centuries [213, 214]. HLA-A*03-B*14 also occurred in hemochromatosis chromosomes from Alabama and Nord-Trøndelag patients. Although this haplotype is also described as a common HH ancestral haplotype in hemochromatosis populations in many northwestern European countries, particularly in Scandinavia [208], its appearance in Alabama HH patients is unlikely to be attributed predominantly to Norwegian or other Scandinavian founders because ancestry reports from these geographic areas of Europe are rare in Alabama hemochromatosis probands and population control subjects [211]. Nevertheless this haplotype could have a common ancestral Irish origin and be spread in

Norway by the close contacts between Ireland and Scandinavia through the Vickings' movements [207, 208]. In the case of Porto patients, the relative low diversity of HH haplotypes could be attributed to the particular demographic characteristics of the Portuguese population in the north region namely the unipolar mode of migration and the low rate of mobility from other regions [215]. Significant regional differences were previously found in the distribution of the C282Y mutation in Portugal with the highest frequencies found in the north of the country [216]. In terms of historical population settlements, it is well recognized that there is a geographical and cultural boundary between the north and the south of Portugal documented by archeological, ethnographic and linguistic records [215], all favoring the notion that a stronger Celtic influence in the north could map the founder HH chromosomes in this region by the 6th century BC. The hypothesis that the later Nordic/Suevian occupation and settlement, which also occurred only in the north of the present country, could also contribute to the increased frequency of the mutation cannot be excluded. The present results of divergent patterns of haplotype conservation and genotype/phenotype associations in patients from Porto and Nord-Trøndelag do not favor a strong Scandinavian HH founder effect in north Portugal.

Effect of haplotype conservation on the CD8+ T lymphocyte phenotype

It is well known that the existence of different founder effects and different recombination histories at the MHC region affect the transmission of other genetic traits encoded in the same chromosomal region [182].The previously demonstration that CD8+ T lymphocyte numbers are transmitted in association with particular HLA haplotypes in Portuguese HH patients [41, 43] prompt us to analyze if the same association was also observed in the other HH populations. We confirmed that the phenotype of low CD8+ T lymphocytes was commonly observed in each of the three populations, but their respective distributions (Fig. 2) and their genotype/phenotype correlations (Table 4) varied. The "low CD8 phenotype" was significantly associated with the most conserved ancestral haplotype carrying A*03-A-A-T in the cohorts from Porto (n=50) and Alabama (n=51) but it was not associated in a much greater series from Nord-Trøndelag (n=148). This lack of association of the common ancestral haplotype with the "low CD8 phenotype" in Nord-Trøndelag patients is intriguing. One should stress however, that discrepancies in expected genotype/phenotype correlations can also be highly informative regarding the localization of genetic traits. That individual chromosomes with the same alleles (A*03, A-A-T) may or may not be associated with the "low CD8 phenotype" indicates that these alleles are not, by themselves, determinants of the trait, further supporting the hypothesis of another independent, still unidentified, genetic marker in the region. The time and place, during the evolutionary history of the HH chromosomes, when the association occurred remains unknown. Further studies

of genotype/phenotype correlations in other populations with different founder effects could clarify this question. As suggested by Olsson and co-workers [207], it would be of great interest to explore further the HLA haplotype/phenotype correlations in an extended population of patients from the Trøndelag region, because of its long historic close contacts with the British islands, the supposed origin of founders of the "Celtic" haplotypes in Scandinavia [207]. On the other hand, results from Porto and Alabama support the postulate that a major genetic determinant of CD8$^+$ T-lymphocyte numbers is transmitted in linkage disequilibrium with *HFE* in this ancestral haplotype and suggest these populations as good targets to further position a candidate locus associated with the transmission of low CD8$^+$ T lymphocyte phenotypes. The evidence that the association is lost not only in chromosomes without the A-A-T SNP microhaplotype but also, within the A-A-T conserved haplotypes, in chromosomes without the ancestral A*03 allele (Table 4), favors the localization of such a putative trait between *HLA-A* and *PGBD1*. Future studies in these populations should consider selecting "non-conserved" chromosomes, i.e., those with discontinuous regions of conservation to the consensus haplotypes, to facilitate the search for individual loci contributing to the trait.

Effect of the SNP microhaplotypes on the iron overload phenotype

In addition to its association with a "low CD8 phenotype", the conservation of the ancestral A-A-T microhaplotype had been previously shown to be associated with a more severe iron overload phenotype [44]. In the present study we showed that, although in general, the presence in homozygosity of the A-A-T microhaplotype was associated to higher values of serum ferritin and total body iron stores in male patients, this association was not significantly sustained at the individual populations' level and therefore cannot be used as a reliable universal marker of the phenotypic expression in HH (Table 5). The lack of statistical power in individual populations could be explained by the low numbers of non-A-A-T homozygous patients found in each region together with a high phenotypic diversity in these patients (reflected in the high range of values shown in Table 5), but it could also be influenced by genetic differences among populations, namely the loss of association of the A-A-T microhaplotype with the putative "low CD8 phenotype" marker in the Nord-Trøndelag patients. One should also note that these patients were mainly identified by screening of asymptomatic subjects, therefore unselected for clinical severity. On the contrary, Porto and Alabama, patients were mainly diagnosed on a clinical setting. Nevertheless, even using the same selection criteria, there are also great differences in iron loading between Porto and Alabama patients that could be related with different environmental factors or local life-style habits, including regular alcohol consumption. Therefore, further studies are still needed in

larger populations and with a higher density mapping of the region, in order to find a more specific and universal surrogate marker of iron overload severity in HH.

Concluding remarks

We conclude that the evolutionary history of long extended haplotypes on chromosome 6p21.3 could account for heterogeneity within the haplotypes and consequent differences in the phenotypic expression of persons with *HFE* C282Y related HH. These observations have important implications for the interpretation of genotype/phenotype association studies in HH such as in the case of MHC loci associated with the transmission of the phenotype of low CD8^{+} T lymphocyte numbers where differences occur among HH populations from geographically distant regions (namely in north Portugal, Norway and Alabama, USA) or the association of MHC markers with iron overload. The effect of haplotype conservation may also have implications for understanding differences in disease penetrance or the consequences of patients' sampling according to different detection methods. Although no consistent evidence is given about the predictive value of the A-A-T microhaplotype for individual purposes, one may predict that, in general, any cohort of severe or symptomatic HH patients may contain a high frequency of this conserved ancestral haplotype associated with a "low CD8 phenotype", such as we have consistently found in Portuguese patients. On the contrary, in populations where programs for screening of asymptomatic cases are implemented, such as in Norway, it will be more probable to find HH patients with non-conserved haplotypes that are not associated with low CD8^{+} T lymphocytes. It remains unknown whether the severity of iron overload depends directly on the "low CD8 phenotype" or whether another independent modifier of the iron phenotype is inherited in linkage disequilibrium. Naturally, future positional cloning of a long-sought major genetic trait in MHC associated with the transmission of CD8^{+} T lymphocyte numbers [181] should provide answers to this question.

Supplementary Data

Table S1 - Comparison of the most common HLA allele, HLA A-B haplotype (uncorrected data) and SNP microhaplotype frequencies among three different populations of HH patients.

HH chromosomes of patients from:	Porto (n=130)	Alabama (n=114)	Nord-Trøndelag (n=364)	*P**
HLA- A alleles	[%(n)]	[%(n)]	[%(n)]	
HLA-A*01	12.3 (16)	14.9 (17)	12.9 (47)	n.s.
HLA-A*02	17.7 (23)	15.8 (18)	20.9 (76)	n.s.
HLA-A*03	40.8 (53)	47.4 (54)	42.0 (153)	n.s.
HLA-A*11	3.1 (4)	3.5 (4)	8.0 (29)	n.s.
HLA-A*24	3.8 (5)	3.5 (4)	5.8 (21)	n.s.
HLA-B alleles	[%(n)]	[%(n)]	[%(n)]	
HLA-B*07	23.8 (31)	30.7 (35)	28.8 (105)	n.s.
HLA-B*08	10.0 (13)	11.4 (13)	9.1 (33)	n.s.
HLA-B*14	3.8 (5)	9.6 (11)	7.1 (26)	n.s.
HLA-B*15	1.5 (2)	1.8 (2)	6.0 (22)	n.s.
HLA-B*35	12.3 (16)	3.5 (4)	5.5 (20)	*.009***
HLA-B*40	7.7 (10)	0.9 (1)	9.6 (35)	*.008***
HLA-B*44	12.3 (16)	14.0 (16)	16.2 (59)	n.s.
HLA Haplotypes	[%(n)]	[%(n)]	[%(n)]	
A1-B8	5.4 (7)	7.9 (9)	7.7 (28)	n.s.
A2-B44	3.1 (4)	7.0 (8)	6.3 (23)	n.s.
A3-B7	16.9 (22)	27.2 (31)	21.4 (78)	n.s.
A3-B14	1.5 (2)	7.0 (8)	6.0 (22)	n.s.
SNP microhaplotypes	[%(n)]	[%(n)]	[%(n)]	
A-A-T	90.8 (118)	86.0 (98)	76.5 (276)	0.0003
G-G-G	6.2 (8)	9.6 (11)	16.0 (59)	0.003
Non A-A-T nor G-G-G	3.1 (4)	4.4 (5)	7.5 (27)	n.s.

*Comparisons among populations were done using the Chi-square test (*P* values indicated)

** not statistically significant after Bonferroni correction

3.2

High-density mapping of the genomic region between HFE and HLA-B in Hereditary Hemochromatosis: is there a selective recombination suppression of the classical ancestral?

Costa M (1), Cruz E (1,2), Carracedo A (3), Vieira CP (4), Vieira J (5), Porto G (1,2,6)

1. Basic and Clinical Research on Iron Biology, Instituto de Biologia Molecular e Celular (IBMC), University of Porto, Porto, Portugal
2. Clinical Hematology, Centro Hospitalar do Porto – Hospital Santo António, Porto, Portugal
3. Galician Foundation of Genomic Medicine (SERGAS) and Genomic Medicine Group-CIBERER-University of Santiago de Compostela, Spain
4. Evolutionary Systems Biology, Instituto de Biologia Molecular e Celular (IBMC), University of Porto, Porto, Portugal 3. Southern Iron Disorders Center and Department of Medicine, University of Alabama at Birmingham, Birmingham, Alabama, USA
5. Molecular Evolution, Instituto de Biologia Molecular e Celular (IBMC), University of Porto, Porto, Portugal
6. Molecular Pathology and Immunology, Instituto de Ciências Biomédicas Abel Salazar (ICBAS), University of Porto, Porto, Portugal

Content

Abstract

Introduction

Material and Methods

Results:

1. Two haplotype groups characterize the MHC region between *HFE* and *HLA*

2. Two ancestral extended haplotypes predominate in HH chromosomes

3. Conservation patterns of AA or CG group haplotypes in HH patients and controls

4. Haplotype associations with the low CD8 phenotype

5. Insight into the evolutionary history of HH carrying haplotypes

Discussion

Abstract

Background: Genetic analyses in patients with Hereditary Hemochromatosis (HH) have shown that the relative frequencies of the most common MHC haplotypes and their associations with a phenotype of low CD8$^+$ T lymphocyte numbers vary amongst distinct populations, reflecting different recombination histories or founder effects.

Aims & Methods: To refine the region of interest to search for quantitative trait loci (QTL) for the inheritance of low CD8$^+$ T lymphocyte numbers in HH, we performed a high-density SNP mapping of the 4 Mb genomic region between *HFE* and *HLA-B* in a cohort of 43 HH patients and in 105 control subjects from the same area in north Portugal. Haplotype genealogies were inferred by phylogenetic analyses and the distribution of CD8$^+$ T lymphocyte numbers in HH patients was analyzed in relation to the inheritance of conserved or recombinant haplotypes.

Results: Two major haplotype groups, defined by a block of 4 SNP markers, were identified in patients and controls. They were designated, according to the two flanking alleles, as the AA and CG haplotype groups. A remarkably higher genetic homogeneity is observed in haplotypes from the AA relative to the CG group, both in HH patients and controls, suggesting that recombination suppression is somehow favored in chromosomes carrying this particular combination of alleles. Accordingly, in HH the most common and conserved HLA-A*03-B*07 associated ancestral haplotype is included in the AA group, while the less common HLA-A*01-B*08 associated ancestral haplotype is included in the CG group. Haplotype genealogies confirmed the distribution of HH chromosomes in two opposite phylogenetic branches and genotype/phenotype distributions support the co-inheritance of a low CD8 phenotype with the more conserved haplotypes of the AA group.

Conclusions: A high-density map of the *HFE-HLA* region in chromosomes from Portuguese HH patients highlights the remarkable conservation of ancestral haplotypes associated with a major QTL determining CD8$^+$ T lymphocyte numbers, and provides evidence to support a selective suppression of recombination in the context of particular haplotypes in this region.

Keywords: Hereditary Hemochromatosis, HFE, HLA haplotypes, CD8$^+$ T lymphocytes

Introduction

The Hereditary Hemochromatosis (HH) associated gene was first localized in 1976 based on its strong association with HLA [162]. This was the first step towards the later positional cloning of the *HFE* gene in 1996 [27]. The 20 years' delay in the discovery of the *HFE* gene is easily understood taking into consideration the extreme linkage disequilibrium known to occur in the 4 Mb region between *HFE* and *HLA* [207, 217-219]. The finding that one single *HFE* mutation (p.C282Y) in homozygosity explains the vast majority of HH cases [27] naturally concentrated all the attention on the HFE molecular defect as the single pathogenic player in HH, generally neglecting the possibility that other MHC linked players could be involved in the disease process. Nevertheless, this chromosomal region is extremely rich in other immune related genes transmitted in linkage disequilibrium with *HFE* which could concur for the disease expression. It is known that HH is clinically highly heterogeneous and this phenotypic variation was shown to be associated with the HLA haplotypes, independently of the *HFE* mutation [43, 190, 192]. Relevant to this concept is not only the demonstration of an iron overload phenotype in various MHC deficient animal models [23, 24, 28, 35] but also the consistent finding of abnormalities of CD8$^+$ T lymphocyte numbers in HH patients, a phenotypic trait that what demonstrated to be inherited in association with the HLA markers [30, 41]. A recent genome wide association study in normal subjects provided more evidence to support the existence of a major quantitative trait loci (QTL) involved in the genetic control of CD8$^+$ T lymphocyte numbers located in the class I cluster of the MHC region [181], thus reinforcing our interest to look for such QTL in HH.

In 2008 Cruz et al. described a new 500kb haplotype (A-A-T) localized between *HLA* and *HFE* which was associated with the transmission of a low CD8 phenotype and a more severe expression of iron overload in Portuguese HH patients [44]. More recently we tested the predictive value of this microhaplotype as a putative useful marker in other geographically different populations by comparing the genotype-phenotype associations in HH patients from Porto, Portugal, Alabama USA and Nord-Trøndelag, Norway. The results (described in detail in chapter 3.1) showed that the A-A-T microhaplotype alone cannot be used as a universal marker of the CD8 phenotype since the genotype-phenotype associations varied significantly among the different HH populations, probably due to different recombination histories or founder effects[220].

In the present study we refined the mapping of the region between *HFE* and *HLA* with a total of 63 genetic markers analyzed in 43 HH patients and 105 normal controls from the same geographical region in north Portugal. Our choice to focus on Portuguese HH patients in this study was justified by the previously demonstrated stronger genotype/phenotype correlations in this population [220]. The results obtained allowed us to characterize the

structure and history of the two major conserved extended haplotypes associated with HH in this population, and better explore their associations with the transmission of a low CD8 phenotype.

Material & Methods

Study Populations

HH Patients

A group of 47 Portuguese HH patients (41 probands and 6 affected relatives) from north Portugal, mainly from the Porto district area, were included in this study. They had been diagnosed between 1985 and 2011 at the Hemochromatosis Outpatient Clinic of CHP-Santo António Hospital, Porto. Most of the patients' clinical information, including available genetic information, has been already described elsewhere [41, 43, 44, 188, 198-200]. The previously available genetic information included, in all cases, *HFE* genotype (all patients are homozygous for the p.C282Y mutation), HLA class I alleles (A, B and C) determined by low-resolution DNA-based techniques (PCR/sequence-specific oligonucleotide probes, Dynal RELI™ SSO) and typing for the microsatellites D6S265, D6S2222, D6S105 and D6S2239. Information on the CD8$^+$ T lymphocyte numbers was available from their medical records. Analyses of novel genetic markers were performed in stored DNA samples previously obtained with proper informed consent in the context of other studies (Cruz 2008, Costa et al 2014) with the approval of the CHP- Santo António Hospital Ethical Committee.

Controls

For the purpose of comparative analyses, the same SNP markers were analyzed in a control population of 105 unrelated Portuguese healthy blood donors from whom we had available stored DNA collected with proper informed consent in the context of another genetic study [42]. Previous genotypic and phenotypic information of these controls included *HFE*, *HLA A, B* and *C*, *ZNF305, PGBD1, ZNF193, ZNF165* genotypes as well as CD8$^+$ T lymphocyte phenotypes.

High-density mapping of the region between *HFE* and *HLA-B*

A high density mapping of the region between *HFE* and *HLA-B* was performed including, besides the previously available information on *HFE, ZNF305, PGBD1, ZNF193, ZNF165* and the microsatellites D6S265, D6S2222, D6S105 and D6S2239 (published in [44]), additional information on the following 46 selected SNP markers: rs10447393, rs10807035, rs10946940, rs12174753, rs12180820, rs12197514, rs13195291, rs13197633, rs13200462, rs13201308, rs13201411, rs13204012, rs13205211, rs13205911, rs13208096, rs13211507, rs13215560, rs13217162, rs13218430, rs16893666, rs16893741, rs16893817, rs16893827, rs16893889, rs16893892, rs16893917, rs16901846, rs17711344, rs17711801, rs17720293, rs17720687, rs17774663, rs4713207, rs4713211, rs6902687, rs6912843,

rs724078, rs7381993, rs7382112, rs7382146, rs7383248, rs9257425, rs9257816, rs9393920, rs9468217, rs9468344.

The chromosomal physical localization of the analyzed markers region is shown in Figure 1.
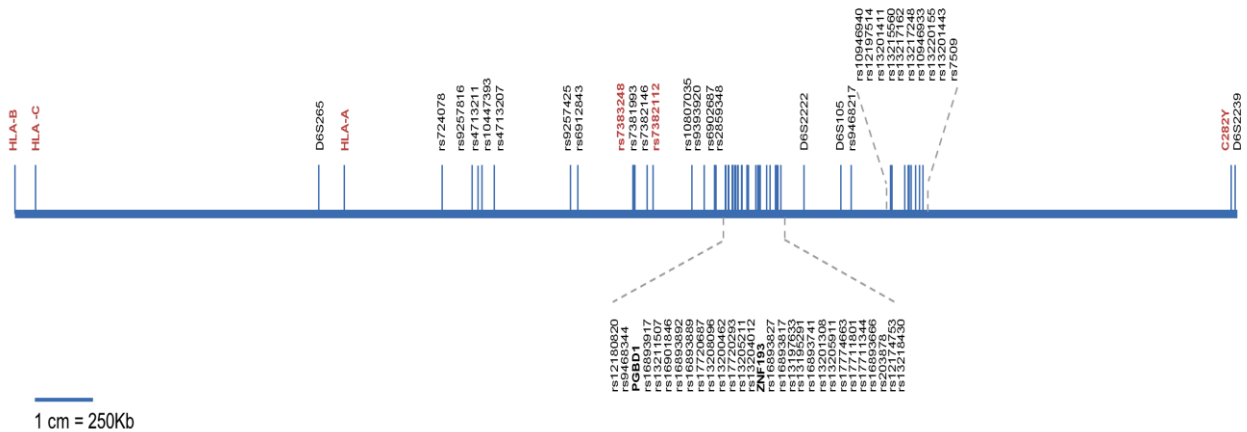
Fig. 1 Distribution of the 63 SNP markers in chromosome 6 along the region from *HLA-B* to the *HFE* gene.

SNPs were typed using the iPLEX™ Gold technology (Sequenom MassARRAY) in the USC node of the Spanish National Genotyping Center (CEGEN). Genotyping call rates were 99% for all individuals included in the analyses. Additional quality control measures included SNP missingness >10% and the use of positive and negative controls. None of the SNPs failed the missingness threshold. More details for SNP analysis can be provided by request.

Generation of phased chromosomes and haplotype construction

HLA A-B haplotypes, as well as the microhaplotypes defined by the genes *PGBD1, ZNF193* and *ZNF165* were defined in HH patients by family segregation whenever there were available informative family members. Otherwise they were inferred by the PHASE program. For the generation of high-density SNP extended haplotypes, we used the PHASE program to infer haplotypes. In the case of HH chromosomes, whenever the phase assignment was known (this happened for the markers: *HLA A, B* and *C, ZNF305, PGBD1, ZNF193, ZNF165* and for microsatellites D6S265, D6S2222, D6S105 and D6S2239), this information was incorporated in the program. In total, high-density extended haplotypes were defined in 86 HH founder chromosomes (these are the two chromosomes from each unrelated proband and the unshared chromosomes in first degree relatives) and in 210 control chromosomes.

Definition of haplotype groups and haplotype conservation

An initial search for groups of conserved haplotypes within HH founder chromosomes identified two groups of chromosomes with a specific consensus sequence defined by 4 SNPs between rs7382112 and rs7383248, termed "haplotype group." The same haplotype groups were also found in control chromosomes. Chromosomes within each group were then compared to the respective consensus sequences that were defined as the most common sequence with complete SNP identity between *HFE* and *HLA-B* (respectively in HH patients and controls). We defined "loss of conservation" when one or more SNPs did not match the consensus sequence. Chromosomes were aligned and compared at 5 consecutive blocks from *HFE* to *HLA-B* and the conservation pattern (conserved vs non-conserved) was defined for each block.

Statistical methods

SNP data from all chromosomes was analyzed with MEGA4 to create a neighbor joining tree. Input data consisted in 302 chromosomes (210 from controls and 86 from HH patients), 53 SNPs per chromosome and ID numbers encoding HLA data (neither HLA nor microsatellite data were used to create the tree). To create the tree we used a pair wise comparison option with pairwise deletion and the neighbor-joining method (a distance based method) implemented in MEGA4.

To analyze the impact of haplotype conservation on the CD8$^+$ T lymphocyte numbers, patients were classified in three classes according to the inheritance of conserved or non-conserved haplotypes: class 1 patients were the homozygous for the ancestral haplotype of the AA group, class 2 and 3 patients were the compound heterozygous for the ancestral AA group haplotype with a non-conserved haplotype of the AA or the CG groups respectively. Distributions of CD8$^+$ T lymphocyte numbers were fitted to a normal curve in each class. Values above 1,5 SD of the mean value in the whole group of patients were assigned as "CD8 expansions". Because of sample size limitations in multiple comparisons, statistical inferences were not applied. Data were analysed by SPSS software for statistical Analysis (SPSS Statistics for Windows, Version 17.0. Chicago: SPSS Inc.).

Results

1 -Two haplotype groups characterize the MHC region between *HFE* and *HLA*

We generated extended haplotypes with genetic information of 63 markers in the region from *HFE* to *HLA-B* in 86 HH founder chromosomes (see Methods). These are illustrated in Figure 2 (left panel), where the extended haplotypes are aligned by allele similarity. A detailed observation of the region between *HFE* and *HLA-A* reveals that this region is composed of several spread blocks of complete allele identity (highlighted in Figure 2 by dark yellow boxes) alternated with other blocks of some variability. In one block, defined by 4 SNP markers from rs7382112 to rs7383248, there is a clear segregation of all (except one) HH chromosomes into two major groups, each maintaining its identity defined by the four selected markers (highlighted in Figure 2 by framed boxes, bold lettering and different colours). The two groups were designated, according to the two flanking alleles, as the AA and GC haplotype groups, respectively. Of the two haplotype groups, AA was the most common (66/86) and the CG group the less common (19/86). All chromosomes carrying the previously described classical HH ancestral HLA haplotype A*03-B*07 were contained in the AA group, whereas all chromosomes carrying the HLA haplotype A*01-B*08 were contained in the CG group. Analysis of the same SNP markers in a sample of 210 control chromosomes derived from 105 normal subjects from the corresponding geographical regions as the HH patients showed that the same haplotype groups are also found in normal chromosomes. Results are illustrated in Figure 2 (right panel) where, for the purpose of comparisons with HH derived haplotypes, the same color coding was used. Such as in HH patients, the AA haplotype group was the most common (113/210) and the CG group the less common (91/210). A small proportion of chromosomes (6/210) could not be included in either of the two defined haplotype groups. Since these haplotypes were inferred using PHASE (see methods) we admit that wrong inferences could account for these few apparent exceptions.
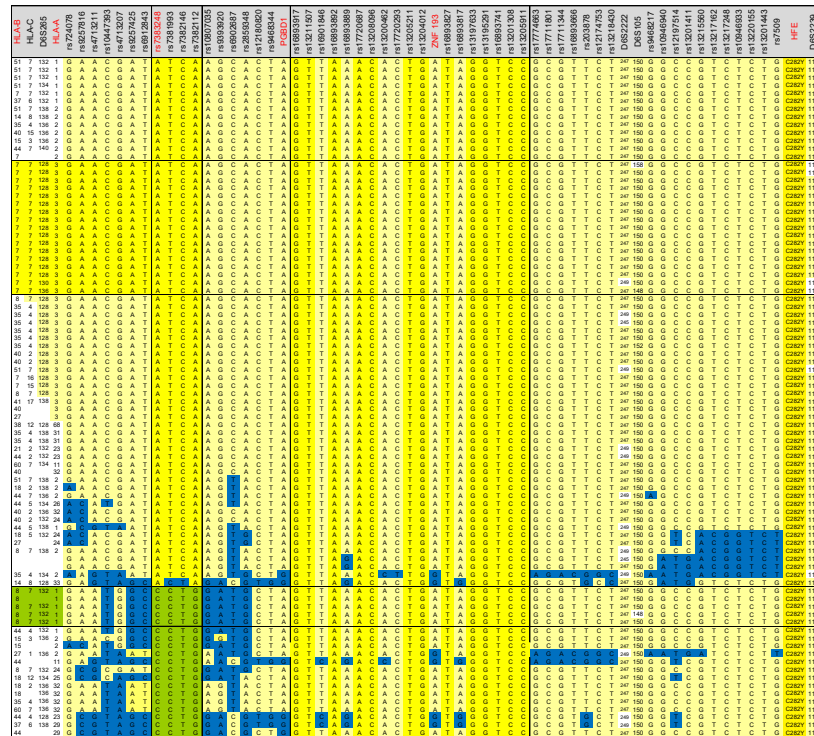
Fig. 2 <u>**Left panel**</u>**: Consensus sequences of 86 extended haplotypes from HH founder chromosomes organized by haplotype group.** Each raw represents the sequence from one HH founder chromosome (arbitrarily ordered by overall homology) and each column one genetic marker, ordered by relative physical position. Yellow boxes show that the allele matches the most common consensus sequence, whereas blue boxes represent the opposite (or alternative) alleles. Blocks of complete allele identity are highlighted by dark yellow boxes. A block defined by the 4 SNP markers from rs7382112 to rs7383248, segregates all (except one) chromosomes in the two haplotype groups, assigned according to their flanking alleles as AA or CG. These two haplotype groups are highlighted by framed boxes, bold lettering and different coloring (dark yellow vs green). <u>**Right panel: Consensus sequences of 210 extended haplotypes from normal chromosomes organized by haplotype group**</u>. For comparisons with HH chromosomes, the same color coding was used.

68
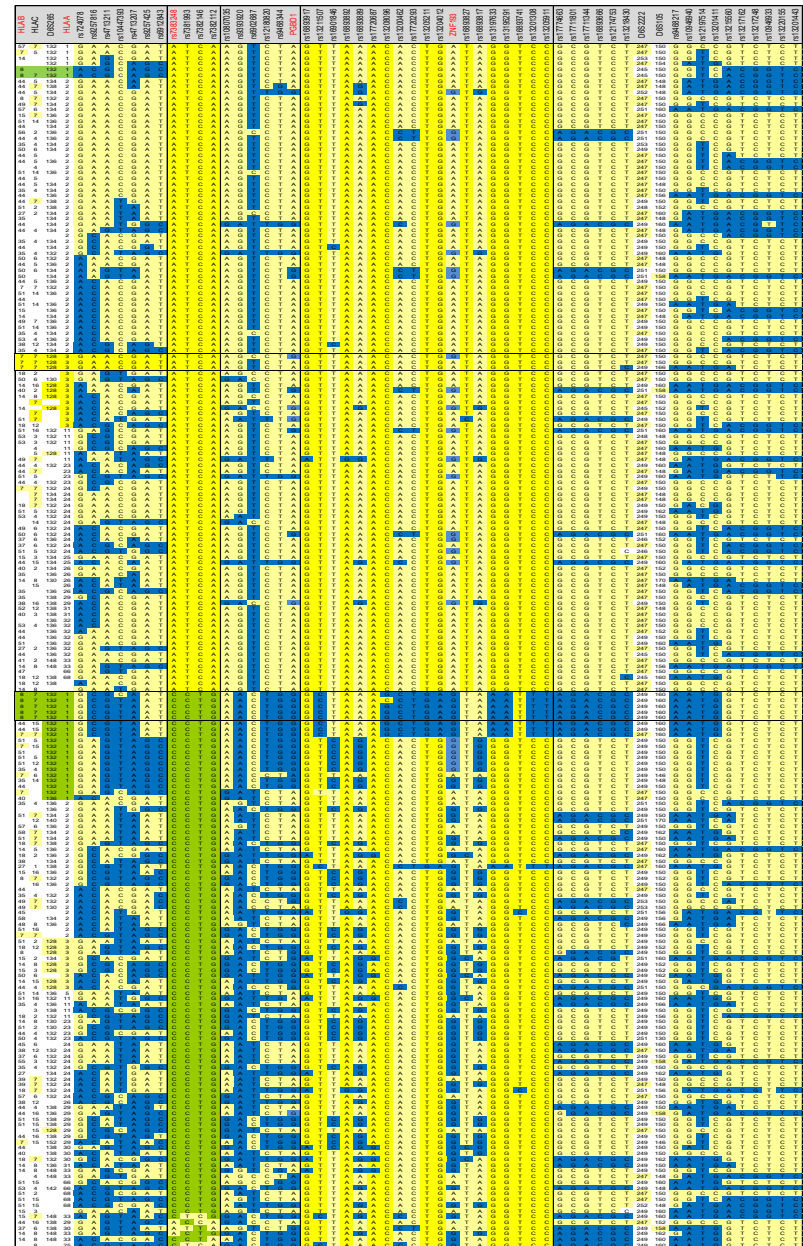
2 - Two ancestral extended haplotypes predominate in HH chromosomes

An identical SNP consensus sequence was observed between *HFE* and *HLA-A* in 80% of the HH chromosomes of the AA haplotype group (53/66). This conservation extended in a centromeric direction to *HLA-A* (62% of these carrying the A*03 allele) and to *HLA-B* (52% of these carrying also the B*07 allele). For further analyses, this consensus sequence was defined as the "ancestral extended haplotype of the AA group". An identical SNP consensus sequence was also observed between *HFE* and *HLA-A* in 32% of the HH chromosomes of the CG haplotype group (6/19). Each of these conserved extended haplotypes contained the HLA-A*01 allele and all but one carried HLA-B*08. For the purpose of further analyses, this consensus sequence was designated as the "ancestral extended haplotype of the CG group".

3 - Conservation patterns of AA or CG group haplotypes in HH patients and controls

All chromosomes within each group were compared looking for their patterns of conservation or non-conservation, relative to the respective ancestral sequence, in five sub-regions: from *HFE* to *ZNF*193; from *ZNF*193 to *PGBD1*; from *PGBD1* to rs7382112; from rs7383248 to *HLA-A*; and from *HLA-A to HLA-B*. We defined, for each region, loss of conservation if one or more SNPs differed from the respective consensus ancestral sequence in HH patients (Figure 3 left panel) or in controls (Figure 3 right panel). In the case of controls we defined as the ancestral sequence the most common consensus sequence found among 210 control chromosomes. In general, haplotype conservation was much higher in HH than in normal chromosomes, as expected by their assumed recent common ancestry. Control chromosomes belonging to the AA haplotype group (but not to the CG group) also show a strong degree of conservation, but this is restricted to the region between *ZNF*193 and the SNP marker rs7383248, while in HH chromosomes it extends to the entire region between *HFE* and *HLA*. In spite of their presumed common ancestry, HH chromosomes display different patterns of conservation according to the different haplotype groups*,* suggesting that they had different recombination histories. While a progressive loss of conservation is observed from *HFE* to *HLA* in chromosomes from the CG group (probably reflecting historical recombination events), chromosomes from the AA group, in contrast, maintain a high degree of conservation at the entire region between *HFE* and *HLA*, diversity becoming apparent only centromeric to *HLA-A*. Considering the recent origin of the HH chromosomes, this result could suggest a more recent origin (founder effect) of the AA group chromosomes than of the CG group. Alternatively, considering that the stronger conservation of AA group haplotypes is also observed in normal chromosomes, the results may also suggest the existence of a selective stronger recombination suppression in this region for the particular haplotypic combination of alleles in the AA than for the CG haplotype group.
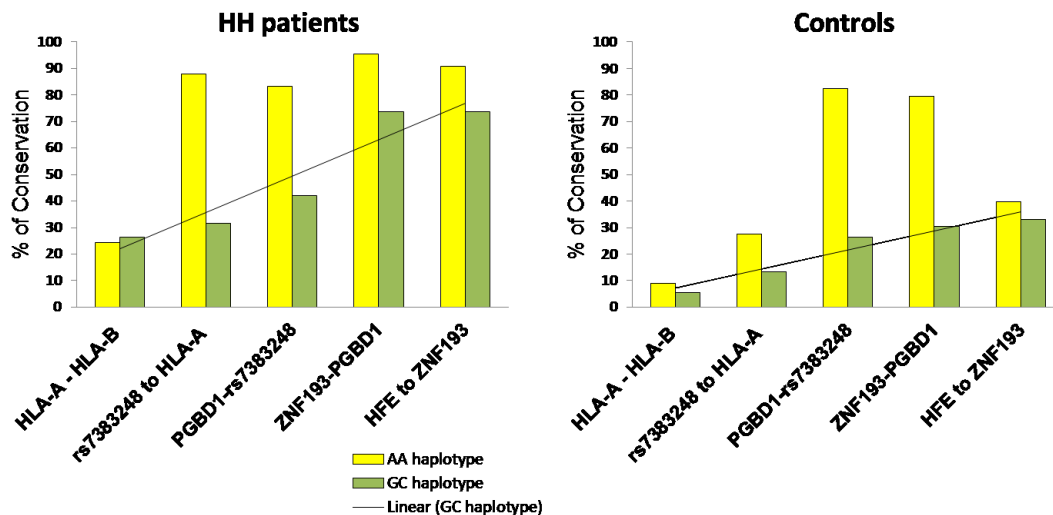
Fig. 3 Percent conservation of HH patients (left graph) and controls (right graph) chromosomes in 5 consecutive regions from HFE to HLA-B. The percentages of conserved chromosomes from the AA haplotype group are represented in blue bars and the percentage of conserved chromosomes from the CG haplotype group are represented in red bars.

4 - Haplotype associations with the low CD8 phenotype

The distribution of CD8^{+} T lymphocyte numbers was analyzed and compared among groups of HH patients classified according to the inheritance of the most common ancestral or the non-conserved haplotypes as described in Methods. Results are illustrated in Figure 4 where fitting curves are displayed without (dashed red line) or with (continuous black line) exclusion of CD8 expansions (see Methods). By simple inspection of the curves it is evident that HH patients carrying non-conserved CG group haplotypes do not display the characteristic left deviation of values (relative to the normal median) as seen in patients homozygous for the most ancestral AA haplotype and, to a lesser extent, in compound heterozygous for the ancestral with a recombinant haplotype of the AA group. Notably, CD8 expansions were more common in the group of homozygous patients who carry a low CD8 phenotype relative to the other groups. An interpretation of this finding is provided in the discussion below.

CD8$^+$ T lymphocytes numbers (x10^3/mL)
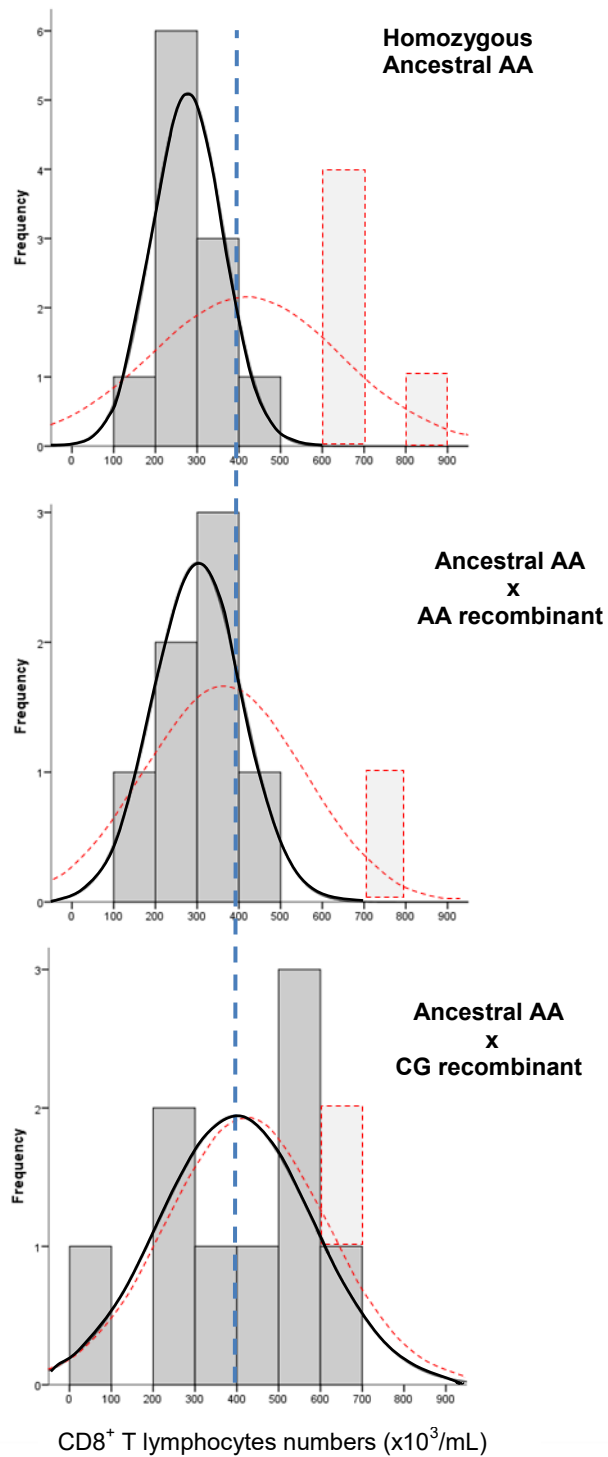
Fig. 4: Distribution of CD8+ T lymphocytes in HH patients according to the inheritance of two ancestral haplotypes (upper graph), one ancestral and one recombinant of the AA group haplotype (middle graph) or one ancestral and one recombinant of the CG group haplotype (lower graph). Dashed red lines represent the distribution fitting to normal with uncensored data. Continuous black lines represent the distribution fitting to normal excluding CD8 expansions. The vertical blue dashed line indicates the median value in the control population.

71

5 - Insight into the evolutionary history of HH carrying haplotypes

Insight into the evolutionary history of a gene region can be gained by inferring haplotype genealogies. To address the hypothesis of different recombination histories in HH chromosomes belonging to the two distinct haplotype groups, we used the genetic information obtained to construct HH haplotype genealogies using the neighbor-joining method implemented in MEGA. In this method we did not use HLA allele information; this was only encoded in ID numbers and used for the tree illustration in Figure 4. In general, chromosomes from the two haplotype groups are distributed in opposite clusters in the tree (CG haplotypes on the left, AA haplotypes on the right). In the particular case of HH chromosomes, these are mainly clustered in two different branches: one integrating the AA haplotype group (including all the HLA-A*03-B*07 carrying chromosomes, highlighted in red) and another one integrating the CG haplotype group (including all the HLA-A*01-B*08 carrying chromosomes, highlighted in green). Other HH-linked haplotypes localized in distant and spread branches of the tree could correspond to the result of more recent re-combinational events or the result of wrong haplotype inferences by PHASE. Distances are shorter (and more distant from the tree origin) among the AA haplotypes carrying the HLA-A*03-B*07 than in the CG haplotypes carrying the HLA-A*01-B*08. This result may support the hypotheses that the origin of the AA group chromosomes, including the ancestral HLA-A*03-B*07, is either more recent or subject to a stronger selective advantage by selective recombination suppression.
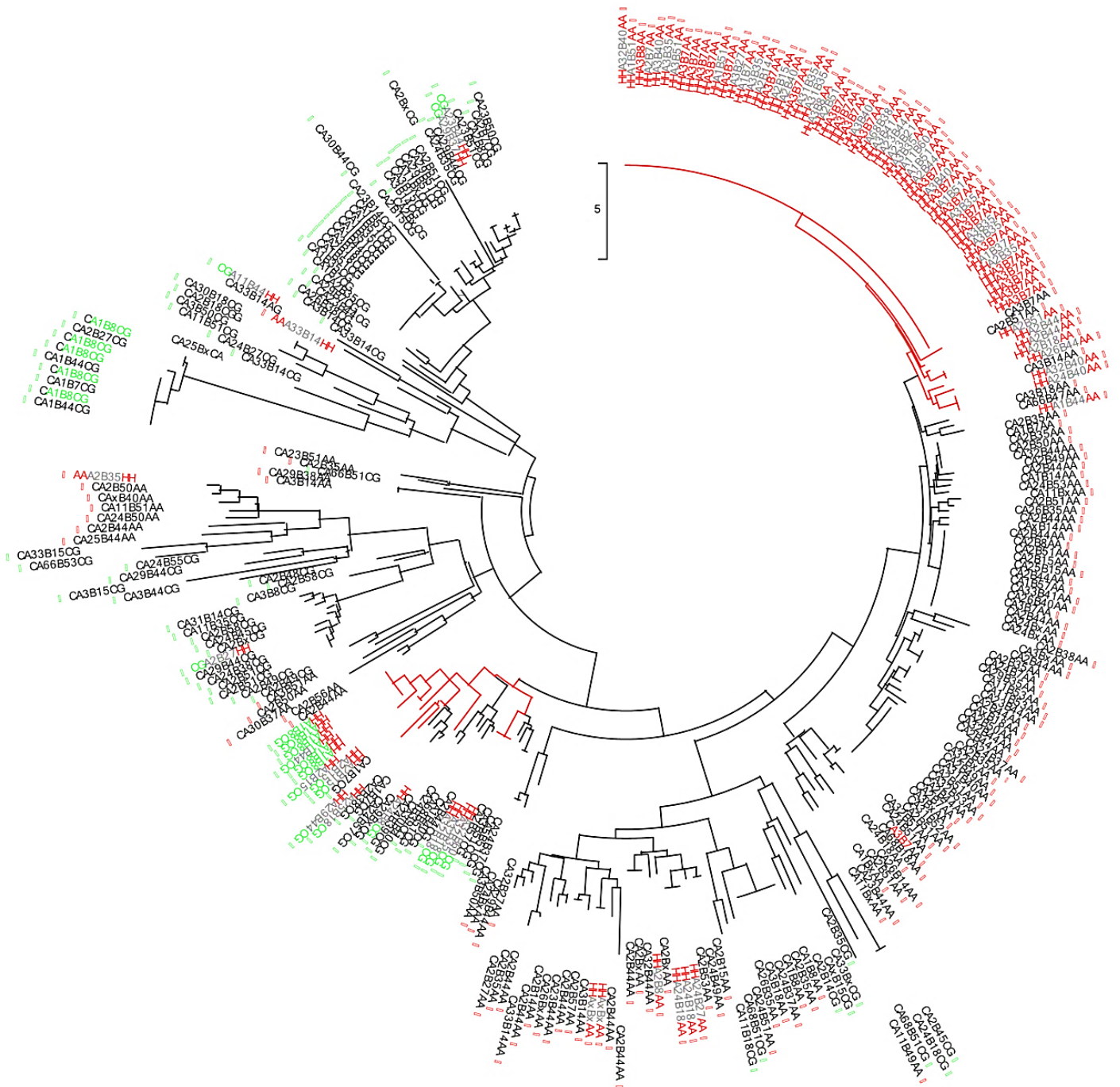
Fig. 5. HFE-HLA neighbor joining tree. SNP data for 86 HH founder chromosomes and 210 control chromosomes was analyzed with MEGA4 and a neighbor joining tree using pairwise comparisons (see Methods). HLA data was not used to create the tree but it is encoded within the ID characters associated with each chromosome [analytic ID (case=HH, control=C)_HLA-A_HLA-B_haplotype group (AA in red or CG in green)]. For a better visualization, chromosomes from the two major haplotype groups (AA or CG) are marked with an additional mark (respectively ■ or ▨).

Discussion

Factors controlling the frequency and location of recombination events on human chromosomes are still not well understood. In this respect, studies of the MHC-class I are of particular interest. The more-localized variation in this region, including "hot" and "cold" spots [221] suggest the existence of localized structures or functional elements that affect crossover occurrence or product viability by means similar to those demonstrated in lower eukaryotes (reviewed by Lichten and Goldman [222]). In a study of the 6-Mb region between D6S265 (70 kb centromeric of HLA-A) and D6S276, Malfroy and co-workers demonstrated the existence of a nonrandom pattern of recombination throughout this region with a recombination rate of 0.19% within the 4-Mb interval centromeric to *HFE* , contrasting with the approximate 1% rate observed within the most telomeric two megabases [221]. In the present study we explored the haplotype structure and recombination history of the *HFE* p.C282Y carrying chromosomes, including their association with a quantitative trait for CD8^{+} T lymphocyte numbers, through a high-density SNP mapping of the 4 Mb region between *HLA-A* and *HFE* in 86 founder chromosomes from Portuguese HH patients and 210 chromosomes from normal individuals from the same region.

The overall haplotype analysis showed that most HH chromosomes in the Portuguese HH population seem to derive from two major ancestral haplotypes, one (more common) containing HLA-A*03B*07 and the other (more rare) containing HLA-A*01B*08. The pattern of haplotype conservation, however, was significantly different in the two cases. While haplotypes derived from the ancestral HLA-A*03B*07 branch were, in general, highly conserved in the whole region between *HFE* and *HLA-A*, the same was not observed in haplotypes derived from the ancestral HLA-A*01B*08 branch. These results showing a differential conservation of SNP markers in the two major ancestral haplotypes are in accordance with results of microsatellite markers in other populations, namely in the Swedish population, where the general conservation of A*03 carrying chromosomes was shown to be stronger than that observed in A*01 carrying chromosomes [207].

Although the two described ancestral haplotypes in Portuguese HH patients can be distinguished by a set of highly conserved unique SNP sequences (belonging respectively to the AA and CG haplotype groups), they also share a long and highly conserved region from *HFE* to the SNP marker rs7382112 (Fig. 2), suggesting a common ancestry. However, the observation that the two haplotypes cluster in two separate branches of a phylogenetic tree (see Fig. 5) seem to indicate that independent founder effects occurred at different times in the Portuguese HH population and that, apparently, the HLA-A*01B*08 carrying CG haplotypes have a more ancient origin (with higher diversity) than the HLA-A*03B*07 carrying AA group haplotypes. This interpretation, however, does not fit with the current view

on the origin and spread of the HH-associated mutation (reviewed in Distante et al [194]), favoring the hypothesis that the most ancient HH founder chromosome should be the one carrying the HLA-A*03-B*07 from which all other haplotypes derive. This assumption is generally based on the high frequency and linkage disequilibrium of this haplotype in all populations studied throughout the world. Nevertheless, the fact that HLA-A*03B*07 carrying chromosomes, besides having the highest frequency in all worldwide spread populations, is also much more conserved than the HLA-A*01B*08 carrying chromosomes, favor an alternative hypothesis that the HLA-A*03B*07 could be maintained at a higher frequency due to a stronger selective pressure, as elegantly shown by Toomajian and co-workers [165]. In this context, it is worth mentioning that another HH-associated classical ancestral HLA haplotype, A*03B*14, described as having the strongest linkage disequilibrium in Scandinavian populations [207] does not occur in general at high frequencies among other HH populations. This suggests that either A*03B*14 results from more recent recombination events in some particular populations and/or that, in contrast to A*03B*07 carrying chromosomes, it was not favored by a putative selective pressure [184].

The observation of a reduced rate of recombination at the MHC region in a particular haplotype group not only in HH chromosomes but also apparent in normal chromosomes (illustrated in Figure 2) brings some new light to the question of the recombination suppression in this region. A selective suppression of recombination may be due to structural variations hampering proper meiotic pairing of homologous sequences and/or due to selective constraints depending on environmental factors. In this case, it could be related to immunity and iron status. The consistent observation that HLA haplotypes influence not only the inheritance of CD8$^+$ T lymphocyte numbers in HH patients but also the severity of iron overload [43] together with the present demonstration that the inheritance of the most conserved ancestral haplotype impacts on the distribution of CD8$^+$ T lymphocyte numbers, all point either to the existence of important selective forces acting upon immune responses or simply a bystander effect on the genetic transmission of a major QTL for CD8 numbers in this highly conserved chromosomal region. This hypothesis is favored by the previous finding that HH patients from Nord-Trøndelag, in Norway, do not display the same genotype/phenotype correlation. Further studies with complete covering of this genetic region with the use of High-throughput sequencing are still necessary to clarify this point, taking into account that recombination takes place more frequently in regions flanking conserved blocks than within them.

A final comment should be given relative to the surprising observation that HH patients homozygous for the ancestral conserved haplotype, strongly associated with a low CD8 phenotype, were also the ones with a higher frequency of CD8 expansions (Fig. 4). A possible explanation for this finding derives from very recent evidence that CD8$^+$ T

lymphocytes from *Hfe* deficient mice display an expression profile compatible with more activated cells in the peripheral blood [223], and that HFE acts "*in vitro*" as a suppressor of CD8^{+} T lymphocyte activation [224]. It is plausible to assume that, the same effect on T cell activation which may lead to the shifting and eventual exhaustion of the more mature effector memory cells in the periphery, could also, in particular conditions and in the context of particular antigen epitopes, lead to expansions of the CD8^{+} T lymphocyte pool. Whether these expansions are maintained throughout life or are eventually exhausted, this can only be clarified with appropriate long follow-up longitudinal studies in those patients.

Conclusion

In conclusion, this study of extended haplotypes in Portuguese HH patients reveals novel aspects of the haplotype nature and recombination history of *HFE* p.C282Y carrying chromosomes, and provides one more step towards the possibility of localizing a major quantitative trait for the setting of CD8^{+} T lymphocyte numbers in humans.

3.3

In vitro response of T lymphocytes to iron and how they may act as modifiers of the clinical expression in HH

Content

Introduction

Iron is an essential nutrient in several biological processes such as oxygen transport, DNA replication and erythropoiesis. After intestinal absorption iron circulates in plasma bound to the plasma protein called transferrin. Circulating iron which is not bound to transferrin, heme or ferritin (here designated as non-transferrin-bound iron - NTBI) becomes important in iron overload disorders, in which plasma iron is present in excess of transferrin-binding capacity [101, 102]. NTBI is responsible for the toxicity associated with iron-overload pathologies leading not only to formation of free oxygen radicals but also causing organ failure through cell death. NTBI is avidly taken up by the liver but this clearance mechanism has a threshold beyond which iron accumulation inside hepatocytes becomes toxic, leading to the development of liver pathologies such as fibrosis, cirrhosis and hepatocarcinoma. The chemical nature of NTBI is very diverse, the most common form is iron-citrate but the mechanisms by which the cells take up NTBI are not fully understood. Besides hepatocytes, a variety of other cell types have also been shown to take up NTBI [225]. The specific iron uptake kinetics displayed by distinct cell types [112, 226, 227], together with the observation of distinct patterns of affected organs in different iron overload diseases [228], all suggest that either the different cell types may differ in the expression of the same NTBI-carrier molecule(s) or that they possess different uptake systems capable of discriminating between the various circulating NTBI species. Until now little was known about the capacity of T lymphocytes to take up NTBI. Here we show for the first time that T lymphocytes are able to take up and accumulate NTBI. Moreover, we found that the iron-citrate specie preferentially taken up by T lymphocytes is the oligomeric Fe_3Cit_3 form, suggesting the existence of a still elusive selective NTBI carrier. Furthermore, we tested the hypothesis if there were differences in the NTBI retention capacity of the circulating immune cells between HH patients and if that could contribute to the heterogeneity of iron load in HH patients. Total NTBI retention showed a significantly different distribution between HH patients and controls, with a high proportion of HH patients showing values below the lower limit found in controls. NTBI retention was strongly negatively correlated with the TfSat of HH patients at the time of the experiment. Differences in plasma iron re-accumulation were also observed in patients when divided according to NTBI retention: patients with lower NTBI retention capacity had a faster and higher re-accumulation pattern (stabilizing TfSat values at an average of 70,6%) than patients with higher NTBI retention capacity, who had a slower and lower re-accumulation pattern (stabilizing TfSat at values <50%). These preliminary results *in vitro* point out for biological differences between CD8$^+$ T cells from HH patients and normal controls which are of great interest to be further addressed.

Methods

Ethics Statement

Peripheral blood samples were obtained from healthy blood donors and HH patients at Santo António General Hospital (Porto, Portugal), who gave their written informed consent to participate in this study, which was approved by the Santo António Hospital Ethical Committee.

Isolation of human peripheral blood cells

Peripheral Blood Mononuclear Cells (PBMCs) were obtained from buffy coat product processed at Santo António General Hospital. Cells were isolated by gradient centrifugation over Lymphoprep (Nycomed). After lysis of erythrocytes, cells were resuspended in RPMI (GibcoBRL) supplemented with 10% fetal calf serum (FCS; GibcoBRL) and plated. $CD3^+$, $CD4^+$ and $CD8^+$ cells were purified from PBMCs using magnetic-activated cell sorting (MACS), after incubation with anti-CD4, -CD8 or -CD14 Microbeads (Miltenyi Biotec, Bergisch Gladbach, Germany), following the manufacturer's instructions. The purity of each cell population in the suspension was randomly assessed by flow cytometry and was always > 95%.

Statistical analysis

The results are expressed as mean values +/−1 standard deviation (SD). The existence of correlations between iron uptake and concentration of Fe-citrate species was assessed by simple regression analysis, performed with STATGRAPHICS Centurion XV (Statpoint Technologies). Statistical significance was set using Chi-square test for group comparisons between controls and HH patients.

NTBI uptake by T lymphocytes

Uptake of non-transferrin-bound iron (NTBI) was assessed using ^{55}Fe- citrate [229]. ^{55}Fe- citrate stock solutions were prepared by mixing ^{55}FeCl$_3$ (PerkinElmer, Inc, USA) with unlabelled trisodium citrate, at different Fe:citrate molar ratios. The pH was maintained at 7.4 and solutions were allowed to rest for 20 minutes before being diluted 33-fold in uptake medium and added to cells. Specific activity in the uptake medium was approximately 30 counts.min^{-1}.pmol^{-1} Fe. All Fe:citrate solutions were prepared immediately before use and discarded after each experiment. Unless otherwise indicated, cells were depleted of intracellular transferrin by incubation for 1 hour in serum-free/iron-free RPMI, washed and incubated with RPMI+20% HH plasma+5 µM ^{55}Fe-citrate (as 5 µM ^{55}FeCl$_3$+100 µM citric acid), at 37°C. 5 µM is the typical NTBI concentration reported in sera from *thalassemia*

major patients [230] and 100 µM citric acid corresponds to the levels normally present in human blood plasma [229]. The pH of the uptake medium was maintained at 7.4. After incubation, cells were washed 3× with ice-cold buffer [20 µM desferrioxamine (DFO) in PBS, pH 7.4], lysed with 0.1% NaOH, 0.1% Triton X-100 and intracellular Fe was measured in a MicroBeta Trilux β-counter (Perkin Elmer), for 1 minute. No significant changes in cell viability with iron treatments was observed, using trypan blue exclusion and maintenance of proliferative potential following activation with anti-human anti-CD3 and anti-human anti-CD28 for CD3^{+}, CD4^{+} and CD8^{+}T lymphocytes (Arezes et al. 2013).To distinguish between intracellular and membrane-bound Fe and citrate, cells incubated for 30 minutes with varied Fe:citrate ratios were washed four times with PBS, pH 7.4, at 4°C, and were then incubated with 1 mg/ml of the proteolytic cocktail Pronase (Sigma) for 30 min, at 4°C. The cell suspension was centrifuged at 12,000 g for 30 s, and the supernatant (containing membrane-bound radioactivity) transferred to new tubes. Cell pellets containing [55]Fe radioactivity were solubilized as described above.

Speciation plots for ferric citrate species

Speciation plots were developed for Fe-citrate complexes formed under different ferric ion and citrate concentrations, using the Hyperquad simulation and speciation (HySS) program [231] and iron affinity constants previously described [232, 233]. The plots report the species present at equilibrium.

NTBI export by T lymphocytes

T lymphocytes were depleted of transferrin, as described above, and incubated, unless otherwise stated, in RPMI + 5µM Fe-citrate (or 5µM [55]Fe-citrate) + 20% FCS for 2h. Cells were washed 2× with washing buffer and incubated for different time-periods in RPMI + 20% FCS + 5µM DFO (for short-term experiments),to prevent re-uptake of exported iron, or in RPMI+ 20% FCS (for long-term experiments). At each time-point, the supernatants were collected and Fe was quantified as described in NTBI uptake.

NTBI retention experiment in HH patients

NTBI retention experiment was assessed in CD4^{+} and CD8^{+} T cells and CD14^{+} monocytes isolated from peripheral blood from normal healthy blood donors and HH patients (C282Y homozygous) regularly followed at the Santo António Hospital (CHP-HSA; Porto, Portugal) Hemochromatosis Clinic. HH patients were consecutively recruited into the study at the time of their visit for maintenance therapeutic phlebotomy. Transferrin saturation and haematological parameters were available for all individuals at the time of the experiment. Retrospective biochemical data were reviewed from clinical files by the clinician in charge.

^{55}Fe- citrate stock solutions were prepared by mixing ^{55}FeCl$_3$ with unlabelled trisodium citrate, at Fe:citrate molar ratio (1:20) as previously described. Cells were depleted of intracellular transferrin by incubation for 1 hour in serum-free/iron-free RPMI, washed and incubated with RPMI +5 μM ^{55}Fe-citrate (as 5 μM ^{55}FeCl$_3$+100 μM citric acid), at 37°C. The pH of the uptake medium was maintained at 7.4. Each experiment of NTBI uptake was performed in a normalized number of cells (1x10^5 cells). Cells were incubated *in vitro* with ^{55}Fe- citrate (5μM) for 3 hours. After incubation, cells were washed 3× with ice-cold buffer [5 μM desferrioxamine (DFO) in PBS, pH 7.4], lysed with 0.1% NaOH, 0.1% Triton X-100 and intracellular Fe was measured in a MicroBeta Trilux β-counter (Perkin Elmer), for 1 minute. No significant changes in cell viability, using trypan blue, were observed with the iron treatments. Systemic NTBI retention capacity by PBMCs was calculated by the sum of NTBI retention (at 3 hours) of the CD8$^+$, CD4$^+$ T-lymphocytes and CD14$^+$ monocytes multiplied by the respective cell numbers in each individual.

Results

1 - Quantification and pattern of NTBI uptake by T lymphocytes

Both $CD4^+$ and $CD8^+$ human T lymphocytes accumulate approximately 250 pmol of $Fe/10^6$ cells *in vitro*, when incubated with 5 µM of ^{55}Fe-citrate (5:100) at 37°C (Fig. 1A). The rate of NTBI uptake is higher during the first 30 minutes of incubation (6.4 and 7.1 pmol/min./10^6cells, respectively for $CD4^+$- and $CD8^+$-lymphocytes), followed by a second component in which uptake is maintained at a significantly lower rate (4×10^{-4} and 7×10^{-2} pmol/min./10^6 cells, respectively for $CD4^+$- and $CD8^+$- lymphocytes) until the last time point analyzed (3 hours). A *plateau* in intracellular iron levels is reached after approximately 60 minutes. The rate of uptake at 37°C during the initial 30 minutes was significantly higher than at 4°C (0.02 pmol/min./10^6cells). Treatment with pronase and trypsin following incubation with Fe-citrate did not significantly change cell-associated radioactivity in $CD3^+$ T lymphocytes (representing total T lymphocytes), suggesting that the measured Fe is mostly intracellular (Fig. 1B). In contrast, at 4°C most of the NTBI is associated with the plasma membrane since cell-associated radioactivity was markedly decreased upon treatment with pronase (Fig. 1C).
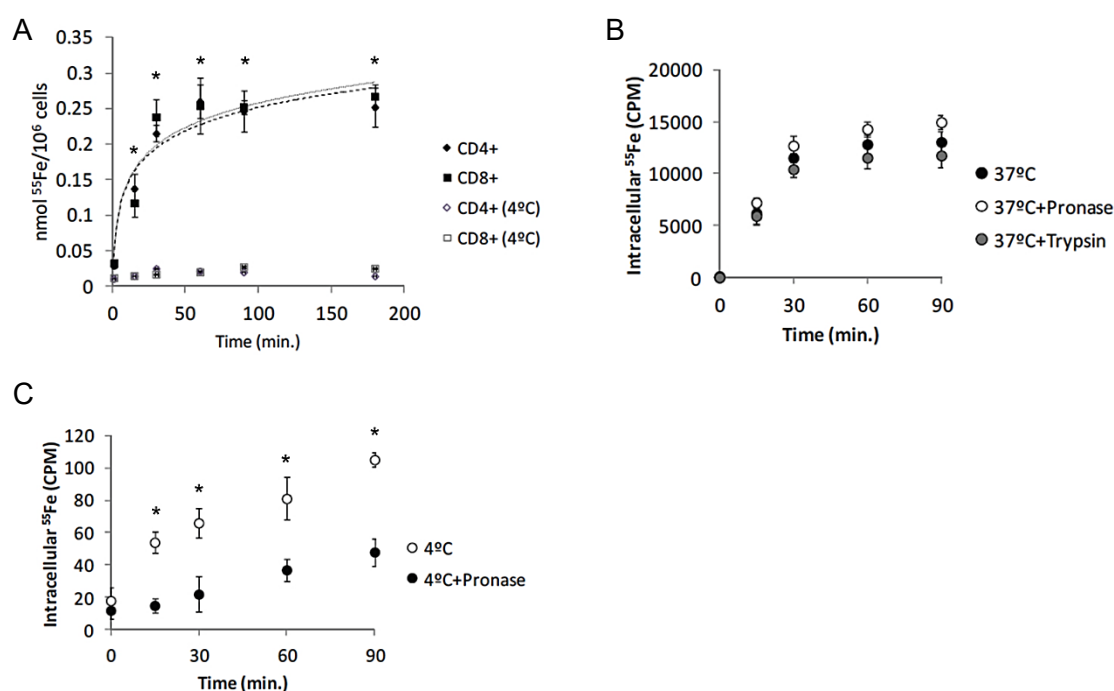
Fig. 1 NTBI uptake by T lymphocytes (A) NTBI uptake by human T-lymphocytes. $CD4^+$ and $CD8^+$ human T-lymphocytes were incubated with 5 µM of ^{55}Fe-citrate (5:100) at 37°C and 4°C and intracellular iron quantified at each time-point. Each point = average (n≥3) ±1SD. (B–C) Specificity of NTBI uptake. $CD3^+$ cells were incubated with 5 µM of ^{55}Fe-citrate (5:100) for up to 90 min, at 37°C (B) or 4°C (C), and at each time point washed either with PBS (with or without pronase) or incubated for 15 min with serum-free RPMI with trypsin. Cell-associated ^{55}Fe levels at each time point were measured. Each point is a mean value (n = 3) ± SD. The similar results obtained at 37°C together with the differences at 4°C suggest that most of the measured iron is intracellular.

Statistical significance between samples at 37°C and controls at 4°C is indicated by * symbols (*p<0.01) (Arezes et al.2013)

In addition to the previous time-dependent experiment a dose dependent experiment was performed by incubating CD3$^+$ T lymphocytes with various concentrations of Fe-Citrate (ranging from 1 µM to 500 µM). We observed that Fe-citrate uptake in T lymphocytes reaches saturation at 200 µM, with a Michaelis constant (K_M) of 92.6 nmol and maximum velocity (Vmax) of 0.4 nmol/min./10^{6}cells (Fig. 2).
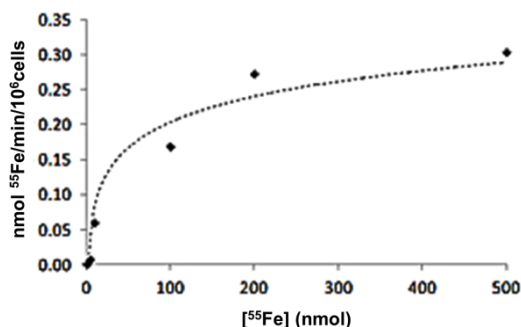
Fig. 2 Kinetics of NTBI uptake in T lymphocytes. Cells were incubated with different concentrations of ^{55}Fe-citrate (1 µM, 5 µM, 10 µM, 100 µM, 200 µM and 500 µM) at 37°C and intracellular iron quantified at various time points (0, 15, 30, 60 and 120 min) (n = 3). The values obtained during the first 30 min of incubation, when the transport system is not saturated, were used to calculate the rate of uptake for each concentration. CD3$^+$ cells reach saturation at 200 µM of Fe-citrate and present a maximum rate of 0.4 nmol/min/10^6 cells (Arezes et al. 2013).

2 - Characterization of the ferric citrate species taken up by T lymphocytes

Although it is commonly accepted that Fe-citrate is one of the most relevant NTBI forms in iron overload disorders, nothing is known regarding the selectivity for particular Fe-citrate species by cells. Taking advantage of the recent development of a speciation model for Fe-citrate [232], we investigated iron uptake by T lymphocytes in the presence of various Fe:citrate ratios, for which the model predicts the formation of distinct Fe-citrate species. In the presence of 100 µM citrate, increase of Fe concentration from 0.1 to 100 µM is predicted to induce a shift from the FeCit$_2$ species to the oligomeric Fe$_3$Cit$_3$, this latter species being essentially the only one present for iron concentrations equal or above 100 µM (Fig. 3A and Table 1). CD3$^+$ lymphocytes were incubated with an equal volume of each of these Fe-citrate solutions, a dose-dependent increase in Fe uptake was observed up to 100 µM Fe (Fig. 3B), with a strong positive correlation observed between NTBI uptake and the presence of [Fe$_3$Cit$_3$] in the solution (Fig. 3C).

In contrast, when CD3$^+$ lymphocytes were exposed to media predicted to contain increasing concentrations of Fe$_3$Cit$_3$ and FeCit$_2$ (Fig. 4A and Table 2), Fe uptake by T cells increased only while [Fe$_3$Cit$_3$] was increasing and stabilized or was inhibited when [Fe$_3$Cit$_3$]

remained stable (Fig. 4 A and B). Finally, a predicted 10-fold increase in [FeCit$_2$] (with constant [Fe$_3$Cit$_3$]; Table 2) significantly inhibited Fe uptake by the lymphocytes, with no correlation found between [FeCit$_2$] and NTBI uptake by these cells (*P*=0.15) (Figure 4C). No association was found between the concentration of any other Fe-citrate species predicted to be present and Fe uptake (data not shown).
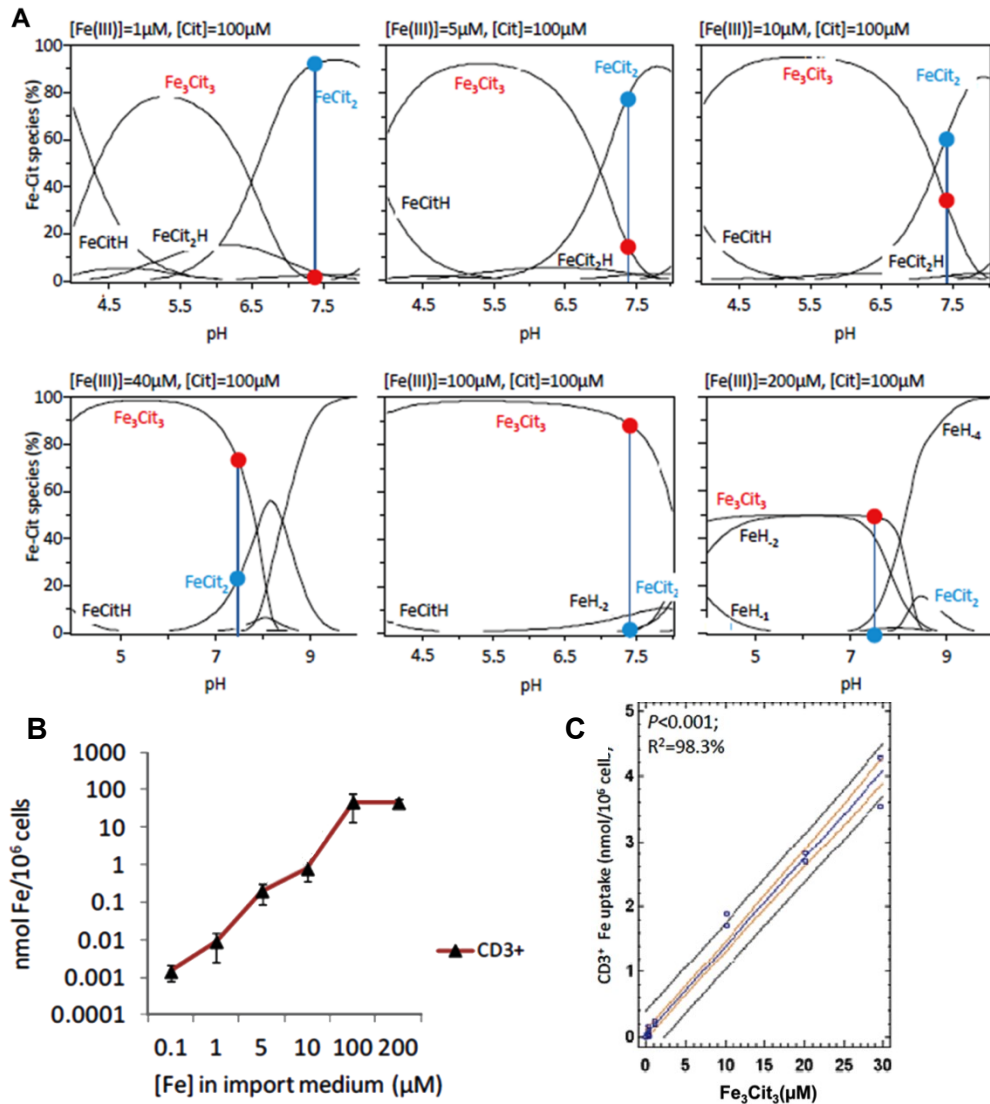
Fig. 3 Fe uptake by T lymphocytes correlates with [Fe$_3$Cit$_3$]. (A) Speciation plots for Fe-citrate species were calculated for Fe:citrate ratios from 1:100–200:100 using the Hyperquad simulation and speciation (HySS) program. Predicted relative abundance (%) of the two most common Fe-citrate species, at pH 7.4, is marked by a blue vertical line and a red (Fe$_3$Cit$_3$) or blue (FeCit$_2$) dot. (B) Fe uptake by T lymphocytes incubated with different iron:citrate ratios increases with the relative abundance of Fe$_3$Cit$_3$. Experiments were performed at least three times with three replicates per experiment. Each point represents the mean (n = 3) ±1SD. (C) Regression analysis showing a significant correlation between Fe uptake by CD3+ cells with predicted [Fe$_3$Cit$_3$] concentration at pH 7.4 (Adapted from Arezes et al.2013).

Table 1 Calculated concentrations of Fe-Citrate (FeCit) species for increasing doses of Fe and 100uM Citrate.

	0.1µM Fe: 100µM Cit	1µM Fe: 100µM Cit	5µM Fe: 100µM Cit	10µM Fe: 100µM Cit	40µM Fe: 100µM Cit	100µM Fe: 100µM Cit	200µM Fe: 100µM Cit
Fe$_3$Cit$_3$ (µM)	2.37×10^{-6}	2.44×10^{-3}	2.40×10^{-1}	1.12	10	29.6	33
FeCit$_2$ (µM)	9.3×10^{-2}	9.22×10^{-1}	3.95	6.09	8	1.65	0
FeCit$_2$H (µM)	3.92×10^{-3}	3.89×10^{-2}	1.67×10^{-1}	2.57×10^{-1}	NA	6.97×10^{-2}	NA
FeCitH (µM)	9.22×10^{-6}	9.31×10^{-5}	4.30×10^{-4}	7.19×10^{-4}	NA	2.14×10^{-3}	NA
FeCit$_2$H$_2$ (µM)	1.22×10^{-5}	1.21×10^{-4}	5.19×10^{-4}	7.99×10^{-4}	NA	2.17×10^{-4}	NA
Fe free (µM)	6.74×10^{-12}	6.92×10^{-11}	3.44×10^{-10}	6.24×10^{-10}	NA	2.04×10^{-8}	NA
Cit free (µM)	4.97×10^{-6}	4.88×10^{-6}	4.53×10^{-6}	4.18×10^{-6}	NA	3.81×10^{-7}	NA
H free (µM)	3.98×10^{-2}	3.98×10^{-2}	3.98×10^{-2}	3.98×10^{-2}	NA	3.98×10^{-2}	NA
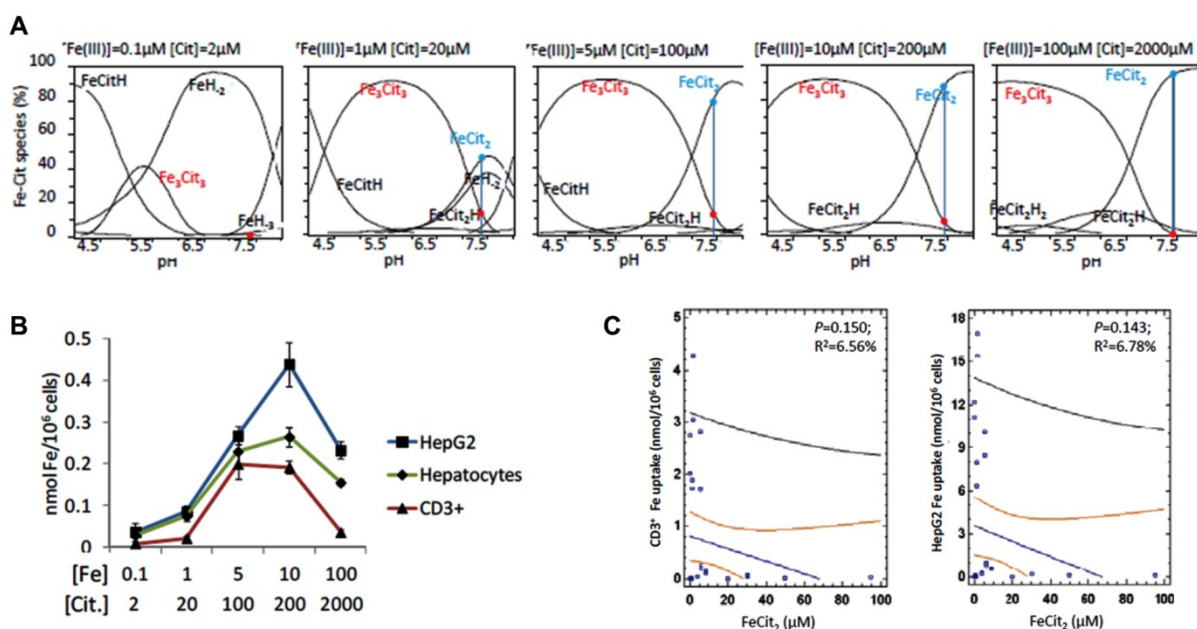
Fig. 4 Fe uptake by T lymphocytes and hepatocytes does not correlate with [FeCit$_2$]. (A) Speciation plots for Fe-citrate species, calculated for increasing Fe-citrate concentrations maintaining a constant Fe:citrate ratio of 1:20 using the Hyperquad simulation and speciation (HySS) program. Predicted relative abundance (%) of the two most common Fe-Cit species at pH 7.4 is marked by a blue vertical line and a red (Fe$_3$Cit$_3$) or blue (FeCit$_2$) dot. (B) Fe uptake by CD3$^+$ lymphocytes in the presence of increasing Fe-citrate concentrations, maintaining a constant Fe:citrate ratio of 1:20 (same conditions as in panel A). Experiments were performed at least three times with three replicates per experiment. Each point represents the mean (n = 3) ±1SD. (C) Regression analysis showing no significant correlation between Fe uptake by CD3$^+$ cells with predicted [FeCit$_2$] concentration at pH 7.4 (Adapted from Arezes et al.2013).

Table 2 Calculated concentrations of Fe-citrate (FeCit) species for increasing doses of Fe and a constant Fe:Citrate ratio of 1:20.

	0.1µM Fe: 2µM Cit	1µM Fe: 20µM Cit	5µM Fe: 100µM Cit	10µM Fe: 200µM Cit	100µM Fe: 2000µM Cit
Fe_3Cit_3 (µM)	6.21×10^{-7}	3.91×10^{-2}	2.40×10^{-1}	3.15×10^{-1}	4.26×10^{-1}
$FeCit_2$ (µM)	1.19×10^{-3}	4.49×10^{-1}	3.95	8.61	94.7
$FeCit_2H$ (µM)	5.02×10^{-5}	1.90×10^{-2}	1.67×10^{-1}	3.63×10^{-1}	3.99
FeCitH (µM)	5.90×10^{-6}	2.35×10^{-4}	4.30×10^{-4}	4.71×10^{-4}	5.21×10^{-4}
$FeCit_2H_2$ (µM)	1.56×10^{-7}	5.90×10^{-5}	5.19×10^{-4}	1.13×10^{-3}	1.24×10^{-2}
Fe free (µM)	2.16×10^{-10}	9.04×10^{-10}	3.44×10^{-10}	1.89×10^{-10}	2.11×10^{-11}
Cit free (µM)	9.95×10^{-8}	9.44×10^{-7}	4.53×10^{-6}	9.02×10^{-6}	8.97×10^{-5}
H free (µM)	3.98×10^{-2}	3.98×10^{-2}	3.98×10^{-2}	3.98×10^{-2}	3.98×10^{-2}

3 - Quantification and pattern of NTBI export by T lymphocytes

In order to have a relevant role as a component of the iron storage compartment, T lymphocytes would need to selectively retain or, alternatively, export intracellular iron acquired as NTBI according to systemic signals. To test this hypothesis we analyzed the export of iron acquired as Fe-citrate by T lymphocytes. $CD4^+$ and $CD8^+$ T cells were exposed to 5µM Fe-citrate for 2h, a time point at which cells have reached the maximum iron content (Fig. 1A), and allowed to export iron into an iron-free medium for up to 6h. We observed that iron export by T lymphocytes follows a linear pattern, $CD8^+$ cells export a little slower matching the $CD4^+$ lymphocyte's export rate after 60min of export (Fig. 5A). After 60min in an iron-free medium, iron export by T lymphocytes corresponds to approximately 3% of intracellular levels, demonstrating as low release of iron acquired as NTBI by these cells. This is confirmed by the quantification of intracellular ^{55}Fe remaining in both T lymphocyte populations throughout time, which further shows that, after 72h of export, T lymphocytes maintain approximately 20% of the initial iron load acquired as NTBI (Fig. 5B).

To test whether iron export by T lymphocytes is dependent on the extracellular NTBI concentration, cells were incubated with increasing ratio of Fe (5, 20, 40 and 100 µM) to 100 µM citrate for 2 hours and allowed to export iron into an iron–free medium. We observed a dose-dependent increase in iron export with increasing NTBI concentrations (Fig. 5C).
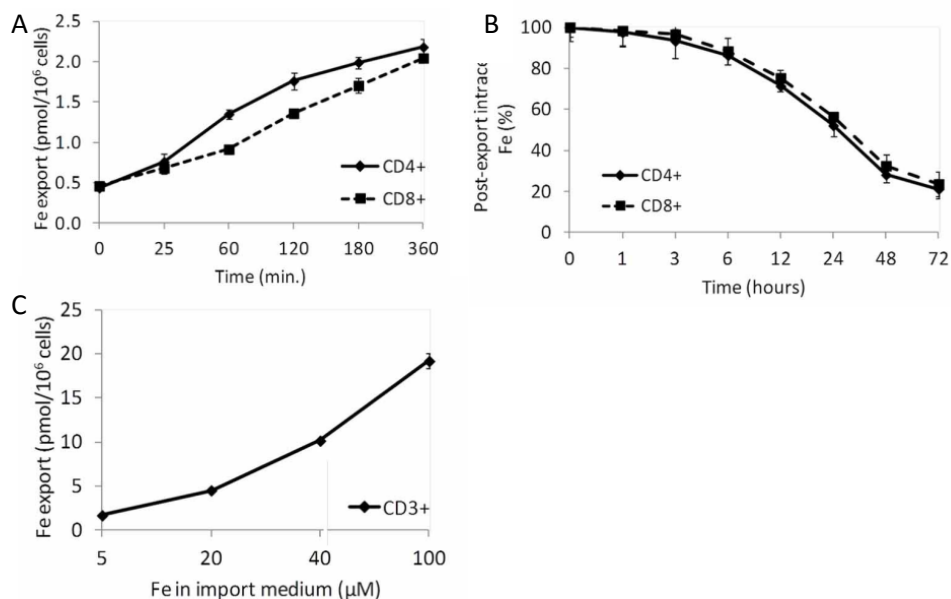
Fig. 5 Iron export by T lymphocytes. A) Time-dependent iron export by T lymphocytes. Each point is a mean value (n=3) ± 1SD. B) Impact of iron export in intracellular Fe levels. Each point is a mean value ± 1SD of two experiments each with three replicates. C) Dose-dependent iron export by T lymphocytes. Each point is the mean of two experiments with two replicates each (Pinto et al.2014).

4 - NTBI retention capacity by CD4^{+} and CD8^{+} T lymphocytes and CD14+ monocytes from healthy controls and HH patients (Unpublished results)

The potential of NTBI sequestration by PBMCs as a modifier of human systemic iron overload was then tested by the quantification of the *ex vivo* uptake of NTBI by T lymphocytes and monocytes obtained from Hereditary Hemochromatosis (HH) patients and from healthy blood donors. CD4^{+}, CD8^{+} T-lymphocytes and CD14^{+} monocytes were isolated from peripheral blood and were incubated for three hours with 5 µM of Fe-citrate. The NTBI retention capacity was measured in a normalized number of cells ($1x10^5$) of each sub-population. Results are presented in Figure 6 with transformed values of Log CPM. The average of NTBI uptake by CD4^{+} T cells was 3.83±0.12 in controls and 3.77±0.40 in HH patients, by CD8^{+} T cells was 3.70±0.11 in controls and 3.70±0.39 in HH patients and by the monocytes was 3.57±0.17 in controls and 3.65±0.37 in HH patients. Although the averages were very similar between patients and controls, the standard deviation denotes the existence of a remarkable higher variability in HH patients.

All HH patients were in maintenance treatment and patient's systemic iron status, as measured by the percentage of plasma transferrin saturation (TfSat) at the time of experiment, varied from 40 to 85%. These TfSat values were significantly correlated with the average TfSat levels measured serially during the previous 12 months (r=0.97; R^2=57%; *P*=0.0299), reflecting the existence of highly stable individual profiles.
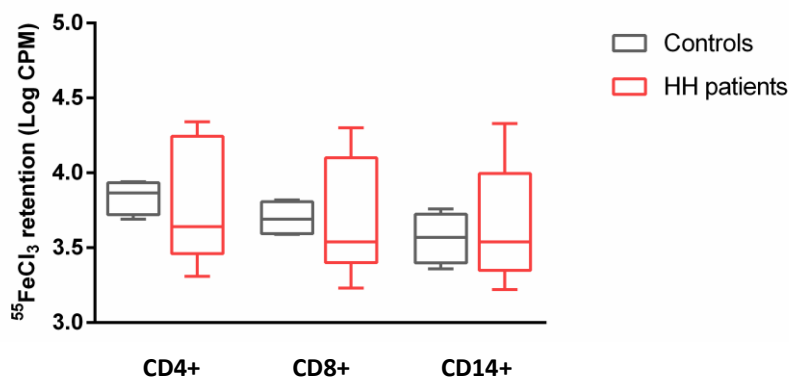
Fig. 6 NTBI retention capacity by CD4+, CD8+ T lymphocytes and CD14+ monocytes isolated from healthy blood donors as controls (n=4) and HH patients (n=9). Box-whiskers graph with minimum and maximum values represented.

5 - Systemic NTBI retention capacity by total PBMCs distinguish two groups of HH patients with different re-accumulation pattern (Unpublished results)

The systemic NTBI retention capacity by the PBMCs, estimated as the sum of NTBI accumulated by T lymphocytes and monocytes multiplied by total numbers of these cells in each individual, showed a significantly different distribution between HH patients and controls (Fig. 7A). In HH patients two groups could be identified, respectively with normal (in the same range of controls) and defective NTBI retention (Chi-square test χ^2=4.952; *P*=0.026; Table 3), with values correlating inversely with the TfSat levels at the time of each experiment (r=-0.76; R^2=58%; *P*=0.017; Fig. 7B). This finding prompted us to analyze retrospectively if there were differences between the two groups of HH patients in the pattern of iron re-accumulation into the plasma transferrin pool following the completion of the iron depletion treatment (at this point all patients displayed similar TfSat values). The results clearly showed that patients with a lower NTBI retention capacity by PBMCs had a faster and higher re-accumulation pattern in comparison with patients with a normal NTBI retention profile (Fig. 7C). This set of results demonstrates *in vivo* the relevance of circulating immune system cells in the protection from systemic iron load.

Table 3 Contingency table displaying the association between individual status (HH patient or control) and NTBI retention by PBMCs

NTBI retention (Log CPM)	Controls	HH patients	Statistics
> 9.5	4	3	χ^2=4.952
< 9.5	0	6	*P*=0.026
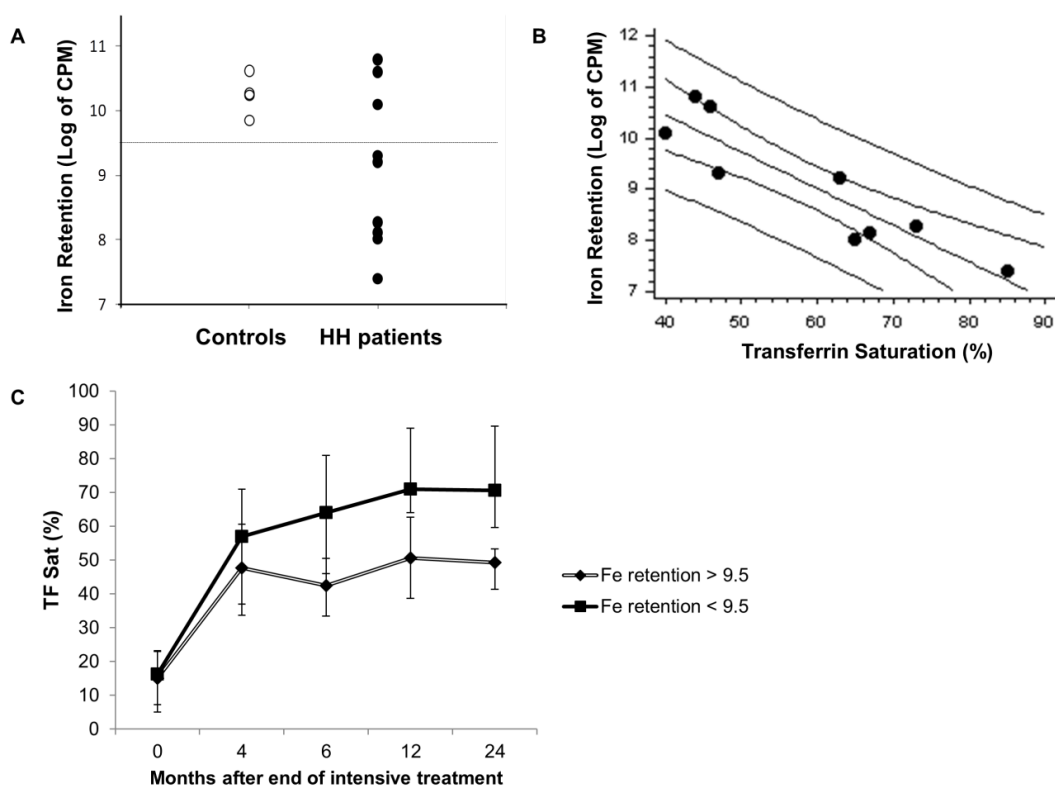
Fig. 7 Impact of NTBI retention by PBMCs in iron parameters of HH patients

(A) NTBI accumulation (Log CPM) by PBMCs (T lymphocytes + monocytes) of HH patients (n=9) and blood donor controls (n=4). Horizontal line signals the cutoff value (9.5) used for division of HH patients in high and low NTBI retainers. (B) Linear regression analysis (r=-0.76; R^2=58%; *P*=0.017) of the correlation between TF saturation at the time of analysis and NTBI retention by PBMCs. Each dot represents one HH patient. (C) Profiles of iron re-accumulation into the plasma TF pool for 24 months after completion of intensive treatment in the two groups of HH patients, divided as normal or low NTBI retainers (Log NTBI retention > 9.5 and < 9.5, respectively). Average of TfSat values for each time point ± maximum and minimum values are represented.

Considering the average total numbers of T lymphocytes and monocytes in a healthy individual, those values correspond to a maximum NTBI retention potential ranging from 45.1-149.9 µmol (for CD4$^+$ cells), 22.5-82.5 (for CD8$^+$) (Table 4), which is well above the physiological systemic NTBI levels commonly present in iron overload conditions.

Table 4 Estimated maximum NTBI retention potential of human CD4$^+$, CD8$^+$ and CD14$^+$ PBMCs.

	CD4$^+$	CD8$^+$	CD14$^+$
Human Total cell number [min-max]	[2.65 – 8.8 x10^9]	[1.5 – 5.15 x 10^9]	[1.05 – 4.60 x 10^9]
Maximum NTBI retention potential (µmol) [min-max]	[45.1 – 149.9]	[22.5 – 82.5]	[18.9 – 82.8]

Discussion

In this chapter, we address the reciprocal interactions between NTBI and lymphocytes which are among the first cell types from the circulating immune system to get in contact with this (and other) iron species, following its entrance into the blood circulation.

The *in vitro* studies here performed aimed to address the kinetics of the interaction between NTBI specie, in the form of iron-citrate, and T lymphocytes. Fe-citrate uptake by $CD4^+$ and $CD8^+$ T cells show that both human T lymphocytes accumulate a maximum of approximately 250 pmol of $Fe/10^6$cells *in vitro*, when incubated with 5µM of ^{55}Fe-citrate (5:100) at 37°C. A plateau in intracellular iron levels is achieved after approximately 60 minutes. The maximum rate of ^{55}Fe uptake by T cells is comparable to the described uptake rate of the hepatoma cell line HepG2 [234] and to what is described for primary hepatocytes [112] although T lymphocytes shown to be incapable to sustain this elevated rate of intake for more than 30 minutes. This difference leads to a lower capacity of each lymphocyte to accumulate NTBI when compared with hepatocytes which are able to increase intracellular NTBI accumulation *in vitro* for at least one week [235].

Several potential iron-binding ligands are present in plasma, including citrate, acetate and albumin. Albumin, the most abundant blood plasma protein [236], has been shown to bind iron both in the presence of citrate, as a ternary complex, or in its absence [237]. Nevertheless, May et al. [238], based on the relative concentrations of potential ligands, predicted that the dominant iron species present in plasma is ferric-citrate, the NTBI form used in the present study. Under the experimental condition of 5µM Fe:100µM Citrate at pH 7.4, we observed a strong and exclusive association between Fe uptake and the predicted presence of the Fe_3Cit_3 oligomer in solution, in contrast with the lack of association with $FeCit_2$ or with any other ferric-citrate species. We recognize that there are differences in the media composition used for the development of the speciation models (salt-buffered aqueous solution) and for the Fe uptake assays (RPMI medium). The simple aqueous solution used for model predictions may not hold several iron binding molecules that RPMI medium possess. However, significant changes in the predicted speciation between the aqueous solution and the uptake medium would only be expected if there is competition for Fe by those ligands. Under our conditions transferrin will not significantly compete with citrate, since it is 85% saturated (20% HH human plasma supplemented). Similarly, acetates, pyruvates and phosphates will not compete with citrate for Fe when the citrate concentration is ≥100 µM [238], as it is the case in our experimental conditions as well as in human plasma. Finally, albumin has been described to efficiently bind iron [237] but its ability to significantly modify citrate-bound iron is dependent on its glycation and oxidation [239]. Healthy individuals have approximately only 1% of their serum albumin glycated, and this

value increases up to 10% in diabetic patients [236]. Iron-overloaded individuals do not display higher levels than the healthy 1% baseline condition, suggesting that, at least on the absence of increased glucose levels, glycated albumin will not significantly compete for iron with citrate. Albumin oxidation, on the other hand, could have a relevant effect, in face of the pro-oxidant conditions expected to be induced by the iron overload. Previous studies have shown that fully oxidized albumin does not show increased iron binding capacities up to 5 µM of iron, but a 2.6- fold increase was observed for 10 µM of Fe [239]. Thus, in pro-oxidant conditions albumin may show an increased capacity to modify citrate-bound concentrations, although we predict that this will only be significant for very high NTBI concentrations and extensive albumin oxidation.

The results here presented also show that the differences in Fe uptake in each experimental condition and the high correlation between Fe_3Cit_3 and Fe uptake are not due to a preferential uptake of membrane-bound Fe in particular conditions but instead may reflect a high specificity of a still unidentified putative receptor for the oligomeric Fe-citrate species. We anticipate that this finding may be instrumental in the search for the elusive Fe-citrate transporter since it represents the identification of the ligand to which the transporter may respond, either at the level of transcription, translation or other form of modification. The high correlation between the presence of the oligomer Fe_3Cit_3 and Fe uptake may be surprising, as donation of Fe by smaller sized mononuclear Fe-citrate species might be expected to be easier, particularly if the uptake involves a channel transporter. However, predictions from models and from kinetics of NTBI chelation by DFO and deferiprone suggested that the dominant species under relevant concentrations of citrate are likely to be oligomeric forms, with a molecular mass around 3.5 kDa [232][240]. It seems thus reasonable to expect that, throughout evolution, cells have specialized in sensing and internalizing this particular species. Nevertheless, it is conceivable that particular tissues and cell types may be equipped with different cellular NTBI uptake systems, which would enable the discrimination between distinct NTBI species and could explain the different patterns of organ iron-loading observed in the various iron overload syndromes [9]. Particularly interesting would be to extend the present analysis to cardiomyocytes, a cell type in which NTBI accumulation has a particularly adverse effect [241, 242] and for which the involvement of specific NTBI transporters have been suggested [116]. Finally, the demonstration that Fe_3Cit_3 represents an important component of the NTBI taken up by hepatocytes and T lymphocytes could be used as a tool for optimization of chelator properties and of chelation regimens presently in use.

Regarding $CD4^+$ and $CD8^+$ T lymphocytes ability to export/retain NTBI, the results show that these two cell types do not differ significantly in the export/retention of iron-citrate, which is in agreement with our findings of similar NTBI uptake by the two cell types. This may

indicated that both cell types are equally equipped to mobilize iron-citrate. These results are supported by previous observations in $\beta_2m^{(-/-)}Rag1^{(-/-)}$ mice—deficient in CD4^{+} and CD8^{+} T lymphocytes and B lymphocytes that displayed higher severity in terms of iron overload than the $\beta_2m^{(-/-)}$ animals—deficient in CD8^{+} T lymphocytes alone [28].

From the observations in mice deficient in CD8^{+} T lymphocytes [23, 24, 34] and also from the recurrently inverse correlation only observed with CD8^{+} T lymphocyte numbers and the severity of iron overload in HFE-HH human patients [30, 32, 171] one may expect that CD8^{+} T cells, although not being the only cell type with NTBI retention ability, may have an important role in systemic iron homeostasis and the lack or a reduced number of these cells may affect the fine-tuning of iron homeostasis, namely NTBI distribution.

After the demonstration of H-ferritin synthesis by human T and not B lymphocytes [243], the present demonstration of the T lymphocytes ability to take up and retain NTBI, is perhaps the strongest piece of evidence supporting the postulate put forward by de Sousa and co-workers that these cells could act as buffers to protect other tissues from iron-mediated toxicity [3]. Our *in vitro* results estimate an elevated potential for the circulating populations of monocytes and T lymphocytes to influence the concentration of circulating NTBI. To address if PBMCs from HH patients had different NTBI retention capacity than cells isolated from healthy blood donors, we performed a NTBI retention assay with ex-vivo CD4^{+} and CD8^{+} T lymphocytes and monocytes isolated from peripheral blood from both groups.

Despite the small sample size of the healthy control group, it should be noticed that each experiment was performed with cells isolated from randomly recruited blood donors and from these independent experiments we observed a very small variation as reflected in a low standard deviation. In contrast, HH patients show a high heterogeneity in the NTBI retention ability by T lymphocytes and monocytes. These results are extended by the observation that the individual profiles of iron re-uptake by HH patients, following the end of intensive treatments, strongly correlate with the NTBI retention potential of each individual's cell types. Although in these patients, as in blood donor controls, the systemic levels of NTBI should be low, we interpret that circulating PBMCs, by sequestering a fraction of the newly exported iron, may modify transferrin saturation, in direct proportion to the retention potential of each individual. These results provide an explanation for the previous observation of spontaneous iron overload in CD8^{+}- and total T lymphocyte-depleted animals [24, 28, 34, 35], as well as for the inverse correlation observed between CD8^{+} T lymphocyte numbers and the severity of iron overload in HH patients [30, 32, 171].

On a broader scope, our results provide a mechanistic support for the possibility of circulating T lymphocytes and monocytes acting *in vivo* as key partners in systemic iron homeostasis. However, a number of questions remain unanswered. Why only CD8^{+} lymphocyte numbers and not CD14^{+} or CD4^{+}, have been associated with iron overload in

human HH patients? What is the fate, in the long term, of the NTBI sequestered by monocytes and T lymphocytes? What is the impact of the intracellular NTBI on the phenotype of each cell population (survival, activation potential, migration, etc.)? These questions prompted us for the following research objective where the CD8$^+$ T cells phenotype and gene expression profile was addressed in the context of *Hfe* ablation.

3.4

Lymphocyte gene expression signatures from patients and mouse models of hereditary hemochromatosis reveal a function of HFE as a negative regulator of CD8^{+} T-lymphocyte activation and differentiation in vivo

This chapter is published in:

Content

Abstract

Abnormally low CD8$^+$ T-lymphocyte numbers is characteristic of some patients with hereditary hemochromatosis (HH), a MHC-linked disorder of iron overload. Both environmental and genetic components are known to influence CD8$^+$ T-lymphocyte homeostasis but the role of the HH associated protein HFE is still insufficiently understood. Genome-wide expression profiling was performed in peripheral blood CD8$^+$ T lymphocytes from HH patients selected according to CD8$^+$ T-lymphocyte numbers and from *Hfe*$^{-/-}$ mice maintained either under normal or high iron diet conditions. In addition, T-lymphocyte apoptosis and cell cycle progression were analyzed by flow cytometry in HH patients. HH patients with low CD8$^+$ T-lymphocyte numbers show a differential expression of genes related to lymphocyte differentiation and maturation namely *CCR7*, *LEF1*, *ACTN1*, *NAA50*, *P2RY8* and *FOSL2*, whose expression correlates with the relative proportions of naïve, central and effector memory subsets. In addition, expression levels of *LEF1* and *P2RY8* in memory cells as well as the proportions of CD8$^+$ T cells in G2/M cell cycle phase are significantly different in HH patients compared to controls. *Hfe*$^{-/-}$ mice do not show alterations in CD8$^+$ T-lymphocyte numbers but differential gene response patterns. We found an increased expression of *S100a8* and *S100a9* that is most pronounced in high iron diet conditions. Similarly, CD8$^+$ T lymphocytes from HH patients display higher S100a9 expression both at the mRNA and protein level. Altogether, our results support a role for HFE as a negative regulator of CD8$^+$ T-lymphocyte activation. While the activation markers S100a8 and S100a9 are strongly increased in CD8$^+$ T cells from both, *Hfe*$^{-/-}$ mice and HH patients, a differential profile of genes related to differentiation/maturation of CD8$^+$ T memory cells is evident in HH patients only. This supports the notion that HFE contributes, at least in part, to the generation of low peripheral blood CD8$^+$ T lymphocytes in HH.

Keywords: Hemochromatosis, HFE, iron, CD8$^+$ T lymphocytes, S100a9, lymphocyte homeostasis

Introduction

Hereditary hemochromatosis is a common genetic disorder of iron overload where the vast majority of patients are homozygous for the C282Y mutation in *HFE*, a non-classical MHC-class I gene localized on chromosome 6 in strong linkage disequilibrium with the HLA-A locus [184, 244]. The conformational change introduced by the C282Y mutation impairs the association of HFE with β(2)-microglobulin and consequently its expression at the cell surface [27]. As an integral part of a membrane-associated protein complex in hepatocytes, HFE is involved in the regulation of hepcidin, a hormone that controls systemic iron levels [245]. Whether HFE is also involved in T-lymphocyte signaling, is still unresolved.

Abnormalities in the pool of CD8$^+$, but not CD4$^+$, T lymphocytes have been consistently reported in HH patients [179]. Low numbers of CD8$^+$ T lymphocytes in the peripheral blood [21, 22, 30] as well as in the liver [33] are associated with severe expression of iron overload. The low numbers of CD8$^+$ T lymphocytes are mostly due to defects in the subpopulation of the effector memory T cells [31]. So far, functional studies have not been conclusive in terms of elucidating the nature of the CD8 defects in HH. Although decreased CD8-associated p56lck activity [170] and diminished cytotoxic activity [29] have been reported, other studies suggested a more activated profile of these cells namely a relative expansion of CD8$^+$CD28$^-$ T-cell populations, a high percentage of CD8$^+$HLA-DR$^+$ cells and an increased production of IL-4 and IL-10 [29, 172]. A possible explanation for the activation profile of CD8$^+$ T cells in HH may be found in a recent work where Reuben and co-workers propose that HFE has a role in antigen processing and presentation leading to an inhibition of CD8$^+$ T-lymphocyte activation [224]. Their studies were based on several T-lymphocyte activation read-outs in cells transfected with wild type and mutated HFE molecules, but no evidence has been provided of an effect on antigen processing and presentation functions *in vivo*.

The anomalies of CD8$^+$ T-lymphocyte numbers in HH could be a consequence of iron overload or a direct effect of HFE on the homeostatic regulation of this cell population. The finding that young, early diagnosed asymptomatic HH subjects already display a low CD8$^+$ phenotype similar to their clinically affected family members, favors the idea of a predominantly primary genetic effect linked to the HFE mutation [22]. On the other hand, the fact that some HH patients despite the same HFE defect do not display the low CD8$^+$ phenotype indicates that environmental and/or genetic factors must compensate for the anomalies in the CD8$^+$ T-cell pool independently of HFE. It is known that modifications in gene expression concur to define the different properties of CD8$^+$ T cells at different differentiation stages and therefore their homeostatic equilibrium [157]. We have shown that particular HLA-A alleles and haplotypes are significantly associated with CD8$^+$ T-cell

numbers in HH patients carrying the same *HFE* mutation [43, 44] but they do not constitute a universal marker in all patients analyzed [220]. Studies are still pending trying to localize other relevant markers in the same chromosomal region. Genomic based studies, however, are not sufficient to distinguish the functional effect of HFE from that of other MHC-class I genes in strong linkage disequilibrium in the same chromosomal region.

In the present study we addressed the question whether HFE shapes the peripheral pools of CD8$^+$ T lymphocytes. We applied two independent RNA-based genome wide approaches in isolated CD8$^+$ T cells from HH patients homozygous for the C282Y *HFE* mutation and disease mouse models lacking the *HFE* gene (*Hfe*$^{-/-}$). While studies in HH patients revealed the impact of HFE on the expression of genes associated with the differentiation and maturation of peripheral CD8$^+$ T-lymphocyte subsets, the transcriptional profile of isolated CD8$^+$ T lymphocytes from *Hfe*$^{-/-}$ mice revealed alterations in CD8$^+$ T-cell activation-related genes, a result also confirmed in peripheral blood lymphocytes from HH patients. Altogether, our results support a mechanistic role for *HFE* as a negative regulator of CD8$^+$ T-lymphocyte activation *in vivo* and provide formal evidence, at least in part, to explain the characteristic low CD8 phenotype of HH patients.

Results

1- A genome-wide transcriptional profile of CD8$^+$ T lymphocytes from HH patients is indicative of the subpopulations' differentiation/maturation states

A transcriptional gene profiling study of sorted CD8$^+$ T lymphocytes from HH patients was performed to identify gene response patterns that may explain lower peripheral blood CD8$^+$ T-lymphocyte numbers in patients with HH and severe iron overload. We took advantage of the known clinical and immune phenotypical variability in HH and selected 10 patients stratified in two distinct groups: group 1 (n=6) shows a typical low CD8 phenotype ($<300 \times 10^3$/ml) (see Methods) hallmarked by a severe clinical expression of iron overload; group 2 (n=4) shows normal/high CD8 phenotype ($\geq 400 \times 10^3$/ml) (see Methods) and very mild clinical expression of HH. Gene expression analysis identified a signature of 16 genes (7 up-regulated and 9 down-regulated) potentially associated with the CD8$^+$ T-cell phenotype (Table 1). The magnitude of gene expression changes was small, generally less than 2-fold. Multiple variable correlation analysis among the 16 gene candidates identified two independent clusters of genes, which are functionally interlinked. One cluster contained the genes: chemokine C-C motif receptor 7 (*CCR7*), lymphoid enhancer-binding factor 1 (*LEF1*) and actinin alpha 1 (*ACTN1*), which are all down regulated in the group of patients with the low CD8 phenotype and are markers of CD8$^+$ T-cell differentiation and/or maturation. The chemokine receptor CCR7 is a differentiation/maturation marker present in naïve (T$_N$) and central memory (T$_{CM}$) cells but absent in the effector memory (T$_{EM}$) pool [246, 247]. *LEF1* has been described as being down-regulated in naïve CD8$^+$ T cells after antigen encounter and differentiation *in vivo* [248]. Of the three genes in this cluster, only *ACTN1* (HS1) was not previously described as a differentiation/maturation marker, but it is known to be involved in cytoskeletal remodeling and calcium mobilization, a fundamental process for T-cell activation [249]. A very distinct picture was observed for the second cluster of functionally related genes which included: N(alpha)-acetyltransferase 50 (*NAA50*), purinergic receptor P2Y (G-protein coupled, 8) (*P2RY8*) and FOS-like antigen 2, (*FOSL2*) that are all up-regulated in the group of patients with a low CD8 phenotype. This group of genes is involved in lymphocyte activation and expansion. Both *P2RY8* and *FOSL2* have been implicated as regulators of cell proliferation, differentiation, and malignant transformation [250, 251] and *NAA50* is described as an anti-apoptotic molecule [252].

Table 1 Summary of differentially expressed genes in total CD8 T-lymphocytes in HH patients with a low CD8 phenotype (n=6) relative to HH patients with a normal/ high CD8 phenotype (n=4).

GeneBank accession #	Gene Symbol	Gene Description	Fold Change (Profile A vs Profile B)
NM_002123.3	*HLA-DQB1*	Major histocompatibility complex, class II, DQ beta1	Up 1.82
NM_002124.2	*HLA-DRB1*	Major histocompatibility complex, class II, DR beta1	Up 1.82
NM_005253	*FOSL2*[a)]	FOS-like antigen 2	Up 1.59
BC096168	*HIST1H1E*	Histone cluster 1, H1e	Up 1.57
NM_178129	*P2RY8*[a)]	Purinergic receptor P2Y, G-protein coupled, 8	Up 1.57
BC009288	*NR4A2*[a)]	Nuclear receptor subfamily 4, group A, member 2	Up 1.52
BC012731	*NAA50*[a)]	N(alpha)-acetyltransferase 50, NatE catalytic subunit	Up 1.51
NR_003330	*SNORD116-15*	Small nucleolar RNA, C/D box 116-15	Down 1.90
BC038982	*IGJ*	Immunoglobulin J polypeptide, linker protein for immunoglobulin alpha and mu polypeptides	Down 1.81
NR_002907	*SNORA73A*	Small nucleolar RNA, H/ACA box 73A	Down 1.74
BC035343	*CCR7*[a)]	Chemokine (C-C motif) receptor 7	Down 1.68
DQ496098	*ACTN1*[a)]	Actinin, alpha 1	Down 1.65
NR_003332	*SNORD116-17*	Small nucleolar RNA, C/D box 116-17	Down 1.57
NR_001290	*SNORD116-19*	Small nucleolar RNA, C/D box 116-19	Down 1.57
AF288571	*LEF1*[a)]	Lymphoid enhancer-binding factor 1	Down 1.56
NM_019111.4	*HLA-DRA*	Major histocompatibility complex, class II, DR alpha	Down 1.52

For definition of low CD8 phenotype and normal/high CD8 phenotype see Methods.

a) Confirmed by custom designed real-time PCR primers

Besides the above described genes, a significant up regulation of the MHC class II genes *HLA-DQB1* and *HLA-DRB1*, as well as the histone cluster 1 gene *HIST1H1e*, was also observed in patients with a low CD8 phenotype, supporting the notion of an activation and cell cycle progression pattern of these cells [253].

In order to explore the significance of the results obtained in this screen, we analyzed the correlations of the expression levels of each gene with the clinical and immune phenotypic variables. These included the number of peripheral blood CD8^{+} T lymphocytes, including the differential pattern of CD8 T_N, T_{CM} and T_{EM} cells as well as the iron overload profile, measured by the estimated total body iron stores (TBIS). The results are given in supplementary S1 Table. They strongly suggest that the differences observed in the gene expression of CD8^{+} T cells between the two HH groups reflect not only upon differences in the relative proportions of their CD8^{+} T-cell subsets but also upon differences in the activation profile of the cells. More specifically, the differentiation markers *CCR7*, *LEF1* and *ACTN1* correlated positively with the number of CD8^{+} T_N and T_{CM} cells in each patient,

reflecting a direct impact of the relative proportion of these subpopulations in the total CD8$^+$ pool expression pattern. In contrast, the activation markers *NAA50*, *P2RY8* and *FOSL2* were negatively correlated with the total number of CD8$^+$ T$_{EM}$ cells in each patient, indicating that subjects with a low CD8 phenotype show more activated effector memory cells. Curiously, variations in the mRNA expression levels of these activation genes had more impact on the total number of CD8$^+$ T lymphocytes than the expression of the differentiation markers *CCR7*, *LEF1* and *ACTN1* (see data on S1 Table).

In general, the TBIS was most significantly correlated with the differentiation markers *CCR7*, *LEF1* and *ACTN1* (see also data on S1 Table) therefore not excluding an effect of iron overload on the most immature CD8$^+$ T lymphocytes or vice-versa. It should be noted, however, that due to the strict selection criteria applied in this screen, it was not possible to discriminate the confounding effects of the CD8$^+$ T-cell numbers and of the iron overload phenotypes, because the two variables are highly correlated (R^2=57%; r=-0.75, p=0.0187).

In order to rule out the hypothesis of a bystander effect of systemic inflammation on the patients' individual immunophenotypes, we retrieved historical measures of their C-reactive protein (CRP) serum levels and compared them with the CD8$^+$ T-lymphocyte counts determined on the same day. No significant correlation was found between the two parameters (R-squared adjusted for d.f.= -1.19185 percent; p=0.379), thus excluding any relevant effect of systemic inflammation on the patients' immunophenotype.

2 - Analysis of CD8$^+$ T-lymphocyte subsets reveals the impact of HFE on the expression profile of central memory and effector memory cells

As shown above, the transcriptional profiles of HH patients with low or normal/high CD8$^+$ T-cell numbers not only highlight the differences in the relative proportions of their subsets but also reflect differences in the activation state of the cells. To understand if the gene expression profiles are informative beyond reflecting upon T-cell numbers, we next focused on the analysis of 6 genes (*CCR7*, *LEF1*, *ACTN1*, *FOSL2*, *P2RY8* and *NAA50*) in the different CD8$^+$ T$_N$, T$_{CM}$ and T$_{EM}$ compartments. Cells were sorted according to the gating strategy illustrated in Fig. 1A, in blood samples from a group of 10 additional and unselected HH patients and 8 healthy control individuals. With this approach we aimed: i) to validate the results of the genome wide screen with independent HH samples ii) to test the impact of HFE on gene expression by comparing HH patients with normal healthy subjects and iii) to address if there was any additional impact of serum iron levels on the expression profiles in individual T-cell populations of HH patients, taking advantage of the fact that patients were at different stages of treatment and therefore showing a wide range of transferrin saturation values.

A.

B.

○ **Controls** ● **HH patients**
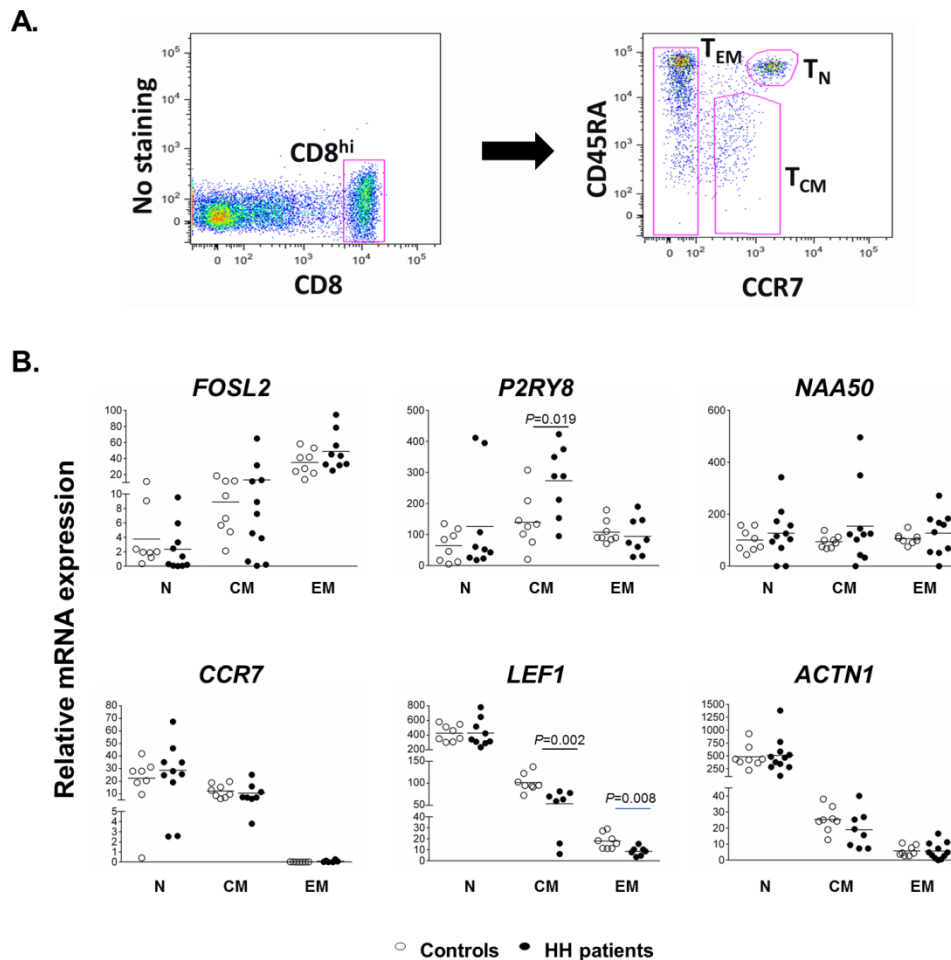
Fig. 1 Gene expression analysis in CD8^{+} T-cell subpopulations

A) Gating strategy used to discriminate the CD8^{+} T subpopulations of naïve, central memory and effector memory cells. **B)** Relative mRNA expression levels of *CCR7*, *LEF1*, *ACTN1, FOSL2*, *P2RY8* and N*AA50* in isolated CD8^{+} T subpopulations. Statistical significant differences were calculated by T-test between HH patients and controls in each subpopulation.

As illustrated in Fig. 1B, the mRNA expression levels of *CCR7*, *LEF1* and *ACTN1* decreased from CD8^{+} T_N to T_{EM} cells, with the lowest values consistently observed in the T_{EM} subset. Once *CCR7* is a well-known maturation marker of T lymphocytes [246] it served as a non-anticipated positive control in our experiment. An opposite pattern was detected for *FOSL2*, which was up-regulated in the most differentiated lymphocyte subpopulation scrutinized, i.e. in T_{EM}. *P2RY8*, in turn, showed the highest expression levels in T_{CM} cells, while *NAA50* was uniformly expressed in all CD8^{+} T-cell subsets. Of note, significant differences were observed in the profile of T_{CM} cells between HH patients and controls, *LEF1* being significantly decreased (*p*=0.002) and *P2RY8* significantly increased (*p*=0.019) in HH patients. In addition, *LEF1* in HH patients was also significantly decreased in T_{EM} (*p*=0.008). These differences between HH patients and controls in the gene transcription of central and effector memory cells, suggest that the HFE defect may affect the homeostatic equilibrium of

these particular populations without affecting the naïve T cells. Importantly, no significant correlations were found between the expression of any of the analyzed genes and the levels of circulating iron as measured by the transferrin saturation (data not shown) further supporting a primary effect of HFE on CD8$^+$ T-lymphocyte signaling independently from circulating iron levels.

3 - Apoptosis and cell cycle studies in CD4$^+$ and CD8$^+$ T lymphocytes from HH patients and controls

The fact that the genes found up regulated in patients with the lowest CD8$^+$ counts were genes involved in activation and proliferation suggests that, in spite of constituting a small pool, these cells must be constantly activated to proliferate. The next question to address was therefore to investigate whether an altered apoptosis/proliferation balance of peripheral blood CD8$^+$ T lymphocytes in HH patients can account for these observations. Since this is the first study analysing apoptosis and cell cycle profiles in T lymphocytes from HH patients, the study was extended to both CD4$^+$ and CD8$^+$ subpopulations of T lymphocytes.

3.1 Apoptosis in CD8$^+$ T lymphocytes correlates with systemic iron levels

In general, a highly significant difference was found between the CD4$^+$ and CD8$^+$ T-lymphocyte subpopulations in terms of the percentages of apoptotic cells (T Test $p=9.4 \times 10^{-8}$, KS-Test $p=0.000002$), with the average apoptosis percentage being 21.8% ±9.9% in CD4$^+$ T cells, and 47.3% ±21.8% in CD8$^+$ T cells. Apoptosis in CD4$^+$ and CD8$^+$ T cells was not influenced by gender but it was influenced by age in CD8$^+$ T cells only ($R^2=13.5$%, $r=0.37$, $p=0.0380$). In general, apoptosis in each of these subsets (CD4$^+$ or CD8$^+$ T cells) was not statistically different between controls and HH patients and, in this later group, it was not influenced by the treatment status i.e. (intensive vs. maintenance treatment) (data not shown). In terms of association with total numbers, no significant correlations were found between apoptosis and either CD4$^+$ or CD8$^+$ T-cell total counts (cells/mm^3) in both HH patients and controls, indicating that defective numbers in HH are not explained by increased apoptosis (data not shown). Nevertheless, the percentage of apoptosis in both CD8$^+$ and CD4$^+$ T cells in HH patients was significantly correlated with the systemic iron load parameters namely serum iron (respectively $R^2=34.6$%, $p=0.008$ and $R^2=20.5$%, $p=0.046$) and transferrin saturation (respectively $R^2=32.9$%, $p=0.006$, and $R^2=20.4$%, $p=0.045$).

3.2 Peripheral blood CD8^{+} T lymphocytes from HH patients show an increased proportion of cells in the G2/M phase

Marked differences were observed between the populations of CD4^{+} and CD8^{+} T cells regarding the proportion of cells along the three phases of cell cycle, particularly in G2M and S (Table 2). Regarding the differences between HH patients and controls, some significant differences could be observed independently of iron status (Table 2). In general, there were more lymphocyte in S and G2/M and less in G0/G1 phase in HH patients than in controls, both in CD4^{+} and CD8^{+}. These differences reached statistical significance in G2/M with values in patients being 2.5 and 11 times higher respectively in CD8^{+} and CD4^{+} cells, and in G0/G1 for CD4^{+} T cells only, although this difference is less than 0.2% of their absolutes levels, probably reflecting the space occupied by the increased numbers of cells in G2/M. No significant correlation was found between the percentages of cells in each cell cycle phase and the percentage of cells in apoptosis, showing that the increase of cells in G2/M observed in patients is not a direct consequence of apoptosis but rather an independent step, possibly related with increased cell activation.

Table 2 Comparisons of CD4^{+} and CD8^{+} T-lymphocyte percentages in different cell cycle phases between HH patients and controls.

Cell Cycle Phase	Cell population	% in Controls	% in HH Patients	KS test[1]
G0G1	**CD4^{+} T cells**	99.65 ± 0.16	99.41 ± 0.33	*P*=0.0256
	CD8^{+} T cells	98.86 ± 1.25	98.13 ± 1.69	n.s
	KS test[2]	0.0337	0.0047	
S	**CD4^{+} T cells**	0.34 ± 0.16	0.49 ± 0.23	n.s
	CD8^{+} T cells	0.94 ± 1.00	1.39 ±1.09	n.s
	KS test[2]	0.0337	0.0015	
G2M	**CD4^{+} T cells**	0.01 ± 0.03	0.11 ± 0.14	*P*=0.0217
	CD8^{+} T cells	0.20 ± 0.36	0.49 ± 0.74	*P*=0.0025
	KS test[2]	<0.0001	0.0135	

[1] Kolmogorov-Smirnov Test comparing HH patients and controls

[2] Kolmogorov-Smirnov Test comparing CD4^{+} T cells and CD8^{+} T cells

In summary, results of cell cycle positioning of total peripheral blood CD8^{+} T lymphocytes from HH patients support the notion that those cells constitute a highly dynamic population in homeostatic equilibrium, compatible with the activation profile revealed before with the gene expression data.

4 - mRNA expression analysis in *Hfe*^{-/-} and wild type mice supports the impact of HFE on the CD8+ T-lymphocyte activation profile

All previous results in HH patients suggesting an impact of HFE on the expression profile of CD8+ T cells were still confounded not only by the known phenotypic heterogeneity among patients, possibly influenced by other MHC linked genetic determinants [44, 220] but also by the strong correlation between the CD8 phenotypes and the severity of iron overload [43]. In order to address the relative impact of HFE and iron overload on the CD8+ T-lymphocyte gene expression profile in the absence of such confounding variables, we used the HFE deficient mouse model (*Hfe*^{-/-}). We performed a differential genome-wide expression analysis comparing *Hfe*^{-/-} and wild-type (wt) mice, in conditions of either normal or iron rich diet. Results showed that few genes were differently expressed in the CD8+ T cells of *Hfe*^{-/-} mice, 66 in total: 37 up-regulated and 29 down-regulated under the standard normal iron condition. A few more genes were differently expressed under high iron diet, 78 in total: 67 up-regulated and 11 down-regulated. Lists of the transcripts differentially regulated in *Hfe*^{-/-} in comparison with wild type C57BL/6 mice are provided in S2 and S3 Tables. Functional clustering analysis was performed to define categories among the differentially regulated genes. The results are presented as supplementary material in S4 Table.

From all differentially expressed genes, only thirteen were found in common in both normal and high iron diet conditions (Fig. 2a), suggesting an impact of HFE on the CD8 expression of these genes regardless of iron levels. Nevertheless, an additional effect of iron cannot be excluded.
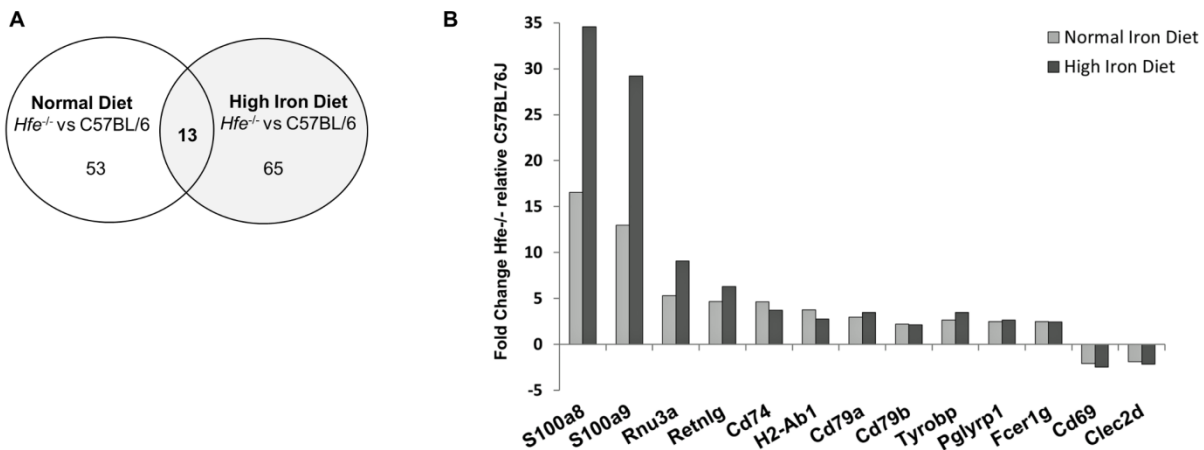
Fig. 2 Genome-wide expression analysis of CD8+ T lymphocytes from *Hfe*^{-/-} and wild type mice A) Venn diagram with comparative analysis between the selected genes found to be differently regulated by the two genotypes under the same iron diet condition. **B)** Differential gene expression of *Hfe*^{-/-} mice with normal and high iron diet relatively to C57BL/6 mice under the same iron diet conditions. Fold Change of the genes found to be differently expressed (T-test, $p<0.05$) and with fold change >1.8 are represented.

As illustrated in Fig. 2b, the most striking differences were found for *S100a8* and *S100a9*, two calcium-binding proteins (calgranulins) involved in the regulation of several cellular processes such as cell cycle progression and differentiation [254, 255]. These genes were increased in *Hfe*$^{-/-}$ mice under normal iron diet (fold-changes of 16.52 for *S100a8* and 12.96 for *S100a9*) but notably, the fold-change differences were even higher under high iron diet conditions (fold-changes of 34.58 for *S100a8* and 29.21 for *S100a9*).

4.1 Correlational analysis of the differential expressed genes between *Hfe*$^{-/-}$ and wild type mice

In order to understand the putative interaction of the calgranulins S100a8 and S100a9 with the other differentially expressed genes, we further analyzed expression data from all individual mice maintained in high iron diet conditions (the condition where differential gene expression was more marked) and performed multi-variable correlation analysis to identify the most significantly co-expressed genes. The results are given as supplementary material illustrated in S1 Fig. In general, correlations with *S100a9* were stronger than those observed with *S100a8*. The gene whose expression was most significantly correlated with *S100a9* was *Tyrobp* (*r*=0.9931; *p*=0.0001) which codes for the tyrosine kinase binding protein *DAP12* (DNAX activation protein 12). Interestingly, *DAP12* has been shown by others to be a marker of self-reactive, non-MHC restricted activated memory-phenotype CD8$^+$ T cells, in contrast to the conventional CD8$^+$ T cells [160]. Two other genes, *Retn1g* and *Fcer1g* were found strongly correlated with *DAP12* expression (*r*=0.9756; *p*=0.0009 and *r*=0.9701; *p*=0.0013, respectively) and, accordingly, they were the next most significantly correlated with *S100a9* expression (*r*=0.9693; *p*=0.0014 and *r*=0.9558; *p*=0.0029, respectively). *Retn1g* codes for a novel resistin-like molecule expressed in hematopoietic tissues and expected to have a cytokine-like role [256] and *Fcer1g* codes for the gama Fc membrane receptor (FcRγ) which, like *DAP12*, is a tyrosine kinase binding protein with a fundamental role in immune effector functions [257]. Two genes, *Cd69* and *Clec2d*, were the only inversely correlated with *S100a9* (*r*=-0.9764; *p*<0.0001 and *r*=-0.9421; *p*=0.0005, respectively). These are respectively the members C and D of the C-type lectin domain family 2, a family of co-stimulatory molecules recently recognized as markers of very early T-cell activation [258]. In particular *Cd69* has been described as a marker of non-circulating resident (resting) memory CD8$^+$ T cells, and characteristically absent in the recirculating central and effector memory CD8$^+$ T-cell populations [259]. The only gene from the initial list of 13 that was not significantly correlated with *S100a9* at the individual level was *CD79a*. In summary, results of a significantly increased expression of *S100a9* in CD8$^+$ T lymphocytes from *Hfe*$^{-/-}$ mice positively correlated with *DAP12* and negatively correlated with *Cd69* suggests that the effect

of HFE on CD8 activation may target preferentially the central/effector memory cells, which are also the cells predominantly decreased in HH patients [31].

None of the genes found altered in HH patients with a low CD8 phenotype (*LEF1* and *P2RY8)* were significantly associated with the up regulation of calgranulins *S100a8* and *S100a9*, showing that the two models of differential gene expression are not equivalent. Hence the putative mechanisms involving HFE as a player in CD8^{+} T-cell activation in mice or those involving HFE as a player in the homeostatic equilibrium of CD8^{+} T-cell subsets in HH patients may be substantially different.

4.2 Genes encoding proteins of iron metabolism are not altered in CD8^{+} T cells from *Hfe*^{-/-} mice

To assess whether iron impacts on the differential gene expression of *Hfe*^{-/-} mice we analyzed the expression of genes related with iron metabolism in normal iron diet conditions, where the differences between the two mouse models in terms of iron loading were more marked (Fig. 3). The expression of most iron related genes was, in general, very low in CD8^{+} T lymphocytes and not significantly different between the two genotypes except for lipocalin 2 (*Lcn2*) that was significantly up-regulated in *Hfe*^{-/-} in comparison with wild-type (*p*=0.0016). *Lcn2* is an antimicrobial protein that acts by capturing and depleting bacterial siderophores and is known to have chemoattractant properties [260]. These results are shown as supplementary material in S5 Table. No significant correlations were found between the expression of any of the 13 genes differentially expressed in Hfe^{-/-} mice and the expression of the iron related genes (data not shown).
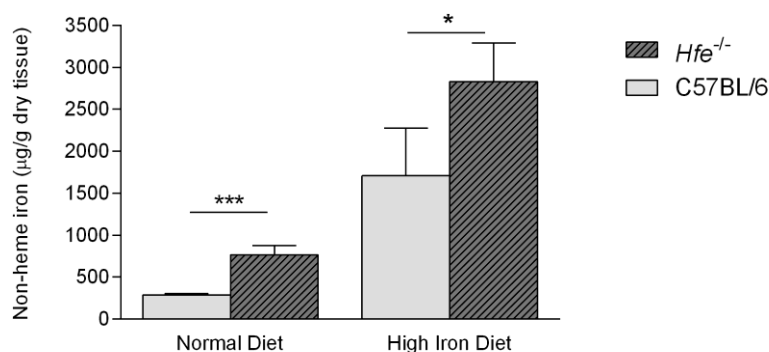
Fig. 3 Hepatic iron concentration of *Hfe*^{-/-} and C57BL/6 mice under a normal or a high-iron diet. Values are expressed as mean ± standard deviation. Statistical significant differences were calculated between mice genotype groups under the same diet condition (T-test * *P*<0.05 and ****P*<0.001).

5. S100a9 mRNA and protein expression are increased in human peripheral blood CD8^{+} T lymphocytes from HH patients

The previous findings that calgranulins are over-expressed in CD8^{+} T lymphocytes of *Hfe*^{-/-} mice, prompted us to investigate these proteins in human patients with HH in comparison to normal controls. This was done first by accessing *S100a8* and *S100a9* expression at mRNA levels with qRT-PCR without any previously activation step. As shown in Fig. 4A, *S100a8* and *S100a9* mRNA expression in isolated CD8^{+} T lymphocytes were significantly higher in HH patients than in controls with fold change of 2.4 for *S100a8* and 3.4 for *S100a9* (Wilcoxon paired test, $p=0.016$ and $p=0.027$ respectively). Although in the *Hfe*^{-/-} mouse model these two proteins were similarly expressed, in humans *S100a9* gene expression was found to be 4.5x higher than *S100a8*. Due to this high expression, we next analyzed S100a9 protein level by flow cytometry.
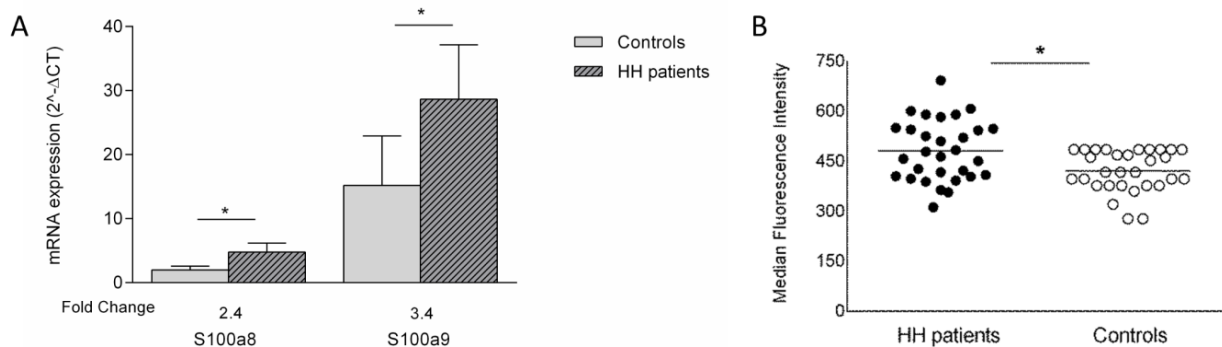
Fig. 4 S100a8 and S100a9 expression in CD8+ T cells from HH patients and controls A) S100a8 and S100a9 mRNA expression in isolated CD8+ T lymphocytes from HH patients and normal controls. Statistical significance was obtained with paired analysis of patient-control of the day using the non-parametric Wilcoxon test, *p<0.05. **B)** Median fluorescence intensity of S100a9 expression in CD8+ T cells from peripheral blood from HH patients and normal controls. Statistical significance was obtained with paired analysis of patient versus control of the day using the parametric T-test, *p<0.0001.

The expression of S100a9 protein was evaluated by MFI (median fluorescence intensity) in total lymphocytes, CD8^{+} and CD4^{+} T subpopulations. In addition, the expression of S100a9 was also evaluated in neutrophils and monocytes that are known to express this protein and were used as positive controls (see Material and Methods). Paired T-Test comparisons of S100a9 MFI values in the several populations were performed between HH patients (n=30) and controls (n=13) tested in the same day under the same conditions. Neutrophils and monocytes had significantly ($p=0.013$ and $p=0.005$ respectively) higher S100a9 MFI values in HH patients (mean±SEM: 13090±1039 and 2947±181 respectively) in comparison with controls (mean±SEM: 10291±293 and 2435±80 respectively). The

expression of S100a9 in total lymphocytes was also consistently higher in HH patients than in controls (mean±SEM: 481±15 in HH and 418±10 in controls, *p*<0.0001), although at a much lower level. Regarding the T-lymphocyte subsets, the expression of S100a9 in CD8$^+$ T lymphocytes was significantly higher in HH patients in comparison to controls (mean±SEM: 481±17 in HH and 421±11 in controls, *p*<0.0001) (Fig. 4B). The same result was obtained for CD4$^+$ T cells (mean±SEM: 469±17 in HH and 388±9 in controls, *p*<0.0001). S100a9 expression in each cell type was not significantly correlated with the total numbers of the respective cells.

Altogether, results in both animal and human models of HH support a direct effect of HFE on the transcriptional profile of CD8$^+$ T lymphocytes, HFE deficiency inducing the up regulation of the calgranulin S100a9. As an HFE-dependent effect, it is not surprising that calgranulins have not been found differentially expressed in the first genome-wide screen in patients, where all subjects carry the same *HFE* mutation. Hence, results of calgranulin expression do not constitute an explanation for the heterogeneity found in HH patients regarding the numbers and subsets of CD8$^+$ T lymphocytes. These were better explained by changes in the signaling pathways described above with the results of the differential expression profiles in CD8 subsets.

Discussion

In this paper we questioned whether or not HFE, a non-classical MHC-class I molecule, affects the triggering/signaling pathways of CD8$^+$ T lymphocytes and if it contributes to the self-renewal and homeostasis of the three main CD8+ subpopulations of naïve, central memory and effector memory cells at the periphery. To do that, we used human and mouse models of HH, both lacking the cell surface expression of HFE. In a first step we analyzed the transcriptional profile of selected CD8$^+$ T lymphocytes from HH patients homozygous for the C282Y *HFE* mutation. Because these patients share a common *HFE* defect but differ in the numbers of CD8$^+$ T lymphocytes and subpopulations, this approach was expected to identify novel candidates associated with the CD8 phenotype independently of HFE. The signaling molecules *CCR7* and *LEF1*, which are normally down regulated in naïve cells after activation [248], as well as *ACTN1*, a calcium dependent remodeling molecule, were significantly decreased in patients with a low CD8 phenotype. Conversely, the expression of *FOSL2*, *P2RY8* and *NAA50* molecules known to be involved in processes of activation/expansions of lymphocytes, were significantly increased in patients with low CD8 phenotype. By mRNA analysis in sorted populations we confirmed the expression patterns of these genes in naïve, central memory and effector memory cells. While *CCR7* and *LEF1* were, as expected, mostly expressed in naïve cells we describe for the first time that and *ACTN1* is also mostly expressed in naïve cells, that *P2RY8* expression is preferentially observed in central memory and that *FOSL2* is preferentially expressed in effector memory cells. This general pattern of subset specific gene expression was found both in HH patients and controls (see Fig. 1).Nevertheless, the expression of *LEF1* and *P2RY8* in central and effector memory CD8 subpopulations of HH patients differed significantly from controls, independently of their total cell numbers or serum iron levels. We interpret these results as evidence of an impact of HFE on the differentiation /maturation of CD8$^+$ T lymphocytes, possibly in the conversion step of central memory into effector memory T cells described by Peixoto and co-workers with *in vitro* experiments [157]. The question remains, however, if a similar expression profile would be also observed in normal subjects displaying a low CD8 phenotype, in spite of a normal HFE. Amongst the healthy controls studied here (n=8), only one subject displayed a low CD8 phenotype (total CD8$^+$ T lymphocytes=197x10^3/ml; total T$_{EM}$ T lymphocytes=0.058 x10^3/ml). But in contrast to HH patients, he had no evidence of a decreased *LEF1* or increased *P2RY8* expression in T$_{CM}$ or T$_{EM}$ subpopulations as compared to the other controls (data not shown), therefore not supporting a defect similar to that observed in HH. A formal proof to this concept, however, would imply an extended analysis of a large normal population, which was out of the scope of the present paper.

The observation that HH patients show an increased proportion of cells in G2/M phase in the periphery is compatible with the hypothesis of an increased activation state. In addition, the present study of apoptosis and cell cycle in human peripheral blood lymphocytes also brought into light a new aspect of lymphocyte biology which is the clear demonstration of marked differences in apoptosis and cell cycle progression between the subpopulations of CD4^{+} and CD8^{+} T lymphocytes. Although a higher percentage of apoptotic cells among the CD8^{+} relative to CD4^{+} T lymphocytes had been already observed in previous studies in the context of sepsis and pulmonary disease, its significance in normal physiological conditions had never been discussed [261, 262]. This is a relevant finding deserving fully consideration in future studies of lymphocyte activation and proliferation in the clinical setting.

One pending question that could not be answered by the simple analysis of CD8 expression data in HH patients was the clarification of the complex interaction between HFE, CD8^{+} T-lymphocyte numbers and the severity of iron overload. As mentioned in the results section, a limitation of the genome-wide screen experiment in HH patients was the fact that, due to the strict selection criteria used, i.e., patients grouped according to exclusive patterns of CD8 phenotypes (low or normal/high) which are significantly associated with the iron overload profiles, it was not possible to distinguish the relative interactions of iron overload or CD8 numbers with the expression profiles. Nevertheless, for the subsequent analysis of expression of the different genes in sorted CD8^{+} T-cell subsets we used a non-selected group of patients who were at different stages of treatment showing a wide range of transferrin saturation values not related to the CD8 phenotype. Although there was, in general, a higher variation in the gene expression of the different CD8^{+} T-cell subsets in HH patients than in controls (see Fig. 1B), we found no correlation with either transferrin saturation or total CD8 numbers, supporting the notion of a primary effect of HFE on CD8^{+} T-cell signaling, independent of actual circulating iron levels.

The above described impact of HFE on the CD8^{+} lymphocyte profile independently of iron levels does not exclude the hypothesis that CD8^{+} T lymphocytes may be equipped with some "sensing" system for iron. In this regard, it was interesting to observe a relationship between higher transferrin saturation and increased CD8^{+} T-cell apoptosis. Iron induced apoptosis had been already reported in human hepatocytes and rat neurons but it had never been described in human lymphocytes [263, 264]. It could be speculated that in this way iron overload could contribute to the decreased numbers of CD8^{+} T cells in HH. However, a direct relationship between apoptosis and cell numbers was not found. The most plausible explanation is a compensatory increased activation of CD8^{+} T cells contributing to a "more dynamic" pool of lymphocytes in HH as shown by an increase in the number of cells in G2/M. We should bear in mind, however, that an increased number of cells in G2/M is not

exclusively due to an increased number of mitotic cells but may also reflect an increased number of cells arrested in G2 for DNA repair, eventually in response to iron-induced oxidative injury. Of note, in a previous study we have shown that HH patients´ lymphocytes had lower DEB-induced chromosome instability possibly due to an adaptive response of the HH lymphocytes with increased DNA repair [265].

Once the question of the relationship of iron overload and the expression profile of $CD8^+$ T lymphocytes could not be clarified in the human model of HH, we decided to address this question in animal models where genetic and environmental variables are controlled. For that purpose, we analyzed the transcriptional profile of $CD8^+$ T lymphocytes from mice $Hfe^{-/-}$ in comparison to normal mice of the same genetic background, experiments performed in either normal or high iron diet conditions. Because all mice share the same MHC background, any putative modifier effect of other MHC related molecules could not be a variable here. The results revealed a set of differentially expressed genes between the two strains and three features deserve to be mentioned. First, the differentially expressed genes identified were mostly clustered in functional types related to lymphocyte signaling and activation, supporting the suggested inhibitory effect of wild-type HFE on CD8 activation [224]. Secondly, most of these differentially expressed genes differed in conditions of normal or high iron diet. Nevertheless, the observed impact of a high iron diet is only a partial effect because $Hfe^{-/-}$ mice are already constitutively iron overloaded. Finally the genes previously found altered in HH patients with a low CD8 phenotype were not altered in the $Hfe^{-/-}$ mouse model indicating that the mouse model does not completely recapitulate the phenotype of HH in humans, which is not surprising taking into consideration the fact that abnormalities in $CD8^+$ T-cell numbers have never been described in these mice.

The most striking differences in $Hfe^{-/-}$ mice were observed for the expression $S100a8$ and $S100a9$, belonging to the S100 family of proteins containing two canonical EF-hand calcium-binding motifs involved in the calcium dependent control of cell differentiation, cell cycle progression and growth [254, 255]. The fold-change values of differential expression of these calgranulins between $Hfe^{-/-}$ and wild type mice was superior in mice fed in a high iron diet than for mice under a normal diet. Interestingly, a previously published genome wide mRNA expression study aimed to assess the effect of iron loading in muscle cells from mice also revealed that, among others, $S100a8$ and $S100a9$ were over expressed in iron overload conditions [266]. Further studies are needed to clarify the putative modulatory role of systemic iron on $CD8^+$ T-cell activation.

Results of calgranulins expression in mice was next translated to the human clinical model of HH where patients with a non-functional HFE showed an increased expression in both the mRNA expression and intracytoplasmatic protein expression of S100a9 in $CD8^+$ T lymphocytes. It should be reminded however that an HFE-dependent altered gene

expression in CD8^{+} T lymphocytes does not necessarily mean that HFE is exerting its effect on the surface of these cells. On the contrary, it is more plausible to assume that an HFE-dependent alteration in antigen-presenting cells may indirectly affect the CD8^{+} T-cell signaling. In this context, it was interesting to observe that, at the protein level, an increased expression of S100a9 was also observed in other blood cell types which are known to express this protein in higher amounts, namely neutrophils and monocytes. The additional finding of a strong correlation between the expression of *S100a9* and the adaptor protein *DAP12* is also of particular interest and may open new avenues to better explore the pathways involved in the effect of HFE on CD8^{+} T-cell activation.

The putative role of iron on CD8^{+} T-lymphocyte activation and differentiation deserves some additional considerations. For many years we have reported results of a negative correlation between the numbers of CD8^{+} T lymphocytes and the severity of iron overload in HH [21, 30, 32], supporting the postulate that they may act as systemic "buffers" to protect against systemic iron toxicity [2, 23, 34, 267, 268]. Following that hypothesis, we have recently demonstrated the capacity of peripheral blood lymphocytes to uptake and process NTBI [234] and in that way to protect against tissue iron accumulation [269]. The mechanisms involved in NTBI transport and signaling in lymphocytes are still elusive. It is well known that non-classical MHC I molecules display different features from the classical ones, namely in their capacity to bind non peptide ligands [270]. In the recent paper by Reuben and co-workers on the inhibitory effect of HFE on CD8^{+} T-lymphocyte activation they excluded the interaction with TfR1 as a necessary step for HFE-mediated inhibition of MHC I presentation. It would be interesting to explore if HFE could affect NTBI uptake and in that way somehow influence lymphocyte activation.

The assumption of a mechanistic model of interactions between HFE, lymphocyte activation and S100a9 expression may have important implications for a better understanding of HH and its clinical consequences. We propose that the "low CD8 phenotype" in HH is the result of a homeostatic equilibrium of cells constantly triggered to activate and differentiate into more mature effector cells. This hypothesis is compatible with the concept first advanced by Reuben and co-workers that HFE is a negative regulator of CD8^{+} T-lymphocyte activation and that the lack of HFE may render CD8^{+}T lymphocytes less tolerant to constant stimuli and more susceptible to autoimmune phenomena [224]. Notably, calgranulins have been described as damage-associated molecular pattern molecules (DAMPs) highly up regulated in various autoimmune disorders [255]. Recently Loser and colleagues provided clear evidence, in both animal and human autoimmune disorder models that local calgranulin production is essential for the induction of autoreactive CD8^{+} T cells and the development of systemic autoimmunity, an effect mediated via Toll-like receptor 4 (TLR4) signaling [255]. The idea that a normal surface HFE expression may help preventing

the development of autoimmunity in homeostatic conditions [224] would imply that HH patients should be also more susceptible to autoimmune disorders. Although these are not commonly described in HH, one may recall here the fact that one of the most perturbing clinical features of HH is a severe arthropathy of still unknown pathogenesis that is not prevented by iron depletion, suggesting that other HFE-related mechanisms should be involved. Considering the recently described effect of S100a9 as an inflammation orchestrator in rheumatoid arthritis [255] and lupus erythematosus [271], it is tempting to speculate that an increased expression of S100a9 could also contribute to the arthropathy process in HH. More studies are certainly needed to address this question and to understand if there is any impact of activated CD8$^+$ T lymphocytes on the pathogenesis of HH arthropathy, what is the role of calgranulins in that process and if they could constitute a promising novel therapeutic target.

Methods

Ethics statement

Animal care and procedures were in accordance with institutional guidelines. Conducted experiments in mice were approved by the IBMC.INEB Animal Ethics Committee, in accordance with the Portuguese Veterinary Director General guidelines. Regarding human studies, they were approved by the Institutional Ethical Committee of Santo António Hospital – Centro Hospitalar do Porto and written informed consent was obtained from all participants in accordance with the Declaration of Helsinki.

Mice

Mice models used in this study were C57BL/6 supplied by Charles River and mice homozygous for the disruption of the *Hfe* gene (*Hfe*$^{-/-}$) generated under the same genetic background as described elsewhere [272]. They were females maintained at the IBMC's Animal Care Facility fed *ad libitum* with the standard local rodent diet (Teklan 2014 Harlan with 175ppm of iron) until 14-15 weeks of age. After this, four C57BL/6 wild-type and four *Hfe*$^{-/-}$ mice were fed with the same diet until they were 16-17 weeks old consisting in the "normal iron diet" group. Other four C57BL/6 wild type and four *Hfe*$^{-/-}$ mice were fed, during one week, with a mix of 50% Harlan 2014 and 50% Harlan Iron Rich (supplemented with 2.5% carbonyl iron corresponding to 25000 ppm of iron) (TD.06700) following 100% Harlan Iron Rich one more week until they were 16 -17 weeks old, consisting in the "high-iron diet" group. To confirm the validity of the different diet conditions, non-heme iron concentration was determined in the liver of each mouse (n=16). As expected, significantly higher iron content was observed in the *Hfe*$^{-/-}$ mice in comparison with C57BL/6 under the same diet (Fig. 3).

Human subjects

All patients included in this study were diagnosed and are regularly followed-up at the Hemochromatosis Outpatient Clinic of Santo Antonio Hospital (Porto, Portugal) by the same dedicated clinician. Patients are all unrelated, and genetically characterized as homozygous for the C282Y mutation of the *HFE* gene. They were recruited to participate in the study in a consecutive mode at the time of their regular consultations. Retrospective clinical and laboratory data from patients were obtained from the clinical files under the responsibility of the clinician in charge. These included a) the individual iron overload profile at diagnosis estimated by the total body iron stores measured by quantitative phlebotomies [273], b) the actual iron parameters at the time of experiment measured by serum iron and transferrin saturation; c) the individual immune-phenotype with determinations of total CD8$^+$ T-

lymphocyte numbers as well as measures of the CD8^{+} T subsets of naïve, central memory and effector memory cells, and d) measures of CRP as a marker of systemic inflammation. For the purpose of phenotypic grouping, HH patients were classified into one of these two types: "the low CD8 phenotype" defined as patients with absolute CD8^{+} T-lymphocyte numbers consistently lower than $300x10^3$/ml in at least 5 serial determinations, and the "normal/high CD8 phenotype" defined as patients with CD8^{+} T-lymphocyte numbers consistently higher or equal than $400x10^3$/ml. These limits were defined based on the normal distribution of values described in the Portuguese control population considering the limit for the low CD8 phenotype as the 25% lower percentile and the limit for a normal/high CD8 phenotype the average value in controls [43, 220]. Clinical and laboratory data from the patients have been published previously [30-32, 34, 244].

Healthy controls for the study were consecutively recruited amongst volunteer blood donors at the Blood Bank of Santo Antonio Hospital during their regular visits for blood donation.

Experimental procedures

a) Genome-wide expression analysis of CD8^{+} T lymphocytes from HH patients

Twenty-four HH patients were selected for the present experiment which comprised two parts: a genome-wide gene expression screening, followed by a gene profiling of selected CD8^{+} T-cell subpopulations. In the first part (genome-wide gene expression screening) 10 patients were selected and stratified into the two subgroups of "low" (n=6) or "normal/high" (n=4) as defined above. As expected from previously described data [30-32, 34, 244] , patients in the low group had characteristically a severe iron overload while in the other group subjects were asymptomatic. In the second part, 14 previously unselected patients were consecutively enrolled for gene expression profiling of sorted CD8^{+} T-cell subpopulations, independently of their CD8 phenotype or iron status. They were at different stages of treatment which allowed us to obtain a sample with a wide range of transferrin saturation values. A group of 8 healthy blood donors were used as controls.

For the purpose of genome-wide screening, CD8^{+} T lymphocytes from HH patients were positively selected from peripheral blood mononuclear cells (PBMCs) that were isolated from whole blood or buffy coat samples by density separation over Lymphoprep 1.077g/ml density gradient (Axis-Shield). CD8^{+} T-lymphocytes were positively selected from PBMCs (~$3x10^7$ cells) by Magnetic-Activated Cell Sorting (MACS; Miltenyi Biotec), following the manufacturer's instructions. Total RNA of MACS-purified CD8^{+} T cells was extracted using Mini RNeasy Plus *Kit* Mini (Qiagen, Valencia, CA) as recommended by the manufacturer. RNA concentration and purity were determined using optical density (OD) measurements at 260 and 280 nm. All the samples had an OD260/OD280 ratio of 1.95 or higher. In each

experiment time total RNA concentration was normalized between patients and controls and converted into cDNA with NZY First-Strand cDNA Synthesis kit (Nzytech) as recommended by the manufacturer. Transcriptional profile of CD8$^+$ T lymphocytes was assessed using the GeneChip Human Gene 1.0 ST array (Affymetrix). The RNA processing and hybridization steps, carried out at the Genomics Core facility of the European Molecular Biology Laboratory (EMBL, Heidelberg), were performed as recommended by the manufacturer. Upon filtering and normalization of the raw data, samples were grouped according to the CD8 low or normal/high profiles and subjected to a between-group analysis using the GeneSpring GX software (Agilent). Genes which exhibited at least a 1.5-fold change in expression were considered as up- or down-regulated. Quantitate real-time PCR was used to confirm differential expression.

For the purpose of gene profiling experiments in separated CD8$^+$ T-cell subpopulations, unprocessed peripheral blood samples were stained with the following fluorochrome-conjugated mouse anti-human monoclonal antibodies: anti-CD8a APC-eFluor 780 (eBioscience), anti-CD45RA APC (eBioscience) and anti-CCR7 FITC (R&D System). After red blood cell lysis, the subpopulations of CD8$^+$ T-lymphocytes were flow sorted in a FACS Aria (BD) instrument according to the gating strategy previously described [31] as: naïve (T$_N$, CD8$^+$CCR7$^+$CD45RA$^+$), central memory (T$_{CM}$, CD8$^+$CCR7$^+$CD45RA$^-$) and effector memory (T$_{EM}$, CD8$^+$CCR7$^-$CD45RA$^{+/-}$). Samples were sorted until 3000 cells from each gated subpopulation were collected. Cells were sorted according to the gating strategy illustrated in Fig. 1A. In order to avoid the risk of low representativity after cell sorting, we did not further discriminate effector memory cells according to CD45RA expression as previously described [31]. This decision was supported by our previous observation that the cell subpopulation that mostly contributes to the variation in the total number of peripheral CD8$^+$ T cells, both in HH patients and normal controls, is the entire effector memory population [31]. Total RNA was isolated from sorted cells using the RNeasy Plus Micro Kit (QIAGEN), according to the manufacturer's guidelines. Gene expression in sorted CD8$^+$ T-cell subpopulations: was assessed for a group of specific candidate genes: *LEF1*, *ACTN1*, *CCR7*; *NAA50*; *P2RY8* and *FOSL2*. cDNAs resulting from the reverse transcription reaction with SuperScript First-Strand Synthesis System (Invitrogen) were subjected to a first round of PCR amplification with specific primers (S6 Table). To quantify the expression levels of all genes of interest in each CD8$^+$ T-lymphocyte subpopulation, a second seminested real-time PCR was performed in an iCycler iQ5 (Bio-Rad) using iQ SYBR Green Supermix (Bio-Rad) [274]. At the end of the PCR cycling, melting curves were generated to ascertain the amplification of a single product and the absence of primer dimers. Results were normalized to GAPDH as endogenous control.

b) Apoptosis and cell cycle studies in HH patients

Twenty HH patients and 12 controls were used for apoptosis and cell cycle studies. These included 10 patients classified with the low CD8 phenotype and 10 patients classified as normal/high CD8 phenotype, as described above. During the study period, patients were evaluated at different stages of their treatment course. Four patients were under intensive phlebotomy treatment and the remaining 16 were receiving maintenance therapy. The inclusion of patients at different stages of iron load was also important in order to allow an analysis of cell cycle parameters in relation to a wide range of transferrin saturation values.

For detection of apoptotic T cells, blood samples were collected into tubes containing sodium heparin and PBMCs were separated by centrifugation on the Lymphoprep 1.077g/ml density gradient (Axis-Shield) after 12 hour resting at 4ºC. Apoptotic T cells from HH patients were assessed through flow cytometry, using the Annexin V-FITC/7-AAD Kit (Beckman Coulter, BC), containing FITC conjugated Annexin V, 7-AAD staining solution and Annexin V binding buffer, following the manufactures' instructions. Samples were acquired in a flow cytometer EPICS-XL-MCL (BC) using the System II software (BC). Data were analyzed using the System II software (BC). The percentage of viable (Annexin V negative/7-AAD negative), early apoptotic (Annexin V positive/7-AAD negative) and late apoptotic or already dead (Annexin V positive/7-AAD positive) $CD8^+$ and $CD4^+$ T cells was calculated.

In order to analyze the distribution of $CD8^+$ and $CD4^+$ T cells throughout the cell cycle phases: blood sample was submitted to cell surface immunophenotyping with FITC-conjugated mouse anti-human CD4 or anti-human CD8 IgG mAb followed by staining with FITC conjugated rabbit anti-mouse IgG polyclonal Ab and cellular DNA measurement using the DNA PREP Reagents Kit (BC) according to a protocol that was described in detail elsewhere [275]. After staining, samples were acquired in an EPICS-XL-MCL flow cytometer (BC) using the System II software (BC). Data were analyzed using specific software for DNA analysis Multicyle for Windows (Phoenix Flow System, PFS). The percentages of $CD8^+$ and $CD4^+$ T cells in each cell cycle phase (G0/G1, S and G2/M) were calculated.

c) Genome-wide expression analysis of $CD8^+$ T lymphocytes from Hfe$^{-/-}$ and wild type mice

Peripheral blood from each mice (n=16) was collected by heart puncture (approximately 500µl) and $CD8^+$ T-lymphocyte population was isolated by FACS-ARIA I cell sorting using anti-CD8 APC antibody (BD Bioscience). The purities of isolated $CD8^+$ T cells were measured by flow-cytometric analysis of cell markers (CD8) and in all samples >95% of purity was obtained. The maximum number of $CD8^+$ T cells was sorted by each mouse blood sample. Total RNA was extracted with RNeasy Plus Micro kit (QIAGEN) according to the manufacture`s guidelines. Total RNA integrity was evaluated by Agilent 2010 Bioanalyzer

protocol. To overcome the low RNA concentration, we performed the Ovation Pico WTA system protocol by NuGEN to amplify the RNA samples followed by cDNA synthesis using the WT Ovation Exon module.

Transcriptional profile of CD8$^+$ T lymphocytes from mice was assessed using the GeneChip Mouse Gene ST 1.0 array (Affymetrix, Santa Clara, CA, USA). The RNA processing and hybridization steps, carried out at the Genomics Core facility of the European Molecular Biology Laboratory (EMBL, Heidelberg), were performed as recommended by the manufacturer. Data from the GeneChip were imported into GeneSpring GX 11.5 software (Agilent) and the expression value for each gene was normalized by using the Robust Multichip Average (RMA) 16 algorithm. Results were grouped according to mice genotype and iron diet conditions, i.e. wild type mice with normal or high-iron diet, and *Hfe$^{-/-}$* with normal or high iron diet. Genes which exhibited at least a 1.8-fold change in expression were considered as up- or down-regulated.

d) Human translational study of the candidate genes found differently expressed in Hfe$^{-/-}$ mice

Subsequent studies were done for the most significantly different expressed genes found in mice study, calgranulin genes *S100a8* and *S100a9*, consisting in mRNA and protein expression in HH patients and controls.

Gene expression of *S100a8* and *S100a9* was assessed in sorted CD8$^+$ T cells from HH patients and controls. For this, PBMCs were isolated from whole blood or buffy coat samples by density separation over Lymphoprep and CD8$^+$ T-lymphocytes were selected MACS, as described above. Total RNA, of MACS-purified CD8$^+$ T cells, was extracted as described above. In each experiment time total RNA concentration was normalized between patients and controls and converted into cDNA with NZY First-Strand cDNA Synthesis kit (Nzytech) as recommended by the manufacturer. Quantitative real-time PCR was performed in an iCycler iQ5 (Bio-Rad) using iQ SYBR Green Supermix (Bio$^-$Rad) using specific primers for each gene (S7 Table). At the end of the PCR cycling, melting curves were generated to ascertain the amplification of a single product and the absence of primer dimers. Results were normalized to 18S gene as endogenous control. In order to access the reproducibility of the technique, biological replicates were performed consisting in the analysis of different samples of the same patient in different days. This was always done against a different control for the experiment of the day (n=12). Since reproducibility of the replicates was achieved, all samples were included for analysis (n=12). Paired analysis of patient-control of the day was performed.

Intracellular protein expression of S100a9 was accessed by flow cytometry in total peripheral blood samples from 30 HH patients and 13 controls. For this, peripheral blood was

collected into K3-ethylene-diamine-tetracetic acid (EDTA-K3)-containing tubes. The blood samples were stained with the following fluorochrome-conjugated mouse anti-human monoclonal antibodies: anti-human CD3 FITC (eBioscience) and anti-human CD8 PerCP (eBioscience). Leukocyte fixation and subsequent permeabilization of the cells was then performed using the Fix & Perm Cell Permeabilization Kit (Invitrogen). Anti-human IgG1 S100a9 PE (sc-53187, Santa Cruz, CA) or the PE-conjugated isotype control was used for intracellular staining. Samples were acquired in FACS Canto v.2 flow cytometer (BD) under the same conditions, using the FACSDiva software (BD). In each experiment day at least a control sample was tested in parallel with patient's samples. Data were analyzed in the Infinicyt software (Cytognos SL, Salamanca, Spain) and the median fluorescence intensity (MFI) of the S100a9 expression was determined in neutrophils, monocytes and lymphocytes defined according to SSC and FSC characteristics, in CD8$^+$ lymphocytes defined by the CD3$^+$CD8$^+$ population after lymphocyte gating and in CD4$^+$ lymphocytes defined as CD3$^+$CD8$^-$ population after lymphocyte gating. Results were analyzed as a ratio of patient/control of the day.

Statistical analysis

Correlations among variables were analyzed by multiple-variable correlation analysis with calculation of various statistics, including covariances and partial correlations. Differences in group means or sample distributions were tested respectively by the Student's t-test and the Kolmogorov-Smirnov (KS) two sample test as appropriate. For analysis of Affymetrix expression data we used the normalized values. For analysis of individual expression values in sorted CD8$^+$ T-cell subsets, a systematic outliers' exclusion was performed in HH patients´ data in order to permit comparisons with controls' group means assuming equal variances. The non-parametric Wilcoxon test for paired samples was used to compare mRNA expression levels of *S100a8* and *S100a9* between patients and controls analyzed on the same day. The parametric paired T-test was used to compare protein expression of S100a9 by FACS (MFI) between patients and controls analyzed in the same day.

Analysis of differentially expressed genes, resulting from genome-wide studies in mice, was clustered into biologically relevant categories using the bioinformatics resources: Database for Annotation, Visualization and Integrated Discovery (DAVID, http://david.abcc.ncifcrf.gov/) and Web-based Gene SeT AnaLysis Toolkit (WebGestalt, http://bioinfo.vanderbilt.edu/wg2/). For Gene Ontology (GO) and Kyoto Encyclopedia of Genes and Genomes (KEGG) pathways enrichment analysis, the minimum of two genes were required for identification of relevant biological pathway, with statistically significance. The *p* value of 0.05 was taken as the level of statistical significance. Affymetrix data were

analyzed in GeneSpring GX software (Agilent) and all other statistical analysis were performed with StatGraphics software (Statgraphics Statistical Graphics System, version 16.0).

Supplementary Material

Fig.1 Positive (A) and negative (B) correlations of S100a8 and S100a9 with the other differentially expressed genes. Results were obtained by multi-variable correlation analysis of the normalized gene expression values in individual mice on high iron diet conditions. The partial correlation coefficients and significance levels (P value in brackets) for the different gene combinations are shown. The relative strength of the correlations is highlighted by colour grading of blue (for positive correlations) or yellow (for negative correlation). Genes are ordered by the strength of their associations with S100a9.

A

	Retnlg	Fcer1g	Cd79b	Rnu3a	Pglyrp1	H2Ab1	Cd74	S100a8	S100a9
Tyrobp	0,9756 (0,0009)	0,9701 (0,0013)	0,9621 (0,0021)	0,9322 (0,0067)	0,901 0,0142	0,8377 0,0374	n.s.	0,7838 (0,0214)	0,9931 (0,0001)
Retnlg		0,9369 (0,0058)	0,9186 (0,0097)	0,9140 (0,0108)	0,9029 (0,0137)	n.s.	n.s.	0,8670 (0,0053)	0,9693 (0,0014)
Fcer1g			0,8872 (0,0184)	0,9694 (0,0014)	0,9118 (0,0113)	0,8288 (0,0414)	0,8134 (0,0490)	0,9088 (0,0018)	0,9558 (0,0029)
Cd79b				0,8183 (0,0465)	0,8759 (0,0221)	n.s.	n.s.	0,811 (0,0146)	0,9474 (0,0041)
Rnu3a					0,8491 (0,0324)	0,8355 (0,0383)	0,8408 (0,0360)	0,8222 (0,0123)	0,9403 (0,0052)
Pglyrp1						n.s.	n.s.	0,8409 (0,0089)	0,8537 0,0305
H2Ab1							n.s.	0,8061 (0,0157)	0,8737 0,0229
Cd74								0,8288 (0,0415)	0,8288 (0,0415)

B

	Clec2d	Tyrob	Retnlg	Fcer1g	Cd79b	Rnu3a	Pglyrp1	H2Ab1	Cd74	S100a8	S100a9
Cd69	0,9194 (0,0012)	-0,7969 (0,0179)	-0,8087 (0,0151)	-0,7989 (0,0174)	-0,8428 (0,0086)	-0,8717 (0,0048)	-0,8619 (0,0059)	n.s.	n.s.	-0,9254 (0,0010)	-0,9764 (<0,0001)
Clec2d		-0,7402 (0,0357)	-0,771 (0,0251)	n.s.	-0,8308 (0,0106)	-0,7651 (0,0270)	-0,8724 (0,0047)	-0,9856 (0,0003)	-0,9219 (0,0011)	-0,812 (0,0143)	-0,9421 (0,0005)

S1 Table: **Clinical correlations of the genes identified in the genome-wide differential screen**. Indicated are the correlation coefficient (r) R squared (R^2) and significance level (p) values obtained by simple regression analyses between the mRNA expression levels for each indicated gene and the clinical variables reflecting the immune-phenotype (CD8 T lymphocyte and subset counts) and the iron overload profile defined by estimated total body iron stores (TBIS). For each clinical variable are indicated the ranges of values in the total HH patient population analysed.

			CD8 T cell subsets		
		Total CD8 T lymphocytes $(0,09-0,73 \times 10^6 /ml)$	**naive + central memory** $(0,044-0,459 \times 10^6 /ml)$	**effector memory** $(0,060-0,403 \times 10^6 /ml)$	**TBIS (1,5-17,4g)**
mRNA expression levels	**CCR7**	n.s.	$r=+0,95\ R^2=91\%\ (p=0,0032)$	n.s.	$r=-0,78\ R^2=61\%\ (p=0,0129)$
	LEF1	n.s.	$r=+0,79\ R^2=63\%\ (p=0,0601)$	n.s.	$r=-0,70\ R^2=48\%\ (p=0,0379)$
	ACTN1	n.s.	$r=+0,87\ R^2=75\%\ (p=0,0249)$	n.s.	$r=-0,79\ R^2=62\%\ (p=0,0115)$
	NAT13	$r=-0,79\ R^2=62\%\ (p=0,0070)$	n.s.	$r=-0,91\ R^2=84\%\ (p=0,0108)$	n.s.
	P2YR8	$r=-0,86\ R^2=74\%\ (p=0,0015)$	n.s.	$r=-0,88\ R^2=78\%\ (p=0,0191)$	n.s.
	FOSL2	$r=-0,70\ R^2=49\%\ (p=0,0243)$	n.s.	$r=-0,81\ R^2=65\%\ (p=0,0525)$	n.s.

n.s.=not statistically significant

S2 Table Genes up and down regulated in *Hfe* knockout CD8⁺ T lymphocytes in comparison with C57BL/6 mice under normal diet condition

Transcripts ID	Gene abbreviation	Gene name	Fold Change	*p*-value	Gene ID
10493831	S100a8	S100 calcium binding protein A8 (calgranulin A)	16,53	0,00	20201
10499861	S100a9	S100 calcium binding protein A9 (calgranulin B)	12,96	0,00	20202
10362674	Rnu3a	U3A small nuclear RNA	5,31	0,00	19850
10436100	Retnlg	resistin like gamma	4,67	0,00	245195
10456005	Cd74	CD74 antigen (invariant polypeptide of major histocompatibility complex, class II antigen-associated)	4,62	0,01	16149
10372648	Lyz2	lysozyme 2	4,33	0,01	17105
10444291	H2-Ab1	histocompatibility 2, class II antigen A, beta 1	3,75	0,01	14961
10493812	S100a4	S100 calcium binding protein A4	3,44	0,00	20198
10450154	H2-Aa	histocompatibility 2, class II antigen A, alpha	3,35	0,01	14960
10570434	Ifitm1	interferon induced transmembrane protein 1	3,12	0,00	68713
10551025	Cd79a	CD79A antigen (immunoglobulin-associated alpha)	2,97	0,00	12518
10468517	Mxi1	Max interacting protein 1	2,90	0,03	17859
10512487	Rmrp	RNA component of mitochondrial RNAase P	2,81	0,02	19782
10444236	H2-DMb1/DMb2	histocompatibility 2, class II, locus Mb1 and Mb2	2,76	0,00	15000 | 14999
10508465	Marcksl1	MARCKS-like 1	2,68	0,00	17357
10551883	Tyrobp	TYRO protein tyrosine kinase binding protein	2,63	0,02	22177
10508721	Snora44	small nucleolar RNA, H/ACA box 44	2,59	0,03	100217418
10550509	Pglyrp1	peptidoglycan recognition protein 1	2,50	0,00	21946
10360070	Fcer1g	Fc receptor, IgE, high affinity I, gamma polypeptide	2,49	0,04	14127
10467979	Scd1	stearoyl-Coenzyme A desaturase 1	2,47	0,03	20249
10429520	Ly6d	lymphocyte antigen 6 complex, locus D	2,40	0,03	17068
10538871	Gm4964	predicted gene 4964	2,37	0,04	243420
10440576	Rnf160	ring finger protein 160	2,36	0,00	78913
10392142	Cd79b	CD79B antigen	2,20	0,01	15985
10558769	Ifitm1	interferon induced transmembrane protein 1	2,19	0,01	68713
10379727	Gm11428	predicted gene 11428	2,10	0,03	100034251
10414262	Ear2	eosinophil-associated, ribonuclease A family, member 2	2,08	0,03	13587
10349593	Faim3	Fas apoptotic inhibitory molecule 3	2,06	0,00	69169
10548817	Plbd1	phospholipase B domain containing 1	2,04	0,05	66857
10466172	Ms4a1	membrane-spanning 4-domains, subfamily A, member 1	1,99	0,05	12482
10548535	Klra3	killer cell lectin-like receptor, subfamily A, member 3	1,97	0,03	16634
10430818	Tnfrsf13c	tumor necrosis factor receptor superfamily, member 13c	1,97	0,01	72049
10556113	Rbm3	RNA binding motif protein 3	1,95	0,00	19652
10481627	Lcn2	lipocalin 2	1,91	0,00	16819
10535458	Zdhhc4	zinc finger, DHHC domain containing 4	1,89	0,03	72881
10563338	Ppp1r15a	protein phosphatase 1, regulatory (inhibitor) subunit 15A	1,87	0,03	17872
10422227	Spry2	sprouty homolog 2 (Drosophila)	1,86	0,04	24064
10398286	Mir342	microRNA 342	-4,69	0,01	723909
10515694	Szt2	seizure threshold 2	-3,04	0,02	230676
10503198	Chd7	chromodomain helicase DNA binding protein 7	-3,02	0,01	320790
10405779	Mir23b	microRNA 23b	-2,78	0,03	387217

S2 Table Genes up and down regulated in *Hfe* knockout CD8^{+} T lymphocytes in comparison with C57BL/6 mice under normal diet condition (cont.)

Transcripts ID	Gene abbreviation	Gene name	Fold Change	*p*-value	Gene ID
10456490	Cep192	centrosomal protein 192	-2,66	0,02	70799
10512827	Gm568	predicted gene 568	-2,50	0,03	230143
10351043	Snord47	small nucleolar RNA, C/D box 47	-2,50	0,02	100217446
10410311	Zfp456	zinc finger protein 456	-2,43	0,02	408065
10447036	n-R5s65	nuclear encoded rRNA 5S 65	-2,39	0,04	
10523134	Pf4	platelet factor 4	-2,35	0,04	56744
10503218	Chd7	chromodomain helicase DNA binding protein 7	-2,34	0,05	320790
10434396	Abcf3	ATP-binding cassette, sub-family F (GCN20), member 3	-2,29	0,00	27406
10412900	Nkiras1	NFKB inhibitor interacting Ras-like protein 1	-2,21	0,00	69721
10502934	Rabggtb	RAB geranylgeranyl transferase, b subunit	-2,21	0,00	19352
10531776	Fam175a	family with sequence similarity 175, member A	-2,10	0,00	70681
10548333	Cd69	CD69 antigen	-2,08	0,00	12515
10457838	Zfp397os	zinc finger protein 397 opposite strand	-2,04	0,00	328918
10586250	Dennd4a	DENN/MADD domain containing 4A	-2,03	0,02	102442
10546706	Rybp	RING1 and YY1 binding protein	-2,01	0,02	56353
10574141	Nlrc5	NLR family, CARD domain containing 5	-1,99	0,04	434341
10442032	BC002059	cDNA sequence BC002059, mRNA (cDNA clone MGC:6110)	-1,90	0,01	213811
10410530	Slc6a19	solute carrier family 6 (neurotransmitter transporter), member 19	-1,90	0,04	74338
10542156	Clec2d	C-type lectin domain family 2, member d	-1,89	0,00	93694
10525487	4932422M17Rik	RIKEN cDNA 4932422M17 gene	-1,89	0,03	74366
10522009	Pgm1	phosphoglucomutase 1	-1,87	0,02	66681
10515363	Mmachc	methylmalonic aciduria cblC type, with homocystinuria	-1,87	0,05	67096
10443459	Sfrs3	splicing factor, arginine/serine-rich 3 (SRp20)	-1,85	0,00	20383
10492582	Mir15b	microRNA 15b	-1,85	0,05	387175
10501048	Dennd2d	DENN/MADD domain containing 2D	-1,84	0,02	72121

S3 Table: Genes up and down regulated in *Hfe* knockout CD8^{+} T lymphocytes in comparison with C57BL/6 mice under high iron diet condition

Transcripts ID	Gene abbreviation	Gene name	Fold Change	*p*-value	Gene ID
10493831	S100a8	S100 calcium binding protein A8 (calgranulin A)	34,58	0,00	20201
10499861	S100a9	S100 calcium binding protein A9 (calgranulin B)	29,21	0,00	20202
10362674	Rnu3a	U3A small nuclear RNA	9,10	0,00	19850
10435497	Stfa2l1	stefin A2 like 1	6,49	0,05	268885
10436100	Retnlg	resistin like gamma	6,36	0,00	245195
10456005	Cd74	CD74 antigen (invariant polypeptide of major histocompatibility complex, class II antigen-associated)	3,71	0,05	16149
10551883	Tyrobp	TYRO protein tyrosine kinase binding protein	3,48	0,00	22177
10399428	Snord118	small nucleolar RNA, C/D box 118	3,25	0,00	100216530
10377429	Snord118	small nucleolar RNA, C/D box 118	3,25	0,00	100216530
10383756	Ifitm2	interferon induced transmembrane protein 2	3,18	0,01	80876
10569017	Ifitm3	interferon induced transmembrane protein 3	3,18	0,03	66141
10379727	Gm11428	predicted gene 11428	2,89	0,02	100034251
10444291	H2-Ab1	histocompatibility 2, class II antigen A, beta 1	2,77	0,03	14961
10551025	Cd79a	CD79A antigen (immunoglobulin-associated alpha)	2,74	0,04	12518
10550509	Pglyrp1	peptidoglycan recognition protein 1	2,65	0,01	21946
10539577	Spr	sepiapterin reductase	2,60	0,04	20751
10583286	Gpr83	G protein-coupled receptor 83	2,58	0,04	14608
10545014	Vopp1	vesicular, overexpressed in cancer, prosurvival protein 1	2,51	0,03	232023
10360070	Fcer1g	Fc receptor, IgE, high affinity I, gamma polypeptide	2,46	0,00	14127
10427908	Gm9948	predicted gene 9948	2,45	0,02	791293
10553299	Ifitm2	interferon induced transmembrane protein 2	2,42	0,02	80876
10344799	Cspp1	centrosome and spindle pole associated protein 1	2,42	0,02	211660
10527638	Alox5ap	arachidonate 5-lipoxygenase activating protein	2,40	0,01	11690
10368508	2610036L11Rik	RIKEN cDNA 2610036L11 gene	2,38	0,02	66311
10397536	Gm4005	predicted gene 4005	2,37	0,02	100042747
10588223	Anapc13	anaphase promoting complex subunit 13	2,36	0,01	69010
10493820	S100a6	S100 calcium binding protein A6 (calcyclin)	2,36	0,00	20200
10364293	Ube2g2	ubiquitin-conjugating enzyme E2G 2	2,28	0,04	22213
10473250	Mrpl18	mitochondrial ribosomal protein L18	2,21	0,02	67681
10569014	Ifitm2	interferon induced transmembrane protein 2	2,21	0,01	80876
10437963	Fam128b	family with sequence similarity 128, member B	2,19	0,00	72083
10590298	Eif1b	eukaryotic translation initiation factor 1B	2,18	0,01	68969
10452110	2410015M20Rik	RIKEN cDNA 2410015M20 gene	2,16	0,01	224904
10603833	Usmg5	upregulated during skeletal muscle growth 5	2,14	0,02	66477
10542156	Clec2d	C-type lectin domain family 2, member d	2,14	0,01	93694
10392142	Cd79b	CD79B antigen	2,12	0,01	15985
10412211	Gzma	granzyme A	2,11	0,00	14938
10514466	Jun	jun proto-onogene	2,11	0,01	16476
10575961	Usp10	ubiquitin specific peptidase 10	2,10	0,01	22224
10356999	Prdx2	peroxiredoxin 2	2,09	0,04	21672
10517336	Clic4	chloride intracellular channel 4 (mitochondrial)	2,08	0,02	29876
10440918	Tmem50b	transmembrane protein 50B	2,07	0,04	77975

S3 Table: Genes up and down regulated in *Hfe* knockout CD8⁺ T lymphocytes in comparison with C57BL/6 mice under high iron diet condition (cont.)

Transcripts ID	Gene abbreviation	Gene name	Fold Change	*p*-value	Gene ID
10362896	Cd24a	CD24a antigen	2,05	0,01	12484
10565081	Timm17a	translocase of inner mitochondrial membrane 17a	2,03	0,00	21854
10576391	Rab4a	RAB4A, member RAS oncogene family	1,99	0,03	19341
10416950	Mir18	microRNA 18	1,98	0,03	387135
10605943	Pdzd11|Kif4	PDZ domain containing 11 | kinesin family member 4	1,97	0,01	72621 | 16571
10604019	1810037I17Rik	RIKEN cDNA 1810037I17 gene	1,97	0,05	67704
10574151	Nlrc5	NLR family, CARD domain containing 5	1,96	0,02	434341
10396862	Actn1|Strm	actinin, alpha 1 | striamin	1,93	0,01	109711
10468287	Usmg5	upregulated during skeletal muscle growth 5	1,92	0,03	66477
10414958	Tcra-V8	T-cell receptor alpha, variable 8	1,92	0,04	100043322
10450814	Ppp1r11	protein phosphatase 1, regulatory (inhibitor) subunit 11	1,91	0,05	76497
10487476	1500011K16Rik	RIKEN cDNA 1500011K16 gene	1,91	0,01	67885
10490221	Atp5e	ATP synthase, H+ transporting, mitochondrial F1 complex, epsilon subunit	1,91	0,02	67126
10371002	Lsm7	LSM7 homolog, U6 small nuclear RNA associated (S. cerevisiae)	1,90	0,05	66094
10430778	Phf5a	PHD finger protein 5A	1,90	0,03	68479
10345183	Cdk10	cyclin-dependent kinase 10	1,89	0,01	234854
10349648	Ctse	cathepsin E	1,88	0,04	13034
10603837	Ndufb11	NADH dehydrogenase (ubiquinone) 1 beta subcomplex, 11	1,87	0,02	104130
10492757	Plrg1	pleiotropic regulator 1, PRL1 homolog (Arabidopsis)	1,87	0,02	53317
10416199	Entpd4	ectonucleoside triphosphate diphosphohydrolase 4	1,86	0,04	67464
10512901	Mrpl50	mitochondrial ribosomal protein L50	1,85	0,00	28028
10450640	Mrps18b	mitochondrial ribosomal protein S18B	1,85	0,00	66973
10449356	AI413582	expressed sequence AI413582	1,83	0,03	106672
10373577	Ormdl2|Dnajc14	ORM1-like 2 (S. cerevisiae) | DnaJ (Hsp40) homolog, subfamily C, member 14	1,83	0,02	66844 | 74330
10366043	Dusp6	dual specificity phosphatase 6	1,81	0,04	67603
10548333	Cd69	CD69 antigen	-2,49	0,00	12515
10396862	Actn1|Strm	actinin, alpha 1 | striamin	-1,93	0,01	109711 | 20904
10542156	Clec2d	C-type lectin domain family 2, member d	-2,14	0,01	93694
10345183	Cdk10	cyclin-dependent kinase 10	-1,89	0,01	234854
10575961	Usp10	ubiquitin specific peptidase 10	-2,10	0,01	22224
10574151	Nlrc5	NLR family, CARD domain containing 5	-1,96	0,02	434341
10344799	Cspp1	centrosome and spindle pole associated protein 1	-2,42	0,02	211660
10397536	Gm4005	predicted gene 4005	-2,37	0,02	100042747
10583286	Gpr83	G protein-coupled receptor 83	-2,58	0,04	14608
10416950	Mir18	microRNA 18	-1,98	0,03	387135
10416199	Entpd4	ectonucleoside triphosphate diphosphohydrolase 4	-1,86	0,04	67464

S4 Table: Functional categories of the significantly different expressed genes between *Hfe* knockout and wild type

Category	Term	Count	*P* value	Genes
CLUSTER 1				
SP_PIR_KEYWORDS	Immune response	8	3.41E-07	Cd79a, Cd74, H2-Ab1, H2-Aa, Pglyrp1, Tnfrsf13c, Cd79b, Faim3
GOTERM_BP_FAT	Antigen processing and presentation of exogenous peptide antigen	5	9.42E-07	Cd74, H2-DMb1, Fcer1g, H2-Ab1, H2-Aa
GOTERM_BP_FAT	Positive regulation of leukocyte activation	4	1.95E-03	Cd74, Fcer1g, H2-Aa, Tnfrsf13c
CLUSTER 2				
GOTERM_CC_FAT	Late endosome	4	2.18E-04	Cd79a, Cd74, H2-DMb1, H2-Ab1
KEGG_PATHWAY	Intestinal immune network for iga production	4	4.92E-04	H2-DMb1, H2-Ab1, H2-Aa, Tnfrsf13c
KEGG_PATHWAY	Graft-versus-host disease	4	5.85E-04	Klra3, H2-DMb1, H2-Ab1, H2-Aa
CLUSTER 3				
GOTERM_BP_FAT	Positive regulation of response to stimulus	6	1.02E-04	Cd79a, Fam175a, Fcer1g, H2-Aa, Tnfrsf13c, Cd79b
INTERPRO	Phosphorylated immunoreceptor signaling itam	3	1.31E-04	Cd79a, Fcer1g, Cd79b
GOTERM_BP_FAT	Immune response-activating signal transduction	3	6.86E-03	Cd79a, Fcer1g, Cd79b
GOTERM_BP_FAT	Immune response-regulating signal transduction	3	8.04E-03	Cd79a, Fcer1g, Cd79b
CLUSTER 4				
GOTERM_BP_FAT	Immune response	11	1.83E-07	Pf4, Cd79a, Cd74, H2-DMb1, Fcer1g, H2-Ab1, H2-Aa, Pglyrp1, Tnfrsf13c, Cd79b, Faim3
SP_PIR_KEYWORDS	Disulfide bond	17	1.50E-04	Lcn2, Pf4, Klra3, Tyrobp, Cd79a, Lyz2, H2-Ab1, H2-Aa, Pglyrp1, Tnfrsf13c, Cd79b, Faim3, Cd74, Fcer1g, Ly6d, Clec2d, Cd69
SP_PIR_KEYWORDS	Signal	16	3.59E-03	Lcn2, Pf4, Tyrobp, Cd79a, H2-DMb1, Lyz2, H2-Ab1, H2-Aa, Pglyrp1, Cd79b, Faim3, Retnlg, Gm11428, Fcer1g, Ly6d, Plbd1
INTERPRO	lpr007110:immunoglobulin-like	5	3.44E-02	Cd79a, H2-DMb1, H2-Ab1, H2-Aa, Cd79b
CLUSTER 5				
GOTERM_BP_FAT	Positive regulation of immune system process	6	1.67E-04	Cd79a, Cd74, Fcer1g, H2-Aa, Tnfrsf13c, Cd79b
GOTERM_BP_FAT	Go:0001775~cell activation	5	3.60E-03	Ms4a1, Pf4, Cd79a, Cd74, Fcer1g
GOTERM_BP_FAT	Go:0045321~leukocyte activation	4	1.86E-02	Ms4a1, Cd79a, Cd74, Fcer1g
CLUSTER 6				
UP_SEQ_FEATURE	Calcium-binding region:2; high affinity	3	4.23E-04	S100a8, S100a4, S100a9
UP_SEQ_FEATURE	Calcium-binding region:1; low affinity	3	4.23E-04	S100a8, S100a4, S100a9
PIR_SUPERFAMILY	Pirsf002353:s-100 protein	3	4.73E-04	S100a8, S100a4, S100a9
INTERPRO	lpr001751:s100/cabp-9K-type, calcium binding	3	1.54E-03	S100a8, S100a4, S100a9
SP_PIR_KEYWORDS	Ef hand	3	2.22E-03	S100a8, S100a4, S100a9
SP_PIR_KEYWORDS	Calcium binding	3	6.17E-03	S100a8, S100a4, S100a9
CLUSTER 7				
GOTERM_BP_FAT	Leukocyte chemotaxis	3	2.30E-03	Pf4, Fcer1g, S100a9
GOTERM_BP_FAT	Cell chemotaxis	3	2.30E-03	Pf4, Fcer1g, S100a9
GOTERM_BP_FAT	Chemotaxis	4	2.8E-03	Pf4, S100a8, Fcer1g, S100a9
GOTERM_BP_FAT	Locomotory behavior	5	3.09E-03	Pf4, S100a8, Chd7, Fcer1g, S100a9
CLUSTER 8				
GOTERM_BP_FAT	Defense response	6	5.11E-03	Cd74, Fcer1g, Lyz2, H2-Aa, Pglyrp1, Clec2d
GOTERM_BP_FAT	Defense response to bacterium	3	3.04E-02	Fcer1g, Lyz2, Pglyrp1

S4 Table: **Functional categories of the significantly different expressed genes between** *Hfe* **knockout and wild type (cont.)**

Category	Term	Count	*P* value	Genes
CLUSTER 9				
GOTERM_MF_FAT	**Carbohydrate binding**	5	7.02E-03	**Pf4, Klra3, Pglyrp1, Clec2d, Cd69**
SP_PIR_KEYWORDS	**Signal-anchor**	5	1.81E-02	**Klra3, Cd74, Tnfrsf13c, Clec2d, Cd69**
UP_SEQ_FEATURE	**Domain:c-type lectin**	3	2.21E-02	**Klra3, Clec2d, Cd69**
INTERPRO	**Ipr018378:c-type lectin, conserved site**	3	2.82E-02	**Klra3, Clec2d, Cd69**
INTERPRO	**Ipr001304:c-type lectin**	3	3.50E-02	**Klra3, Clec2d, Cd69**
INTERPRO	**Ipr016186:c-type lectin-like**	3	4.01E-02	**Klra3, Clec2d, Cd69**
SMART	**Sm00034:clect**	3	4.16E-02	**Klra3, Clec2d, Cd69**

Category columm shows the original database/resource from which terms originate. The Term column indicates the enriched terms associated with the gene list. The Count column indicates the number of genes involved in the term. The *P* value was obtained with the modified Fisher exact *test*. BP, biological processes; GO, Gene Ontology Term; KEGG, Kyoto Encyclopedia of Genes and Genomes; MF, molecular functions; PIR, Protein Information Resource; UDP, Uridine 5'-diphospho

S5 Table: Expression levels of iron related genes in CD8^{+} T lymphocytes from *Hfe* knockout and wild type C57BL/6 mice. The relative levels of expression are highlighted by colour grading according to normalized expression values. The significance of the differential expression values is indicated by the *p* value of T-test.

| Gene | Protein | Normal Iron Diet | | *p* value |
		Hfe [-/-]	C57BL/6	
Iron storage				
Ftl1	Ferritin L Chain			ns
FtH	Ferritin Heavy chain			ns
Hmox1	Heme oxigenase			ns
Iron transport				
Slc25a37	Mitoferrin			ns
Slc11a2	Dimetal transporter1			ns
Lcn2	Lipocalin2			0.0016
Sfxn2	Sideroflexin2			ns
Slc40a1	Ferroportin			ns
Abcg2	Bcrp			ns
Receptors				
Tfrc	Transferrin receptor			ns
Lrp1	LRP/CD91			ns
Regulators				
Smad4	Smad4			ns
Smad7	Smad7			ns
Usf2	Usf2			ns
Hamp2	Hepcidin 2			ns
Fxn	Frataxin			ns
Ireb2	IRP2			ns
BMP6	BMP6			ns
BMP9	BMP9			ns
Hamp1	Hepcidin 1			ns
Hfe2	HJV			ns
Hfe	HFE			ns
Oxidoreductases				
Cybrd1	Dcytb			ns

☐ No expression (< 5normalized gene expression value)

☐ low expression ([5 a 7[normalized gene expression value)

☐ medium expression([7 a 9[normalized gene expression value)

☐ high expression(>9 normalized gene expression value)

S6 Table: **Sequences of the oligonucleotide primers used for the first and second PCR experiments in CD8 T lymphocytes from HH patients**. Primers on the top: forward primers; Primers on the bottom: reverse primers

Gene	Accession number	1st PCR primers	2nd PCR primers
LEF1	AF288571	5'-ATCCCGAAGAGGAAGGCGATT-3' 5'-GCACCACGGGCACTTTATTTG-3'	5'-CCGATGACGGAAAGCATCCAG-3' 5'-GCACCACGGGCACTTTATTTG-3'
ACTN1	DQ496098	5'-TGAAGATGACCCTGGGCATGA-3' 5'-CAACGATGTCTTCGGCATCCA-3'	5'-GGAAGGATGGCCTCGGCTT-3' 5'-CAACGATGTCTTCGGCATCCA-3'
CCR7	BC035343	5'-ACTTCCTCCCCAGACAGGGGT-3' 5'-GCCCACGAAACAAATGATGGA-3'	5'-TGGTGGTGGCTCTCCTTGTCA-3' 5'-GCCCACGAAACAAATGATGGA-3'
NR4A2	BC009288	5'-CCCGGTGAGTCTGATCAGTGC-3' 5'-CAATCCATTCCCCAAAGCCAC-3'	5'-GAGAAGATCCCTGGCTTCGCA-3' 5'-CAATCCATTCCCCAAAGCCAC-3'
NAA50	BC012731	5'-AGCTGGGAGATGTGACACCACA-3' 5'-GCCGACTCATTGCTGATCTGG-3'	5'-GGCACCTTACCGAAGGCTAGGA-3' 5'-GCCGACTCATTGCTGATCTGG-3'
P2RY8	NM_178129	5'-CCTTTGCAAGGTTGCTGGACA-3' 5'-AGAGAAGAGGTTGCCCGGGAT-3'	5'-TTCTGCCGCTGCTTCTGCA-3' 5'-AGAGAAGAGGTTGCCCGGGAT-3'
FOSL2	NM_005253	5'-GCTCAGGCAGTGCATTCATCC-3' 5'-TGCAGCCAGCTTGTTCCTCTC-3'	5'-GCGTGATCAAGACCATTGGCA-3' 5'-TGCAGCCAGCTTGTTCCTCTC-3'
GAPDH	M33197	5'-GGTCGGAGTCAACGGATTTGG-3' 5'-ATGGTGGTGAAGACGCCAGTG-3'	5'-CAAATTCCATGGCACCGTCAA-3' 5'-ATGGTGGTGAAGACGCCAGTG-3'

S7 Table: **Sequences of the oligonucleotide primers used for S100a8 and S100a9 expression studies in sorted CD8 from HH patients and controls**

Gene	Primer forward	Primer reverse
18S rRNA human	5`-CGCCGCTAGAGGTGAAATTC-3`	5`-TTGGCAAATGCTTTCGCTC-3`
S100a8 human	5`-GTCTCTTGTCAGCTGTCTTTCA-3`	5`-CCTGTAGACGGCATGGAAAT-3`
S100a9 human	5`-GGAATTCAAAGAGCTGGTGC-3`	5`-TCAGCATGATGAACTCCTCG-3`

Chapter 4

General Discussion

Conclusions and future perspectives

General discussion

The general objective of this thesis was to clarify the role of lymphocytes in iron homeostasis, using the clinical model of Hereditary Hemochromatosis (HH). Due to some of its genetic characteristics, HH offers an excellent biological context to study the interactions between the immune system and iron. First, the gene implicated in this iron-overload disorder, *HFE*, is a non-classical MHC-class I gene, localized in the MHC genetic region, a cluster of highly related genes involved in immune responses [27]. HH patients are homozygous for the p.C282Y mutation in the *HFE* gene which is found in strong linkage disequilibrium with particular HLA-A alleles. Moreover, the inheritance of some specific HLA haplotypes predisposes HH patients to display a phenotype of low numbers of peripheral CD8^{+} T lymphocytes strongly associated with their clinical severity in terms of iron overload. These special features led to the definition of two specific goals in this thesis: i) to clarify the genetic contribution of the MHC-class I region to the setting of CD8^{+} T lymphocyte numbers, and ii) to elucidate the mechanisms through which lymphocytes may act as modifiers of the clinical expression in HH.

HH and its MHC heritage

The MHC genetic region is one of the most gene-dense and polymorphic regions of the human genome. It is also the genomic region most strongly associated with disease susceptibility, especially with autoimmune and infectious diseases [276]. This is a fact largely attributed to the high density of genes related with immune functions found in this region, in particular the human leukocyte antigen (HLA) class I and class II genes. In this context, it is interesting to note that HH provides one of the most remarkable examples of HLA-disease association. The finding of a very high frequency of the HLA-A*03 allele associated with hemochromatosis [19] constituted the first step leading to the later positional cloning of the *HFE* gene 4Mb distant from the HLA-A cluster. The finding that the vast majority of HH patients are homozygous for a single mutation (p.C282Y) that abrogates HFE function [27], and the evidence of iron overload in mouse models lacking *Hfe*, all constitute strong evidence to support a causal effect for this genetic alteration. Nevertheless, considering this strong association to the disease in the context of the MHC high gene density, the strong linkage disequilibrium and the extreme polymorphism and clustering of genes with related functions in so many diverse immune cell functions, it turns highly complex to determine the true causative effect of the disease-associated HFE allelic product. Relevant to this concept was the finding that a highly conserved microhaplotype (A-A-T) localized in the region between *HFE* and *HLA* was associated with both a phenotype of low CD8^{+} T lymphocyte

numbers and a more severe iron overload in Portuguese patients [44], suggesting that other genes in this region could also be involved in the disease process.

One of the specific objectives of this thesis was to test if the previously found association of the A-A-T microhaplotype as a predictive phenotype marker in Portuguese patients was also observed in other geographically distant populations. The results, described in detail in chapter 3.1, clearly show that the predictive value of this haplotype cannot be generalized worldwide. We found that the low CD8 phenotype was associated with the most conserved haplotypes carrying A-A-T and the HLA-A*03 allele in the populations from Porto (Portugal) and Alabama (USA) but not in the population from Nord-Trøndelag (Norway). Because the low CD8 phenotype is generally associated with a more severe iron overload phenotype, we speculate that these genotype/phenotype differences could explain the presence of clinical symptomatology in Alabama and Porto patients while Nord-Trøndelag patients are mostly asymptomatic [171, 197]. Assuming the existence of a major genetic determinant of CD8$^+$ T-lymphocyte numbers that is transmitted in linkage disequilibrium with *HFE* in its ancestral haplotype, we considered that the population from Porto, by keeping the strongest genotype-phenotype association, would be the ideal population to allow further narrowing of the region of interest to look for a candidate locus associated with the transmission of the trait. With that purpose, 43 HH patients and 105 normal individuals from north Portugal were genotyped for 63 markers in the chromosomal region between *HFE* and *HLA-B*. The results, described in detail in chapter 3.2, were somehow surprising in the sense that the inclusion of additional markers did not narrow the region previously defined by the A-A-T microhaplotype. Instead, a higher homology was found among patients with different phenotypes suggesting that either the putative major quantitative trait locus (QTL) is localized beyond the defined limits, or the coverage of the region was still insufficient to find better markers. One additional possibility is that the low CD8 trait may be defined by the combination of multiples genes in a more extended region. Although this study did not provide, as originally expected, a great advance in the positional cloning of a major QTL for CD8$^+$ T lymphocyte numbers, it revealed, however, a novel important aspect of MHC genetics. This was the evidence that the long recognized recombination suppression found in this chromosomal region depends on the haplotype structure and allele combination in highly conserved haplotypes, observed in both HH and normal chromosomes. This finding not only helps explaining the evolutionary history of HH carrying haplotypes and its strong association with a low CD8 phenotype (in particular in HLA-A*03B*07 carrying haplotypes), but also suggests, for the first time, that the process of recombination suppression involves the combination of particular gene alleles in a restricted region close to HLA [277, 278].

While providing new insights on the commonly reported phenotype of low CD8$^+$ T lymphocytes in HH patients, the study described above followed a purely genomic approach and could thus not provide any indication of how lymphocytes may influence iron overload. In order to approach this question, a series of functional studies were performed, both *in vitro* and *in vivo*, which are referred to in the next paragraphs.

The Lymphocyte pool: a new circulating iron storage compartment

Iron homeostasis classically involves four major compartments: the *uptake* compartment (enterocytes), the *functional* compartment (erythroid precursors or other proliferating cells), the *recycling* compartment (spleen macrophages), and the *storage* compartment (hepatocytes and macrophages). Work performed in the context of this thesis placed, for the first time, the lymphocyte pool as a new "circulating storage compartment". This was mostly based on the demonstration that circulating T lymphocytes are able to take up and retain iron acquired in the form of NTBI. Moreover, we identified Fe$_3$Cit$_3$ as the predominant oligomeric iron-citrate species in iron-overload physiological conditions, and the one that is preferentially taken up by T cells and hepatocytes (published in Arezes et al.2013)[234]. Whilst we argue that T lymphocytes are important players in systemic iron homeostasis, we appreciate that the remaining blood cell types, may also contribute to the fine-tuning of iron homeostasis. As previously described, the ability to take up NTBI was also observed in other circulating blood cells such as reticulocytes and erythrocytes [279, 280], monocytes, eosinophils, basophils, neutrophils and platelets [281]. The ability of these cell types to buffer the NTBI and keeping it away from target organs may depend on their retention capability and selectivity for the NTBI species that is present in circulation.

The observation that T lymphocytes are able to take up and retain NTBI raised the following questions: what is the fate of the NTBI taken up by lymphocytes? What is the physiological implication of these findings *in vivo*?

The fate of intracellular NTBI taken up by T lymphocytes was addressed in the paper published by Pinto et al in 2014 where we describe an increase in the labile iron pool (LIP) content in response to incubation with 5µM Fe-citrate. Besides using intracellular iron to proliferate, T cells also increase their iron-storage capacity in response to NTBI uptake by up-regulating ferritin levels [269]. Previous studies addressing the response of ferritin to NTBI in lymphocytes showed contrasting results [282-285] and this could be explained by the use of distinct iron donors and of non-physiological NTBI concentrations. We argue that the use of ferric citrate as iron donor, the maintenance of citrate concentrations between the physiological interval of 60–140 µM [286] and the use of iron concentrations within the range that is commonly found in iron overload situations [230] are the correct experimental

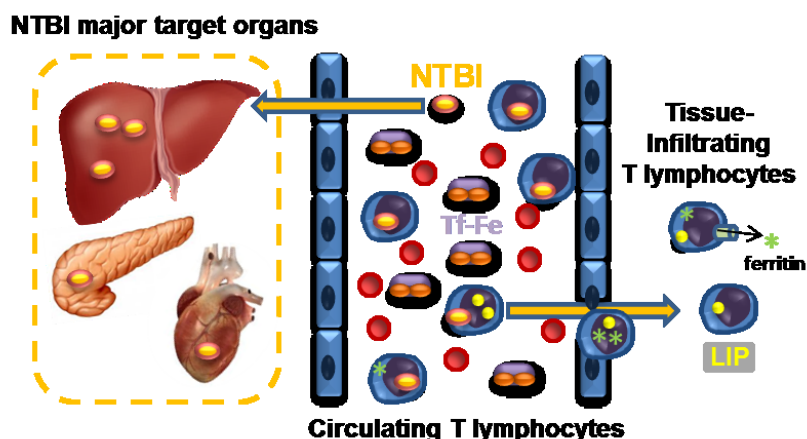conditions and should become the standard procedure for future studies involving biological systems and NTBI.

Fig.1 Proposed model of NTBI storage and further utilization for cell growth. NTBI is rapidly cleared from circulation by hepatocytes. Circulating T lymphocytes are the first cells in contact with the NTBI. NTBI in the blood stream is taken up by T lymphocytes, where it integrates the intracellular labile iron pool (LIP) and the ferritin stores (*). These cells, and possibly others, constitute the "circulating" iron storage compartment. When the circulating and liver NTBI clearance capacities are exceeded, other cell types, such as pancreatic beta cells or cardiomyocytes, also take up NTBI, with iron accumulation in the respective organs (pancreas, heart). Besides constituting a first line "safe" deposit of iron, T lymphocytes (and possibly other circulating cells) could also contribute to iron distribution and delivery to other cells and tissues, either in normal physiological (homeostatic erythroid/lymphoid proliferation) or pathological conditions (stress erythropoiesis, inflammation, tumor growth). T lymphocyte-derived iron uptake by target cells could occur as transferrin-bound iron (Tf-Fe) or as NTBI, which could be exported directly via ferroportin or, eventually, by ferritin secretion, as proposed earlier (Dörner et al., 1980[287]). (Adapted from Pinto et al 2014)

The physiological implications of the capacity of T lymphocytes to store NTBI was addressed *in vivo*, firstly in a mouse model deficient in T lymphocytes, the Foxn1[null] mouse, fed with an iron-sufficient or iron-rich diet (Pinto et al. 2014)[269]. Foxn1[null] mice fed with iron-sufficient diet did not increase the liver iron stores, confirming that the deficiency of T lymphocytes alone is not the cause of iron overload. Under an iron-rich diet, however, Foxn1[null] mice displayed higher stores than the normal T cell phenotype (Foxn1^{+/-}) under the same diet condition. To trace the NTBI, we have injected Foxn1[null] fed iron-rich diet with radiolabeled ^{55}Fe -citrate and ^{55}Fe was measured in the liver. By transferring T lymphocytes from Foxn1^{+/-} into Foxn1[null] mice, we showed that the reposition of circulating T lymphocytes lowers the liver iron stores. This decrease in the liver iron content was directly proportional to the number of transferred CD8 T cells and this effect was not due to alterations in intestinal iron absorption since no changes in liver hepcidin mRNA levels were observed in response to T lymphocyte transfer. As a whole, these results support our hypothesis that T lymphocytes take up circulating NTBI preventing its accumulation within parenchymal cells, therefore protecting the liver, as well as other target organs, from tissue damage.

One important point addressed in this thesis was the extension of the above mentioned question to the human model. Taking the results obtained with the mouse model into consideration, we would expect patients with low numbers of CD8$^+$ T lymphocytes to be more prone to develop a more severe iron accumulation, due to a lower remodelling potential. In fact, results of the *in vitro* human CD8$^+$ T cells experiment (described in detail in chapter 3.3) corroborated the "remodelling hypothesis" observed in the Foxn1^{null} iron-overloaded mice. After assessing the NTBI retention capacity of HH CD8$^+$ T cells, their systemic storage potential was estimated and shown to correlate strongly with the transferrin saturation at the time of the experiment. Moreover, the NTBI retention profile of each patient reflected the pattern of iron re-accumulation after depletion of the iron stores.

It remains elusive whether the patients' low retention capacity by T cells is under a systemic regulation by hepcidin or is only due to a hepcidin-independent higher iron export. The fact that, in spite of a deregulated hepcidin expression, the absolute levels of serum hepcidin in HH patients may be within the normal range supports the idea that an additional mechanism may be directly regulating the iron export by targeting ferroportin independently of hepcidin. A response to this question was, however, out of the scope of this thesis.

HFE and CD8$^+$ T lymphocytes: beyond the iron field

Previous studies in HFE-HH patients consistently reported the existence of specific abnormalities in CD8$^+$ T lymphocyte functions including defective lymphocyte-specific protein tyrosine kinase (p56lck) activity, decreased cytotoxic activity, decreased number of CD8$^+$ T cells expressing the co-stimulatory molecule CD28, a higher number of CD8$^+$ T cells lacking CD28, and an abnormally high percentage of HLA-DR-positive activated T cells [29, 152, 170]. Based on this knowledge, one of the main objectives of this thesis (described in detail in Chapter 3.3) was to question if there was any direct impact of HFE on the differentiation and activation profile of CD8$^+$ T lymphocytes. For that purpose, two gene expression microarray approaches were used. Firstly, we compared the transcriptional profiles of CD8$^+$ T cells of HH patients with high or low numbers of these cells at the periphery. We observed that the fold-changes of the differently expressed genes between the two groups were lower than 2, suggesting that there were no major functional differences in CD8$^+$ T cells from these two groups of patients. Nevertheless, we found a set of differentially expressed genes, which were significantly associated to the relative representation of specific CD8$^+$ T subpopulations of naïve, central and effector memory cells. Genes derived from this screening were further validated in a larger number of HH patients and their expression compared between patients and normal controls. The most differentially expressed genes between these two groups were P2Ry8, which was increased in CD8 central memory cells (CD8$_{CM}$), and LEF1, which was down regulated in CD8 effector memory cells (CD8$_{EM}$) of HH patients in comparison to

controls. These results pointed to HFE as a potential player in the differentiation step of central-memory to effector memory which is in agreement with the previous observation of lower numbers of $CD8_{EM}$ reported in HH patients [31]. Interestingly, in this same study Macedo et al reported that the lower numbers of $CD8_{EM}$ cells in patients carrying the A-A-T haplotype in homozygosity when comparing with patients carrying the G-G-G haplotype is mainly due to reduced numbers of $CD8_{EM}$ $CD27^-CD28^-$ [31]. An effect of other MHC-linked genes on the differentiation process and setting of $CD8^+$ T cells can thus not be discarded.

In order to study the expression profile of $CD8^+$ T cells without the confounding effect of MHC variability, which is seen in human patients, we further addressed the impact of HFE on the transcriptional profile of $CD8^+$ T lymphocytes in the murine disease model of *Hfe* deficiency. One should bear in mind, however, that the *Hfe*$^{-/-}$ mouse model does not fully recapitulate the complete phenotype of HH patients, namely the defects in $CD8^+$ T cell numbers. One of the characteristics of the *Hfe*$^{-/-}$ animal model is that all mice share a common MHC background, which may justify the homogeneity in $CD8^+$ lymphocyte phenotypes. Our genome-wide expression profiling results in the *Hfe*$^{-/-}$ and wild-type mice revealed that the most enriched functional categories of differentially expressed genes in *Hfe*$^{-/-}$ mice when comparing with wild-type mice were related with the signaling and activation of $CD8^+$ T cells. Moreover, we identified calgranulins as the most differentially up-regulated genes in *Hfe*$^{-/-}$, a result further confirmed in $CD8^+$ T cells from human HH patients, which raises the possibility that these mediators may be players on a common pathway with HFE.

The above mentioned results suggesting an activation state of $CD8^+$ T cells in *Hfe* deficiency *in vivo* are supported by a recent *in vitro* study by Reuben et al, who describe that the co-transfection of APC cells with the full length gp100 melanoma antigen in combination with HFE WT inhibits the activation state of $CD8^+$ T lymphocytes [224]. In contrast to the co-transfection with p.H63D mutated HFE, p.C282Y mutated HFE or control HLA-A1 constructs were not able to reproduce the WT inhibitory effect and could not downregulate to the same extent the secretion of several soluble factors such as IL-13, MIP-1β, INF-Y and sTNFR, leaving CD8 T cells in a more activated state. Moreover, Reuben et al identified the α1-2 domains as the participants on the inhibitory effect of CD8+ T-lymphocyte activation. These domains are known to share specific chaperone binding sites with MHC Class I molecules.

Considering the dual role of HFE as a monitor of circulating iron levels and simultaneously a controller of signalling and T cell activation discussed above, one has to consider its implications in two conditions where cells compete for iron in the context of an immune response: one is infection and another is cancer. Infection has been claimed as a potential driving selective force for the observed high frequency of the p.C282Y mutation in normal populations. In the context of epidemics, it is important to consider the putative impact of MHC related selection. It is plausible to accept that during the plague period

caused by *Yersinia pestis*, those individuals with the p.C282Y mutation would be better equipped to resist the infection since their macrophages, kuppfer cells and enterocytes display an iron depleted phenotype that may offer an additional protection against the growth of intracellular pathogens. Considering the possibility of a more activated immune system with increased recognition of MHC-I antigens by CD8^{+} T cells lacking surface HFE, this could be an additional advantage for pathogen clearance.

In terms of the impact of HFE in cancer biology, it was recently shown that tumor cells increase HFE expression at cell membrane [288]. The same study also reported a reciprocal regulation where activated CD3 T cells were able to inhibit the HFE expression in tumor cells lines [288]. Down-regulation of HFE in tumor cells lines was shown to be mediated by CD4^{+} and CD8^{+} T lymphocytes through secretion of IFN-Y and TNF [288]. The increased HFE expression is intriguing in the perspective of tumor growth and any interpretation is, so far, merely speculative. One possible reason why tumour cells increase HFE expression would be to down-regulate the MHC-I antigen processing and presentation, thus escaping immune surveillance.

S100a9 a new mediator in the HFE-CD8 crosstalk

From the clinical point of view, the finding that the S100a8 and S100a9 calgranulins were the most differentially regulated genes in CD8^{+} cells of *Hfe*^{-/-} is of great relevance, especially since we confirmed that the expression of these calgranulins is also increased in peripheral blood cells from HH patients. This was the first description of up-regulated expression of these proteins in the context of HH, an iron overload disorder strongly associated with alterations in the immune system, particularly of CD8^{+} T lymphocytes. Previous studies in a mouse model of autoimmune disease suggested that S100a8 and S100a9 proteins function as TLR4 ligands on CD8^{+} T cells, which in turn upregulate IL-17 expression and induce autoimmunity in mice and humans [255]. The same TLR4 and TLR3 signaling pathways were shown to be able to down-regulate HFE protein and ferroportin expression in the spleen after activation with LPS and polyinosinic:polycytidylic acid, poly(I:C) treatments [289]. Although these studies did not address the eventual autocrine performance of calprotectins, they suggest, however, that the TLR4 signaling pathway may be a common target for both iron regulation and immune activation, and that S100a8 and S100a9 may somehow have an important role in the process. Although these two proteins are known to function as an S100a8/S100a9 heterodimer called calprotectin, they may also act independently. We reported a high expression of S100a9 in CD8^{+} T cells from HH patients, in contrast with a low expression of S100a8. Other authors have also stressed an independent role for S100a9. For example, local production of S100A9 has been described to induce monocyte production of pro-inflammatory cytokines like TNFα, IL-1β and IL-6, and

of chemokines like MIP-1α and MCP-1, which in turn could modulate the whole immune response [271]. Moreover, S100a9 autocrine activation stimulates the production of IL-6 and TNF-α production by T lymphocytes. Considering that, as previously referred, TNF-α production by T lymphocytes is able to down-regulate HFE expression in tumor cell lines [288], and the recent finding that S100a9 local production in breast tumor is associated with a reduced metastatic rate, and therefore a better prognostic [290], we may speculate that S100a9 and HFE could synergistically modulate the immune responses mediated by either iron or inflammation.

Conclusions and future perspectives

Altogether, the data presented in the different chapters of this thesis highlight and strengthen our view of lymphocytes as important players in iron homeostasis, and increase our knowledge of the interaction between CD8$^+$ T lymphocyte anomalies in Hereditary Hemochromatosis (HH) and of its genetic background in the context of the MHC cluster genes.

The extensive linkage disequilibrium at the entire 4Mb region between *HFE* and *HLA*, within the MHC class I cluster, naturally favoured the detection of several genotype-phenotype associations in HH, starting from the historical HLA-disease association to the discovery of the *HFE* p.C282Y causing mutation, and to the most recently described association with a genetic trait involved in the transmission of CD8$^+$ T lymphocyte numbers. Because, in general, recombination is assumed to be lower in the MHC than in other regions of the genome, this fact alone could justify the remarkable genotype/phenotype associations found in HH. The results we describe here, however, suggest for the first time that recombination suppression may be selectively favoured in the context of particular haplotype combinations in the region between *HFE* and *HLA*, and this interpretation offers a good explanation for the differences in genotype-phenotype associations found among geographical distant HH populations, who probably had different recombination histories or founder effects.

Work presented in this thesis also brought into light some mechanisms that may explain how CD8$^+$ T lymphocytes act as modifiers of iron overload. We demonstrated that CD8$^+$ T cells are able to take up and retain NTBI and identified the specific oligomeric species Fe$_3$Cit$_3$, as the most physiological NTBI form that is preferentially internalized by these cells. Based on these findings, we hypothesized that the NTBI clearance from circulation by these cells avoids the accumulation within hepatocytes or other tissues where it may be toxic. Evidence is missing, however, on the mechanisms involved in NTBI uptake, transport and signaling by lymphocytes. From the transcriptional study of the CD8$^+$ T cells in the context of *Hfe* deficiency (*Hfe*$^{-/-}$ mice) we concluded that *Hfe* impacts on their function by up-regulating several genes involved in T cell activation, signaling and differentiation. The observation that the most striking difference in the *Hfe*$^{-/-}$ mice was the higher expression of S100a9, and that its expression is also increased in CD8$^+$ T lymphocytes from HH patients points for the first time to the importance of this calgranulin in the disease process.

In terms of future perspectives, continuing work in this field may prove to be important to clarify some aspects of disease expression in HH that remain elusive. We plan to further characterize the S100a9 protein expression in CD8$^+$ subpopulations and to measure the protein concentration in the serum of HH patients as a new marker to address the clinical

heterogeneity among patients. Based on the previously described role of S100a9 as a major player in autoimmune diseases such as rheumatoid arthritis, and its association with a CD8 autoreactive phenotype, we will be particularly interested on its involvement in HH-related arthropathy. Another implication of our work in terms of future directions is the possibility of better approaching the positioning of a putative major genetic trait involved in the transmission of CD8$^+$ T lymphocyte numbers. We are presently conducting a deep sequencing analysis covering the entire exonic region between *HLA-DRB1* and *HFE* in samples from Portuguese HH patients. Sample selection for this study took into account the information obtained in our high-density mapping. In particular, we have chosen patients with a conserved haplotype structure despite divergent CD8 phenotypes, as well as patients with the highest haplotype heterogeneity despite a common low CD8 phenotype. With this strategy, we hope to effectively narrow the region of interest to look for major quantitative trait loci marking the CD8 phenotype in HH patients.

References

1. De Sousa, M., *Iron and the Lymphomyeloid system: a growing Knowledge*, in *Iron in immunity, cancer, and inflammation*. 1989, John Wiley & Sons Inc.

2. de Sousa, M., A. Smithyman, and C. Tan, *Suggested models of ecotaxopathy in lymphoreticular malignancy. A role for iron-binding proteins in the control of lymphoid cell migration.* Am J Pathol, 1978. **90**(2): p. 497-520.

3. De Sousa, M., *Lymphoid cell positioning: a new proposal for the mechanism of control of lymphoid cell migration.* Symp Soc Exp Biol, 1978. **32**: p. 393-410.

4. Brock, J., *Iron and cells of the immune system*, in *Iron in immunity, cancer and inflammation*. 1989, John Wiley & Sons Chichester. p. 81-108.

5. De Sousa, M., *The Immunology of Iron Overload*, in *Iron in Immunity, Cancer and Inflammation*. 1989, John Wiley & Sons Chichester. p. 247-258.

6. Sousa, M.d., *T lymphocytes and iron overload: novel correlations of possible significance to the biology of the immunological system.* Memórias do Instituto Oswaldo Cruz, 1992. **87**: p. 23-29.

7. Porto, G. and M. De Sousa, *Iron overload and immunity.* 2007.

8. Pietrangelo, A., *Hereditary hemochromatosis: pathogenesis, diagnosis, and treatment.* Gastroenterology, 2010. **139**(2): p. 393-408, 408 e1-2.

9. Fleming, R.E. and P. Ponka, *Iron overload in human disease.* New England Journal of Medicine, 2012. **366**(4): p. 348-359.

10. J., L., *De morbo virgineo. Epistola XXI, Epistolae Medicinales. 1554*, in *Classic descriptions of disease.*, C.C. Thomas, Editor. 1932: Springfield and Baltimore.

11. Loudon, I.S., *Chlorosis, anaemia, and anorexia nervosa.* Br Med J, 1980. **281**(6256): p. 1669-75.

12. Patek, A.J., Jr, and C.W. Heath, *CHlorosis.* Journal of the American Medical Association, 1936. **106**(17): p. 1463-1466.

13. Beutler, E., *History of iron in medicine.* Blood Cells Mol Dis, 2002. **29**(3): p. 297-308.

14. Verso, M., *Some nineteenth-century pioneers of haematology.* Medical history, 1971. **15**(01): p. 55-67.

15. Recklinghausen, V., *Uber Haemochromatose.* Tagebl Versamml Natur Arzte Heidelberg, 1889. **62**.

16. Trousseau, A., *Glycosurie, diabete sucre.* Clin Med Hotel Dieu Paris, 1865. **2**: p. 663-98.

17. Sheldon, J.H., *Haemochromatosis*. 1935: Oxford University Press, Humphrey Milford, publisher to the University.

18. Davis, W.D., Jr. and W.R. Arrowsmith, *The effect of repeated bleeding in Hemochromatosis.* J Lab Clin Med, 1950. **36**(5): p. 814-5.

19. Simon, M., et al., *Letter: Idiopathic hemochromatosis associated with HL-A 3 tissular antigen.* La Nouvelle presse medicale, 1975. **4**(19): p. 1432.

20. Keown, P. and B. Descamps, *Suppression de la reaction lymphocytaire mixte par des globules rouges autologues et leurs constituants.* Comptes Rendus de l'Académie des Sciences, Paris, Serie D, 1978. **287**: p. 749-752.

21. Reimao, R., G. Porto, and M. de Sousa, *Stability of CD4/CD8 ratios in man: new correlation between CD4/CD8 profiles and iron overload in idiopathic haemochromatosis patients.* C R Acad Sci III, 1991. **313**(11): p. 481-7.

22. Porto, G., et al., *Haemochromatosis as a window into the study of the immunological system: a novel correlation between CD8+ lymphocytes and iron overload.* Eur J Haematol, 1994. **52**(5): p. 283-90.

23. de Sousa, M., et al., *Iron overload in beta 2-microglobulin-deficient mice.* Immunol Lett, 1994. **39**(2): p. 105-11.

24. Santos, M., et al., *Defective iron homeostasis in beta 2-microglobulin knockout mice recapitulates hereditary hemochromatosis in man.* J Exp Med, 1996. **184**(5): p. 1975-85.

25. Koller, B.H. and O. Smithies, *Inactivating the beta 2-microglobulin locus in mouse embryonic stem cells by homologous recombination.* Proceedings of the National Academy of Sciences, 1989. **86**(22): p. 8932-8935.

26. Zijlstra, M., et al., *Germ-line transmission of a disrupted β2microglobulin gene produced by homologous recombination in embryonic stem cells.* 1989.

27. Feder, J.N., et al., *A novel MHC class I-like gene is mutated in patients with hereditary haemochromatosis.* Nat Genet, 1996. **13**(4): p. 399-408.

28. Santos, M.M., et al., *Iron overload and heart fibrosis in mice deficient for both beta2-microglobulin and Rag1.* Am J Pathol, 2000. **157**(6): p. 1883-92.

29. Arosa, F.A., et al., *Anomalies of the CD8+ T cell pool in haemochromatosis: HLA-A3-linked expansions of CD8+CD28- T cells.* Clin Exp Immunol, 1997. **107**(3): p. 548-54.

30. Cruz, E., et al., *The CD8+ T-lymphocyte profile as a modifier of iron overload in HFE hemochromatosis: an update of clinical and immunological data from 70 C282Y homozygous subjects.* Blood Cells Mol Dis, 2006. **37**(1): p. 33-9.

31. Macedo, M.F., et al., *Low numbers of CD8+ T lymphocytes in hereditary haemochromatosis are explained by a decrease of the most mature CD8+ effector memory T cells.* Clin Exp Immunol, 2010. **159**(3): p. 363-71.

32. Porto, G., et al., *Relative impact of HLA phenotype and CD4-CD8 ratios on the clinical expression of hemochromatosis.* Hepatology, 1997. **25**(2): p. 397-402.

33. Cardoso, E.M., et al., *Hepatic damage in C282Y homozygotes relates to low numbers of CD8+ cells in the liver lobuli.* Eur J Clin Invest, 2001. **31**(1): p. 45-53.

34. Cardoso, E.M., et al., *Increased hepatic iron in mice lacking classical MHC class I molecules.* Blood, 2002. **100**(12): p. 4239-41.

35. Miranda, C.J., et al., *Contributions of beta2-microglobulin-dependent molecules and lymphocytes to iron regulation: insights from HfeRag1(-/-) and beta2mRag1(-/-) double knock-out mice.* Blood, 2004. **103**(7): p. 2847-9.

36. Pietrangelo, A., et al., *Hereditary hemochromatosis in adults without pathogenic mutations in the hemochromatosis gene.* N Engl J Med, 1999. **341**(10): p. 725-32.

37. Krause, A., et al., *LEAP-1, a novel highly disulfide-bonded human peptide, exhibits antimicrobial activity.* FEBS Lett, 2000. **480**(2-3): p. 147-50.

38. Ahmad, K.A., et al., *Decreased liver hepcidin expression in the Hfe knockout mouse.* Blood Cells Mol Dis, 2002. **29**(3): p. 361-6.

39. Nemeth, E., et al., *The N-terminus of hepcidin is essential for its interaction with ferroportin: structure-function study.* Blood, 2006. **107**(1): p. 328-33.

40. Pinto, J.P., et al., *Hepcidin messenger RNA expression in human lymphocytes.* Immunology, 2010.

41. Cruz, E., et al., *Involvement of the major histocompatibility complex region in the genetic regulation of circulating CD8 T-cell numbers in humans.* Tissue Antigens, 2004. **64**(1): p. 25-34.

42. Vieira, J., et al., *A putative gene located at the MHC class I region around the D6S105 marker contributes to the setting of CD8+ T-lymphocyte numbers in humans.* Int J Immunogenet, 2007. **34**(5): p. 359-67.

43. Cruz, E., et al., *A study of 82 extended HLA haplotypes in HFE-C282Y homozygous hemochromatosis subjects: relationship to the genetic control of CD8+ T-lymphocyte numbers and severity of iron overload.* BMC Med Genet, 2006. **7**: p. 16.

44. Cruz, E., et al., *A new 500 kb haplotype associated with high CD8+ T-lymphocyte numbers predicts a less severe expression of hereditary hemochromatosis.* BMC Med Genet, 2008. **9**: p. 97.

45. de Almeida, S.F., et al., *HFE cross-talks with the MHC class I antigen presentation pathway.* Blood, 2005. **106**(3): p. 971-7.

46. Weinberg, E.D., *Iron and infection.* Microbiological reviews, 1978. **42**(1): p. 45.

47. Hiyeda, K., *The cause of Kaschin-Beck's disease.* Jpn. J. Med. Sci. Biol, 1939. **4**: p. 91-106.

48. Faulk, W.P., B.-L. Hsi, and P. Stevens, *Transferrin and transferrin receptors in carcinoma of the breast.* The Lancet, 1980. **316**(8191): p. 390-392.

49. Troisier, M., *Diabète sucré.* Bull Soc Anat Paris, 1871. **44**: p. 231-5.

50. Laufberger, V., *Sur la cristallisation de la ferritine.* Bull. Soc. chim. biol, 1937. **19**(1575): p. 4582.

51. Widdowson, E.M. and R.A. McCance, *The absorption and excretion of iron before, during and after a period of very high intake.* Biochem J, 1937. **31**(11): p. 2029-34.

52. Schade, A.L. and L. Caroline, *An Iron-binding Component in Human Blood Plasma.* Science, 1946. **104**(2702): p. 340-1.

53. Davis, W.D., Jr. and H. Laurens, Jr., *Correlation of results of liver function tests and liver biopsy in hepatic disease.* South Med J, 1950. **43**(3): p. 217-23.

54. Plattner, H.C., T. Nussbaumer, and A. Rywlin, *[Juvenile and familial hemochromatosis with endocrinomyocardiac syndrome].* Helv Med Acta, 1951. **18**(4-5): p. 499-502.

55. Alper, T., D.V. Savage, and T.H. Bothwell, *Radioiron studies in a case of hemochromatosis.* J Lab Clin Med, 1951. **37**(5): p. 665-75.

56. Finch, S.C. and C.A. Finch, *Idiopathic hemochromatosis, an iron storage disease. A. Iron metabolism in hemochromatosis.* Medicine (Baltimore), 1955. **34**(4): p. 381-430.

57. Macdonald, R.A., *Idiopathic hemochromatosis. A variant of portal cirrhosis and idiopathic hemosiderosis.* Arch Intern Med, 1961. **107**: p. 606-16.

58. Crosby, W.H., *The Control of Iron Balance by the Intestinal Mucosa.* Blood, 1963. **22**: p. 441-9.

59. Williams, R., et al., *Venesection therapy in idiopathic haemochromatosis. An analysis of 40 treated and 18 untreated patients.* Q J Med, 1969. **38**(149): p. 1-16.

60. Zahringer, J., et al., *Mechanism of iron induction of ferritin synthesis.* Biochem Biophys Res Commun, 1975. **65**(2): p. 583-90.

61. Bacon, B.R., et al., *Hepatic lipid peroxidation in vivo in rats with chronic iron overload.* J Clin Invest, 1983. **71**(3): p. 429-39.

62. Niederau, C., et al., *Survival and causes of death in cirrhotic and in noncirrhotic patients with primary hemochromatosis.* N Engl J Med, 1985. **313**(20): p. 1256-62.

63. Aziz, N. and H.N. Munro, *Iron regulates ferritin mRNA translation through a segment of its 5' untranslated region.* Proc Natl Acad Sci U S A, 1987. **84**(23): p. 8478-82.

64. Hentze, M.W., et al., *Identification of the iron-responsive element for the translational regulation of human ferritin mRNA.* Science, 1987. **238**(4833): p. 1570-3.

65. Edwards, C.Q., et al., *Prevalence of hemochromatosis among 11,065 presumably healthy blood donors.* N Engl J Med, 1988. **318**(21): p. 1355-62.

66. Fillet, G., Y. Beguin, and L. Baldelli, *Model of reticuloendothelial iron metabolism in humans: abnormal behavior in idiopathic hemochromatosis and in inflammation.* Blood, 1989. **74**(2): p. 844-51.

67. McLaren, G.D., et al., *Regulation of intestinal iron absorption and mucosal iron kinetics in hereditary hemochromatosis.* J Lab Clin Med, 1991. **117**(5): p. 390-401.

68. Fleming, M.D., et al., *Microcytic anaemia mice have a mutation in Nramp2, a candidate iron transporter gene.* Nat Genet, 1997. **16**(4): p. 383-6.

69. Gunshin, H., et al., *Cloning and characterization of a mammalian proton-coupled metal-ion transporter.* Nature, 1997. **388**(6641): p. 482-8.

70. Kawabata, H., et al., *Molecular cloning of transferrin receptor 2. A new member of the transferrin receptor-like family.* J Biol Chem, 1999. **274**(30): p. 20826-32.

71. Camaschella, C., et al., *The gene TFR2 is mutated in a new type of haemochromatosis mapping to 7q22.* Nat Genet, 2000. **25**(1): p. 14-5.

72. Abboud, S. and D.J. Haile, *A novel mammalian iron-regulated protein involved in intracellular iron metabolism.* J Biol Chem, 2000. **275**(26): p. 19906-12.

73. Donovan, A., et al., *Positional cloning of zebrafish ferroportin1 identifies a conserved vertebrate iron exporter.* Nature, 2000. **403**(6771): p. 776-81.

74. McKie, A.T., et al., *A novel duodenal iron-regulated transporter, IREG1, implicated in the basolateral transfer of iron to the circulation.* Mol Cell, 2000. **5**(2): p. 299-309.

75. Montosi, G., et al., *Autosomal-dominant hemochromatosis is associated with a mutation in the ferroportin (SLC11A3) gene.* J Clin Invest, 2001. **108**(4): p. 619-23.

76. Pigeon, C., et al., *A new mouse liver-specific gene, encoding a protein homologous to human antimicrobial peptide hepcidin, is overexpressed during iron overload.* J Biol Chem, 2001. **276**(11): p. 7811-9.

77. Powell, L.W., et al., *Screening for hemochromatosis in asymptomatic subjects with or without a family history.* Arch Intern Med, 2006. **166**(3): p. 294-301.

78. Bulaj, Z.J., et al., *Disease-related conditions in relatives of patients with hemochromatosis.* N Engl J Med, 2000. **343**(21): p. 1529-35.

79. Beutler, E., et al., *Penetrance of 845G--> A (C282Y) HFE hereditary haemochromatosis mutation in the USA.* Lancet, 2002. **359**(9302): p. 211-8.

80. Olynyk, J.K., et al., *A population-based study of the clinical expression of the hemochromatosis gene.* N Engl J Med, 1999. **341**(10): p. 718-24.

81. Roetto, A., et al., *Mutant antimicrobial peptide hepcidin is associated with severe juvenile hemochromatosis.* Nat Genet, 2003. **33**(1): p. 21-2.

82. Bridle, K.R., et al., *Disrupted hepcidin regulation in HFE-associated haemochromatosis and the liver as a regulator of body iron homoeostasis.* Lancet, 2003. **361**(9358): p. 669-73.

83. Gehrke, S.G., et al., *Expression of hepcidin in hereditary hemochromatosis: evidence for a regulation in response to the serum transferrin saturation and to non-transferrin-bound iron.* Blood, 2003. **102**(1): p. 371-6.

84. Papanikolaou, G., et al., *Mutations in HFE2 cause iron overload in chromosome 1q-linked juvenile hemochromatosis.* Nat Genet, 2004. **36**(1): p. 77-82.

85. Nemeth, E., et al., *Hepcidin regulates cellular iron efflux by binding to ferroportin and inducing its internalization.* Science, 2004. **306**(5704): p. 2090-3.

86. Andersen, R.V., et al., *Hemochromatosis mutations in the general population: iron overload progression rate.* Blood, 2004. **103**(8): p. 2914-9.

87. Allen, K.J., et al., *Iron-overload-related disease in HFE hereditary hemochromatosis.* N Engl J Med, 2008. **358**(3): p. 221-30.

88. Jacolot, S., et al., *HAMP as a modifier gene that increases the phenotypic expression of the HFE pC282Y homozygous genotype.* Blood, 2004. **103**(7): p. 2835-40.

89. Babitt, J.L., et al., *Bone morphogenetic protein signaling by hemojuvelin regulates hepcidin expression.* Nat Genet, 2006. **38**(5): p. 531-9.

90. Goswami, T. and N.C. Andrews, *Hereditary hemochromatosis protein, HFE, interaction with transferrin receptor 2 suggests a molecular mechanism for mammalian iron sensing.* J Biol Chem, 2006. **281**(39): p. 28494-8.

91. Vecchi, C., et al., *ER stress controls iron metabolism through induction of hepcidin.* Science, 2009. **325**(5942): p. 877-80.

92. Andriopoulos, B., Jr., et al., *BMP6 is a key endogenous regulator of hepcidin expression and iron metabolism.* Nat Genet, 2009. **41**(4): p. 482-7.

93. Meynard, D., et al., *Lack of the bone morphogenetic protein BMP6 induces massive iron overload.* Nat Genet, 2009. **41**(4): p. 478-81.

94. Corradini, E., et al., *Bone morphogenetic protein signaling is impaired in an HFE knockout mouse model of hemochromatosis.* Gastroenterology, 2009. **137**(4): p. 1489-97.

95. Kautz, L., et al., *BMP/Smad signaling is not enhanced in Hfe-deficient mice despite increased Bmp6 expression.* Blood, 2009. **114**(12): p. 2515-20.

96. Bothwell, T.H., et al., *Nutritional iron requirements and food iron absorption.* J Intern Med, 1989. **226**(5): p. 357-65.

97. Hentze, M.W., et al., *Two to tango: regulation of Mammalian iron metabolism.* Cell, 2010. **142**(1): p. 24-38.

98. Carpenter, C.E. and A.W. Mahoney, *Contributions of heme and nonheme iron to human nutrition.* Crit Rev Food Sci Nutr, 1992. **31**(4): p. 333-67.

99. Hunt, J.R., *Moving toward a plant-based diet: are iron and zinc at risk?* Nutr Rev, 2002. **60**(5 Pt 1): p. 127-34.

100. Gunshin, H., et al., *Cybrd1 (duodenal cytochrome b) is not necessary for dietary iron absorption in mice.* Blood, 2005. **106**(8): p. 2879-83.

101. Esposito, B.P., et al., *Labile plasma iron in iron overload: redox activity and susceptibility to chelation.* Blood, 2003. **102**(7): p. 2670-7.

102. Breuer, W., C. Hershko, and Z.I. Cabantchik, *The importance of non-transferrin bound iron in disorders of iron metabolism.* Transfus Sci, 2000. **23**(3): p. 185-92.

103. Scheiber-Mojdehkar, B., et al., *Non-transferrin-bound iron in the serum of hemodialysis patients who receive ferric saccharate: no correlation to peroxide generation.* J Am Soc Nephrol, 2004. **15**(6): p. 1648-55.

104. Breuer, W. and Z.I. Cabantchik, *A fluorescence-based one-step assay for serum non-transferrin-bound iron.* Anal Biochem, 2001. **299**(2): p. 194-202.

105. Manwani, D. and J.J. Bieker, *The erythroblastic island.* Curr Top Dev Biol, 2008. **82**: p. 23-53.

106. Bleackley, M.R., et al., *Blood iron homeostasis: newly discovered proteins and iron imbalance.* Transfusion medicine reviews, 2009. **23**(2): p. 103-123.

107. Epsztejn, S., et al., *Fluorescence analysis of the labile iron pool of mammalian cells.* Analytical biochemistry, 1997. **248**(1): p. 31-40.

108. Fenton, H., *LXXIII.—Oxidation of tartaric acid in presence of iron.* Journal of the Chemical Society, Transactions, 1894. **65**: p. 899-910.

109. Geissler, C. and M. Singh, *Iron, meat and health.* Nutrients, 2011. **3**(3): p. 283-316.

110. Soe-Lin, S., et al., *Nramp1 promotes efficient macrophage recycling of iron following erythrophagocytosis in vivo.* Proc Natl Acad Sci U S A, 2009. **106**(14): p. 5960-5.

111. Finch, C., et al., *Ferrokinetics in man.* Medicine, 1970. **49**(1): p. 17-54.

112. Chua, A.C., et al., *Nontransferrin-bound iron uptake by hepatocytes is increased in the Hfe knockout mouse model of hereditary hemochromatosis.* Blood, 2004. **104**(5): p. 1519-25.

113. Trinder, D., et al., *Localisation of divalent metal transporter 1 (DMT1) to the microvillus membrane of rat duodenal enterocytes in iron deficiency, but to hepatocytes in iron overload.* Gut, 2000. **46**(2): p. 270-276.

114. Gunshin, H., et al., *Slc11a2 is required for intestinal iron absorption and erythropoiesis but dispensable in placenta and liver.* J Clin Invest, 2005. **115**(5): p. 1258-66.

115. Tsushima, R.G., et al., *Modulation of iron uptake in heart by L-type Ca2+ channel modifiers: possible implications in iron overload.* Circ Res, 1999. **84**(11): p. 1302-9.

116. Oudit, G.Y., et al., *L-type Ca2+ channels provide a major pathway for iron entry into cardiomyocytes in iron-overload cardiomyopathy.* Nat Med, 2003. **9**(9): p. 1187-94.

117. Liuzzi, J.P., et al., *Zip14 (Slc39a14) mediates non-transferrin-bound iron uptake into cells.* Proceedings of the National Academy of Sciences, 2006. **103**(37): p. 13612-13617.

118. Muckenthaler, M.U., B. Galy, and M.W. Hentze, *Systemic iron homeostasis and the iron-responsive element/iron-regulatory protein (IRE/IRP) regulatory network.* Annu Rev Nutr, 2008. **28**: p. 197-213.

119. Dunn, L.L., Y. Suryo Rahmanto, and D.R. Richardson, *Iron uptake and metabolism in the new millennium.* Trends Cell Biol, 2007. **17**(2): p. 93-100.

120. Kaplan, C.D. and J. Kaplan, *Iron acquisition and transcriptional regulation.* Chem Rev, 2009. **109**(10): p. 4536-52.

121. Anderson, G.J. and C.D. Vulpe, *Mammalian iron transport.* Cell Mol Life Sci, 2009. **66**(20): p. 3241-61.

122. Niederau, C., et al., *Long-term survival in patients with hereditary hemochromatosis.* Gastroenterology, 1996. **110**(4): p. 1107-19.

123. Liver, E.A.F.T.S.O.T., *EASL clinical practice guidelines for HFE hemochromatosis.* Journal of hepatology, 2010. **53**(1): p. 3-22.

124. Qaseem, A., et al., *Screening for hereditary hemochromatosis: a clinical practice guideline from the American College of Physicians.* Ann Intern Med, 2005. **143**(7): p. 517-21.

125. Brissot, P., et al., *Iron disorders of genetic origin: a changing world.* Trends Mol Med, 2011. **17**(12): p. 707-13.

126. Piperno, A., et al., *Blunted hepcidin response to oral iron challenge in HFE-related hemochromatosis.* Blood, 2007. **110**(12): p. 4096-100.

127. Ganz, T., et al., *Immunoassay for human serum hepcidin.* Blood, 2008. **112**(10): p. 4292-7.

128. Gao, J., et al., *Interaction of the hereditary hemochromatosis protein HFE with transferrin receptor 2 is required for transferrin-induced hepcidin expression.* Cell Metab, 2009. **9**(3): p. 217-27.

129. Schmidt, P.J., et al., *The transferrin receptor modulates Hfe-dependent regulation of hepcidin expression.* Cell metabolism, 2008. **7**(3): p. 205-214.

130. Gao, J., et al., *Hepatocyte-targeted HFE and TFR2 control hepcidin expression in mice.* Blood, 2010. **115**(16): p. 3374-3381.

131. Ryan, J.D., et al., *Defective bone morphogenic protein signaling underlies hepcidin deficiency in HFE hereditary hemochromatosis.* Hepatology, 2010. **52**(4): p. 1266-73.

132. Almeida, A.R., B. Zaragoza, and A.A. Freitas, *Indexation as a novel mechanism of lymphocyte homeostasis: the number of CD4+CD25+ regulatory T cells is indexed to the number of IL-2-producing cells.* J Immunol, 2006. **177**(1): p. 192-200.

133. Starr, T.K., S.C. Jameson, and K.A. Hogquist, *Positive and negative selection of T cells.* Annu Rev Immunol, 2003. **21**: p. 139-76.

134. Sprent, J. and D.F. Tough, *T cell death and memory.* Science, 2001. **293**(5528): p. 245-8.

135. Sallusto, F., et al., *Two subsets of memory T lymphocytes with distinct homing potentials and effector functions.* Nature, 1999. **401**(6754): p. 708-12.

136. Goldrath, A.W. and M.J. Bevan, *Selecting and maintaining a diverse T-cell repertoire.* Nature, 1999. **402**(6759): p. 255-62.

137. Jameson, S.C., *Maintaining the norm: T-cell homeostasis.* Nat Rev Immunol, 2002. **2**(8): p. 547-56.

138. Kirberg, J., A. Berns, and H. von Boehmer, *Peripheral T cell survival requires continual ligation of the T cell receptor to major histocompatibility complex-encoded molecules.* J Exp Med, 1997. **186**(8): p. 1269-75.

139. Butcher, E.C. and L.J. Picker, *Lymphocyte homing and homeostasis.* Science, 1996. **272**(5258): p. 60-6.

140. Banchereau, J. and R.M. Steinman, *Dendritic cells and the control of immunity.* Nature, 1998. **392**(6673): p. 245-52.

141. MacLennan, I.C., et al., *The changing preference of T and B cells for partners as T-dependent antibody responses develop.* Immunol Rev, 1997. **156**: p. 53-66.

142. Garside, P., et al., *Visualization of specific B and T lymphocyte interactions in the lymph node.* Science, 1998. **281**(5373): p. 96-9.

143. Ahmed, R. and D. Gray, *Immunological memory and protective immunity: understanding their relation.* Science, 1996. **272**(5258): p. 54-60.

144. Dutton, R.W., L.M. Bradley, and S.L. Swain, *T cell memory.* Annu Rev Immunol, 1998. **16**: p. 201-23.

145. Gunn, M.D., et al., *A chemokine expressed in lymphoid high endothelial venules promotes the adhesion and chemotaxis of naive T lymphocytes.* Proc Natl Acad Sci U S A, 1998. **95**(1): p. 258-63.

146. Campbell, J.J., et al., *Chemokines and the arrest of lymphocytes rolling under flow conditions.* Science, 1998. **279**(5349): p. 381-4.

147. Campbell, J.J., et al., *6-C-kine (SLC), a lymphocyte adhesion-triggering chemokine expressed by high endothelium, is an agonist for the MIP-3beta receptor CCR7.* J Cell Biol, 1998. **141**(4): p. 1053-9.

148. Mackay, C.R., W.L. Marston, and L. Dudler, *Naive and memory T cells show distinct pathways of lymphocyte recirculation.* J Exp Med, 1990. **171**(3): p. 801-17.

149. Baggiolini, M., *Chemokines and leukocyte traffic.* Nature, 1998. **392**(6676): p. 565-8.

150. Gunn, M.D., et al., *Mice lacking expression of secondary lymphoid organ chemokine have defects in lymphocyte homing and dendritic cell localization.* J Exp Med, 1999. **189**(3): p. 451-60.

151. Michie, C.A., et al., *Lifespan of human lymphocyte subsets defined by CD45 isoforms.* Nature, 1992. **360**(6401): p. 264-5.

152. Arosa, F.A., *CD8+CD28- T cells: certainties and uncertainties of a prevalent human T-cell subset.* Immunol Cell Biol, 2002. **80**(1): p. 1-13.

153. Fonseca, A.M., et al., *Red blood cells inhibit activation-induced cell death and oxidative stress in human peripheral blood T lymphocytes.* Blood, 2001. **97**(10): p. 3152-60.

154. Bluestone, J.A. and A.K. Abbas, *Natural versus adaptive regulatory T cells.* Nat Rev Immunol, 2003. **3**(3): p. 253-7.

155. Almeida, A.R., et al., *Homeostasis of T cell numbers: from thymus production to peripheral compartmentalization and the indexation of regulatory T cells.* Semin Immunol, 2005. **17**(3): p. 239-49.

156. Freitas, A.A. and B. Rocha, *Population biology of lymphocytes: the flight for survival.* Annu Rev Immunol, 2000. **18**: p. 83-111.

157. Peixoto, A., et al., *CD8 single-cell gene coexpression reveals three different effector types present at distinct phases of the immune response.* J Exp Med, 2007. **204**(5): p. 1193-205.

158. Sung, H.C., et al., *Cognate antigen stimulation generates potent CD8(+) inflammatory effector T cells.* Front Immunol, 2013. **4**: p. 452.

159. Tanchot, C., et al., *Differential requirements for survival and proliferation of CD8 naive or memory T cells.* Science, 1997. **276**(5321): p. 2057-62.

160. Dhanji, S., et al., *Self-reactive memory-phenotype CD8 T cells exhibit both MHC-restricted and non-MHC-restricted cytotoxicity: a role for the T-cell receptor and natural killer cell receptors.* Blood, 2004. **104**(7): p. 2116-23.

161. Klein, J., *Natural history of the major histocompatibility complex*. 1986: Wiley.

162. Simon, M., et al., *Association of HLA-A3 and HLA-B14 antigens with idiopathic haemochromatosis.* Gut, 1976. **17**(5): p. 332-4.

163. Milman, N., et al., *HLA determinants in 70 Danish patients with idiopathic haemochromatosis.* Clinical genetics, 1988. **33**(4): p. 286-292.

164. *An integrated map of genetic variation from 1,092 human genomes.* Nature, 2012. **491**(7422): p. 56-65.

165. Toomajian, C., et al., *A method for detecting recent selection in the human genome from allele age estimates.* Genetics, 2003. **165**(1): p. 287-97.

166. Olynyk, J.K., *Hereditary haemochromatosis: diagnosis and management in the gene era.* Liver, 1999. **19**(2): p. 73-80.

167. McCune, A. and M. Worwood, *Penetrance in hereditary hemochromatosis.* Blood, 2003. **102**(7): p. 2696; author reply 2696-7.

168. Adams, P.C., et al., *Hemochromatosis and iron-overload screening in a racially diverse population.* N Engl J Med, 2005. **352**(17): p. 1769-78.

169. Gandon, Y., et al., *Non-invasive assessment of hepatic iron stores by MRI.* Lancet, 2004. **363**(9406): p. 357-62.

170. Arosa, F.A., et al., *Decreased CD8-p56lck activity in peripheral blood T-lymphocytes from patients with hereditary haemochromatosis.* Scand J Immunol, 1994. **39**(5): p. 426-32.

171. Barton, J.C., et al., *Total blood lymphocyte counts in hemochromatosis probands with HFE C282Y homozygosity: relationship to severity of iron overload and HLA-A and -B alleles and haplotypes.* BMC Blood Disord, 2005. **5**: p. 5.

172. Fabio, G., et al., *Peripheral lymphocytes and intracellular cytokines in C282Y homozygous hemochromatosis patients.* J Hepatol, 2002. **37**(6): p. 753-61.

173. Rohrlich, P.S., et al., *Direct recognition by alphabeta cytolytic T cells of Hfe, a MHC class Ib molecule without antigen-presenting function.* Proc Natl Acad Sci U S A, 2005. **102**(36): p. 12855-60.

174. Ten Elshof, A.E., et al., *Gamma delta intraepithelial lymphocytes drive tumor necrosis factor-alpha responsiveness to intestinal iron challenge: relevance to hemochromatosis.* Immunological reviews, 1999. **167**: p. 223-232.

175. De Almeida, S.F., et al., *HFE cross-talks with the MHC class I antigen presentation pathway.* Blood, 2005. **106**(3): p. 971-977.

176. de Almeida, S.F., et al., *Chemical chaperones reduce endoplasmic reticulum stress and prevent mutant HFE aggregate formation.* Journal of Biological Chemistry, 2007. **282**(38): p. 27905-27912.

177. Tomatsu, S., et al., *Contribution of the H63D mutation in HFE to murine hereditary hemochromatosis.* Proc Natl Acad Sci U S A, 2003. **100**(26): p. 15788-93.

178. Porto G., C.C., Macedo MF, Cruz E., *Hereditary hemochromatosis type I: Genetic, clinical and immunological aspects*, in *Iron Metabolism and Disease*, H. Fuchs, Editor. 2008. p. 435-460.

179. Porto, G. and M. De Sousa, *Iron overload and immunity.* World J Gastroenterol, 2007. **13**(35): p. 4707-15.

180. Macedo, M.F., et al., *Low serum transferrin levels in HFE C282Y homozygous subjects are associated with low CD8(+) T lymphocyte numbers.* Blood Cells Mol Dis, 2005. **35**(3): p. 319-25.

181. Ferreira, M.A., et al., *Quantitative trait loci for CD4:CD8 lymphocyte ratio are associated with risk of type 1 diabetes and HIV-1 immune control.* Am J Hum Genet, 2010. **86**(1): p. 88-92.

182.   Vandiedonck, C. and J.C. Knight, *The human Major Histocompatibility Complex as a paradigm in genomics research.* Brief Funct Genomic Proteomic, 2009. **8**(5): p. 379-94.

183.   Porto, G. and M.D. Sousa, *Variation of hemochromatosis prevalence and genotype in national groups*, in *Hemochromatosis Genetics, Pathophysiology, Diagnosis, and Treatment*, E. Barton J, CQ, editor, Editor. 2000, Cambridge University Press. p. 51-62.

184.   Simon, M., et al., *A study of 609 HLA haplotypes marking for the hemochromatosis gene: (1) mapping of the gene near the HLA-A locus and characters required to define a heterozygous population and (2) hypothesis concerning the underlying cause of hemochromatosis-HLA association.* Am J Hum Genet, 1987. **41**(2): p. 89-105.

185.   Ajioka, R.S., et al., *Recombinations defining centromeric and telomeric borders for the hereditary haemochromatosis locus.* J Med Genet, 1997. **34**(1): p. 28-33.

186.   Raha-Chowdhury R and Gruen JR, *Localization, allelic heterogeneity, and origins of the hemochromatosis gene*, in *Hemochromatosis Genetics, Pathophysiology, Diagnosis, and Treatment*, Barton JC and Edwards CQ, Editors. 2000, Cambridge University Press: Cambridge. p. 75-90.

187.   Jazwinska, E., *The ancestral haplotype in hemochromatosis*, in *Hemochromatosis Genetics, Pathophysiology, Diagnosis, and Treatment*, Barton JC and Edwards CQ, Editors. 2000, Cambridge University Press: Cambridge. p. 91-99.

188.   Barton, J.C., et al., *Genetic and clinical description of hemochromatosis probands and heterozygotes: evidence that multiple genes linked to the major histocompatibility complex are responsible for hemochromatosis.* Blood Cells Mol Dis, 1997. **23**(1): p. 135-45; discussion 145a-b.

189.   Crawford, D.H., et al., *Evidence that the ancestral haplotype in Australian hemochromatosis patients may be associated with a common mutation in the gene.* Am J Hum Genet, 1995. **57**(2): p. 362-7.

190.   Piperno, A., et al., *The ancestral hemochromatosis haplotype is associated with a severe phenotype expression in Italian patients.* Hepatology, 1996. **24**(1): p. 43-6.

191.   Piperno, A., et al., *Heterogeneity of hemochromatosis in Italy.* Gastroenterology, 1998. **114**(5): p. 996-1002.

192.   Barton, J.C., et al., *Hemochromatosis: association of severity of iron overload with genetic markers.* Blood Cells Mol Dis, 1996. **22**(3): p. 195-204.

193.   Pratiwi, R., et al., *Linkage disequilibrium analysis in Australian haemochromatosis patients indicates bipartite association with clinical expression.* J Hepatol, 1999. **31**(1): p. 39-46.

194.   Distante, S., et al., *The origin and spread of the HFE-C282Y haemochromatosis mutation.* Hum Genet, 2004. **115**(4): p. 269-79.

195.   Sachot, S., et al., *Low penetrant hemochromatosis phenotype in eight families: no evidence of modifiers in the MHC region.* Blood Cells Mol Dis, 2001. **27**(2): p. 518-29.

196.   Barton, J.C., et al., *HLA haplotype A*03-B*07 in hemochromatosis probands with HFE C282Y homozygosity: frequency disparity in men and women and lack of association with severity of iron overload.* Blood Cells Mol Dis, 2005. **34**(1): p. 38-47.

197.   Olsson, K.S., B. Ritter, and N. Hansson, *The HLA-A1-B8 haplotype hitchhiking with the hemochromatosis mutation: does it affect the phenotype?* Eur J Haematol, 2007. **79**(5): p. 429-34.

198.   Barton, J.C. and R.T. Acton, *HLA-A and -B alleles and haplotypes in hemochromatosis probands with HFE C282Y homozygosity in central Alabama.* BMC Med Genet, 2002. **3**: p. 9.

199.   Asberg, A., et al., *Screening for hemochromatosis: high prevalence and low morbidity in an unselected population of 65,238 persons.* Scand J Gastroenterol, 2001. **36**(10): p. 1108-15.

200.   Asberg, A., et al., *Persons with screening-detected haemochromatosis: as healthy as the general population?* Scand J Gastroenterol, 2002. **37**(6): p. 719-24.

201.   Harbo, H.F., et al., *Norwegian Sami differs significantly from other Norwegians according to their HLA profile.* Tissue Antigens, 2009. **75**(3): p. 207-17.

202.   Gonzalez-Galarza, F.F., et al., *Allele frequency net: a database and online repository for immune gene frequencies in worldwide populations.* Nucleic Acids Res, 2011. **39**(Database issue): p. D913-9.

203.   Bengtsson, B.O. and G. Thomson, *Measuring the strength of associations between HLA antigens and diseases.* Tissue Antigens, 1981. **18**(5): p. 356-63.

204.   Thomson, G., *A review of theoretical aspects of HLA and disease associations.* Theor Popul Biol, 1981. **20**(2): p. 168-208.

205.   Thomson, G., U. Motro, and S. Selvin, *Statistical aspects of measuring the strength of associations between HLA antigens and diseases.* Tissue Antigens, 1983. **21**(4): p. 320-8.

206.   Schipper, R.F., et al., *HLA gene haplotype frequencies in bone marrow donors worldwide registries.* Hum Immunol, 1997. **52**(1): p. 54-71.

207.   Olsson, K.S., B. Ritter, and R. Raha-Chowdhury, *HLA-A3-B14 and the origin of the haemochromatosis C282Y mutation: founder effects and recombination events during 12 generations in a Scandinavian family with major iron overload.* Eur J Haematol, 2010. **84**(2): p. 145-53.

208.   Olsson, K.S., et al., *Was the C282Y mutation an Irish Gaelic mutation that the Vikings helped disseminate? HLA haplotype observations of hemochromatosis from the west coast of Sweden.* Eur J Haematol, 2011. **86**(1): p. 75-82.

209.   Baschal, E.E., et al., *Defining multiple common "completely" conserved major histocompatibility complex SNP haplotypes.* Clin Immunol, 2009. **132**(2): p. 203-14.

210.   Thorstensen, K., et al., *Screening for C282Y homozygosity in a Norwegian population (HUNT2): The sensitivity and specificity of transferrin saturation.* Scand J Clin Lab Invest, 2010. **70**(2): p. 92-7.

211.   Barton, E.H., et al., *Countries of ancestry reported by hemochromatosis probands and control subjects in central Alabama.* Ethn Dis, 2004. **14**(1): p. 73-81.

212.   Barton, J.C., E.H. Barton, and R.T. Acton, *Effect of Native American ancestry on iron-related phenotypes of Alabama hemochromatosis probands with HFE C282Y homozygosity.* BMC Med Genet, 2006. **7**: p. 22.

213.   Picket, A.J., *History of Alabama, and Incidentally of Georgia and Mississippi, from the Earliest Period.* 1851, Birmingham: Birmingham Book and Magazine Co. (republisher) Clerk`s Office of the District Court of the United States for the Middle District of Alabama.edn

214.   Southerland, H.L. and J.E. Brown, *The Federal Road Through Georgia, the Creek Nation, and Alabama, 1806-1836.* 1989: University of Alabama Press.

215.   Ribeiro, O., H. Lautensach, and S. Daveau, *Geografia de Portugal: O povo Português.* 1989: Lisboa: Edições Sá da Costa.

216.   Cardoso, C., et al., *T-cell receptor repertoire in hereditary hemochromatosis: a study of 32 hemochromatosis patients and 274 healthy subjects.* Hum Immunol, 2001. **62**(5): p. 488-99.

217.   Toomajian, C. and M. Kreitman, *Sequence variation and haplotype structure at the human HFE locus.* Genetics, 2002. **161**(4): p. 1609-23.

218. Ajioka, R.S., et al., *Haplotype analysis of hemochromatosis: evaluation of different linkage-disequilibrium approaches and evolution of disease chromosomes.* Am J Hum Genet, 1997. **60**(6): p. 1439-47.

219. Gandon, G., et al., *Linkage disequilibrium and extended haplotypes in the HLA-A to D6S105 region: implications for mapping the hemochromatosis gene (HFE).* Hum Genet, 1996. **97**(1): p. 103-13.

220. Costa, M., et al., *Effects of highly conserved major histocompatibility complex (MHC) extended haplotypes on iron and low CD8+ T lymphocyte phenotypes in HFE C282Y homozygous hemochromatosis patients from three geographically distant areas.* PLoS One, 2013. **8**(11): p. e79990.

221. Malfroy, L., et al., *Heterogeneity in rates of recombination in the 6-Mb region telomeric to the human major histocompatibility complex.* Genomics, 1997. **43**(2): p. 226-31.

222. Lichten, M. and A.S. Goldman, *Meiotic recombination hotspots.* Annu Rev Genet, 1995. **29**: p. 423-44.

223. Costa, M., et al., *Lymphocyte gene expression signatures from patients and mouse models of hereditary hemochromatosis reveal a function of HFE as a negative regulator of CD8+ T-lymphocyte activation and differentiation in vivo.* PLoS One, 2015. **10**(4): p. e0124246.

224. Reuben, A., et al., *The WT hemochromatosis protein HFE inhibits CD8(+) T-lymphocyte activation.* Eur J Immunol, 2014. **44**(6): p. 1604-14.

225. Brissot, P., et al., *Non-transferrin bound iron: a key role in iron overload and iron toxicity.* Biochim Biophys Acta, 2012. **1820**(3): p. 403-10.

226. Sturrock, A., et al., *Characterization of a transferrin-independent uptake system for iron in HeLa cells.* J Biol Chem, 1990. **265**(6): p. 3139-45.

227. Lane, D.J. and A. Lawen, *A highly sensitive colorimetric microplate ferrocyanide assay applied to ascorbate-stimulated transplasma membrane ferricyanide reduction and mitochondrial succinate oxidation.* Anal Biochem, 2008. **373**(2): p. 287-95.

228. Craven, C.M., et al., *Tissue distribution and clearance kinetics of non-transferrin-bound iron in the hypotransferrinemic mouse: a rodent model for hemochromatosis.* Proc Natl Acad Sci U S A, 1987. **84**(10): p. 3457-61.

229. Grootveld, M., et al., *Non-transferrin-bound iron in plasma or serum from patients with idiopathic hemochromatosis. Characterization by high performance liquid chromatography and nuclear magnetic resonance spectroscopy.* J Biol Chem, 1989. **264**(8): p. 4417-22.

230. Evans, R.W., et al., *Nature of non-transferrin-bound iron: studies on iron citrate complexes and thalassemic sera.* J Biol Inorg Chem, 2008. **13**(1): p. 57-74.

231. Alderighi, L., et al., *Hyperquad simulation and speciation (HySS): a utility program for the investigation of equilibria involving soluble and partially soluble species.* Coordination Chemistry Reviews, 1999. **184**: p. 311-318

232. Silva, A.M., et al., *Iron(III) citrate speciation in aqueous solution.* Dalton Trans, 2009(40): p. 8616-25.

233. Bates, R.G., *Determination of pH; theory and practice.* 2d ed. 1973, New York,: Wiley. xv, 479 p.

234. Arezes, J., et al., *Non-transferrin-bound iron (NTBI) uptake by T lymphocytes: evidence for the selective acquisition of oligomeric ferric citrate species.* PLoS One, 2013. **8**(11): p. e79870.

235. Parkes, J.G., et al., *Modulation by iron loading and chelation of the uptake of non-transferrin-bound iron by human liver cells.* Biochim Biophys Acta, 1995. **1243**(3): p. 373-80.

236.   Peters, T., *All about albumi biochemistry, genetics and medical applications*. San Diego, CA ed. 1996: Academic press.

237.   Lovstad, R.A., *Interaction of serum albumin with the Fe(III)-citrate complex.* Int J Biochem, 1993. **25**(7): p. 1015-7.

238.   May, P.M., P.W. Linder, and D.R. Williams, *Computer-Simulation of Metal-Ion Equilibria in Biofluids - Models for Low-Molecular-Weight Complex Distribution of Calcium(Ii), Magnesium(Ii), Manganese(Ii), Iron(Iii), Copper(Ii), Zinc(Ii), and Lead(Ii) Ions in Human-Blood Plasma.* Journal of the Chemical Society-Dalton Transactions, 1977(6): p. 588-595.

239.   Silva, A.M.N. and R.C. Hider, *Influence of non-enzymatic post-translation modifications on the ability of human serum albumin to bind iron Implications for non-transferrin-bound iron speciation.* Biochimica Et Biophysica Acta-Proteins and Proteomics, 2009. **1794**(10): p. 1449-1458.

240.   Faller, B. and H. Nick, *Kinetics and Mechanism of Iron(Iii) Removal from Citrate by Desferrioxamine-B and 3-Hydroxy-1,2-Dimethyl-4-Pyridone.* Journal of the American Chemical Society, 1994. **116**(9): p. 3860-3865.

241.   Modell, B., M. Khan, and M. Darlison, *Survival in beta-thalassaemia major in the UK: data from the UK Thalassaemia Register.* Lancet, 2000. **355**(9220): p. 2051-2.

242.   Wood, J.C., et al., *Physiology and pathophysiology of iron cardiomyopathy in thalassemia.* Cooley's Anemia Eighth Symposium, 2005. **1054**: p. 386-395.

243.   Dorner, M.H., et al., *Ferritin synthesis by human T lymphocytes.* Science, 1980. **209**(4460): p. 1019-21.

244.   Porto G, S.M., *Variation of hemochromatosis prevalence and genotype in national groups*, in *Hemochromatosis Genetics, Pathophysiology, Diagnosis, and Treatment*, C. Barton J E, Editor. 2000, Cambridge University Press. p. 51-62.

245.   D'Alessio, F., M.W. Hentze, and M.U. Muckenthaler, *The hemochromatosis proteins HFE, TfR2, and HJV form a membrane-associated protein complex for hepcidin regulation.* J Hepatol, 2012. **57**(5): p. 1052-60.

246.   Sallusto, F. and A. Lanzavecchia, *Heterogeneity of CD4+ memory T cells: functional modules for tailored immunity.* Eur J Immunol, 2009. **39**(8): p. 2076-82.

247.   Monteiro, M., et al., *Cartography of gene expression in CD8 single cells: novel CCR7- subsets suggest differentiation independent of CD45RA expression.* Blood, 2007. **109**(7): p. 2863-70.

248.   Willinger, T., et al., *Human naive CD8 T cells down-regulate expression of the WNT pathway transcription factors lymphoid enhancer binding factor 1 and transcription factor 7 (T cell factor-1) following antigen encounter in vitro and in vivo.* J Immunol, 2006. **176**(3): p. 1439-46.

249.   Babich, A. and J.K. Burkhardt, *Coordinate control of cytoskeletal remodeling and calcium mobilization during T-cell activation.* Immunol Rev, 2013. **256**(1): p. 80-94.

250.   Nakayama, T., et al., *Expression and function of FRA2/JUND in cutaneous T-cell lymphomas.* Anticancer Res, 2012. **32**(4): p. 1367-73.

251.   Adrian, K., et al., *Expression of purinergic receptors (ionotropic P2X1-7 and metabotropic P2Y1-11) during myeloid differentiation of HL60 cells.* Biochim Biophys Acta, 2000. **1492**(1): p. 127-38.

252.   Starheim, K.K., et al., *Knockdown of human N alpha-terminal acetyltransferase complex C leads to p53-dependent apoptosis and aberrant human Arl8b localization.* Mol Cell Biol, 2009. **29**(13): p. 3569-81.

253. Green, A., et al., *Histone H1 interphase phosphorylation becomes largely established in G1 or early S phase and differs in G1 between T-lymphoblastoid cells and normal T cells.* Epigenetics Chromatin, 2011. **4**: p. 15.

254. Khammanivong, A., et al., *S100A8/A9 (calprotectin) negatively regulates G2/M cell cycle progression and growth of squamous cell carcinoma.* PLoS One, 2013. **8**(7): p. e69395.

255. Loser, K., et al., *The Toll-like receptor 4 ligands Mrp8 and Mrp14 are crucial in the development of autoreactive CD8+ T cells.* Nat Med, 2010. **16**(6): p. 713-7.

256. Gerstmayer, B., et al., *Identification of RELMgamma, a novel resistin-like molecule with a distinct expression pattern.* Genomics, 2003. **81**(6): p. 588-95.

257. Mina-Osorio, P. and E. Ortega, *Signal regulators in FcR-mediated activation of leukocytes?* Trends Immunol, 2004. **25**(10): p. 529-35.

258. Okhrimenko, A., et al., *Human memory T cells from the bone marrow are resting and maintain long-lasting systemic memory.* Proc Natl Acad Sci U S A, 2014. **111**(25): p. 9229-34.

259. Schenkel, J.M., K.A. Fraser, and D. Masopust, *Cutting edge: resident memory CD8 T cells occupy frontline niches in secondary lymphoid organs.* J Immunol, 2014. **192**(7): p. 2961-4.

260. Schroll, A., et al., *Lipocalin-2 ameliorates granulocyte functionality.* Eur J Immunol, 2012. **42**(12): p. 3346-57.

261. Nielsen, J.S., et al., *Rough-Form-Lipopolysaccharide Increase Apoptosis in Human CD4(+) and CD8(+) T-Lymphocytes.* Scand J Immunol, 2011.

262. Lim, S.C., et al., *Apoptosis of T lymphocytes isolated from peripheral blood of patients with acute exacerbation of chronic obstructive pulmonary disease.* Yonsei Med J, 2011. **52**(4): p. 581-7.

263. Bresgen, N., et al., *Ferritin--a mediator of apoptosis?* J Cell Physiol, 2007. **212**(1): p. 157-64.

264. Saadeldien, H.M., A.A. Mohamed, and M.R. Hussein, *Iron-induced damage in corpus striatal cells of neonatal rats: attenuation by folic acid.* Ultrastruct Pathol, 2012. **36**(2): p. 89-101.

265. Porto, B., R. Vieira, and G. Porto, *Increased capacity of lymphocytes from hereditary hemochromatosis patients homozygous for the C282Y HFE mutation to respond to the genotoxic effect of diepoxybutane.* Mutat Res, 2009. **673**(1): p. 37-42.

266. Rodriguez, A., et al., *Effects of iron loading on muscle: genome-wide mRNA expression profiling in the mouse.* BMC Genomics, 2007. **8**: p. 379.

267. de Sousa, M., et al., *Iron and lymphocytes: reciprocal regulatory interactions.* Curr Stud Hematol Blood Transfus, 1991(58): p. 171-7.

268. De Sousa, M., et al., *Iron, iron-binding proteins and immune system cells.* Ann N Y Acad Sci, 1988. **526**: p. 310-22.

269. Pinto, J.P., et al., *Physiological implications of NTBI uptake by T lymphocytes.* Front Pharmacol, 2014. **5**: p. 24.

270. Rodgers, J.R. and R.G. Cook, *MHC class Ib molecules bridge innate and acquired immunity.* Nat Rev Immunol, 2005. **5**(6): p. 459-71.

271. Cesaro, A., et al., *An inflammation loop orchestrated by S100A9 and calprotectin is critical for development of arthritis.* PLoS One, 2012. **7**(9): p. e45478.

272. Bahram, S., et al., *Experimental hemochromatosis due to MHC class I HFE deficiency: immune status and iron metabolism.* Proc Natl Acad Sci U S A, 1999. **96**(23): p. 13312-7.

273. Haskins, D., et al., *Iron metabolism; iron stores in man as measured by phlebotomy.* J Clin Invest, 1952. **31**(6): p. 543-7.

274. Peixoto, A., et al., *Quantification of multiple gene expression in individual cells.* Genome Res, 2004. **14**(10A): p. 1938-47.

275. Lima, M., et al., *Immunophenotypic aberrations, DNA content, and cell cycle analysis of plasma cells in patients with myeloma and monoclonal gammopathies.* Blood Cells Mol Dis, 2000. **26**(6): p. 634-45.

276. Price, P., et al., *The genetic basis for the association of the 8.1 ancestral haplotype (A1, B8, DR3) with multiple immunopathological diseases.* Immunol Rev, 1999. **167**: p. 257-74.

277. Miretti, M.M., et al., *A high-resolution linkage-disequilibrium map of the human major histocompatibility complex and first generation of tag single-nucleotide polymorphisms.* Am J Hum Genet, 2005. **76**(4): p. 634-46.

278. Trowsdale, J. and J.C. Knight, *Major histocompatibility complex genomics and human disease.* Annu Rev Genomics Hum Genet, 2013. **14**: p. 301-23.

279. Zhang, A.S., et al., *Use of Nramp2-transfected Chinese hamster ovary cells and reticulocytes from mk/mk mice to study iron transport mechanisms.* Exp Hematol, 2008. **36**(10): p. 1227-35.

280. Prus, E. and E. Fibach, *Uptake of non-transferrin iron by erythroid cells.* Anemia, 2011. **2011**: p. 945289.

281. Hausmann, K., et al., *Sulfide silver amplification of ferritin iron cores in blood and bone marrow cells. Methods, adaptations to microphysical analyses, and the impact of advanced iron overload.* Blut, 1988. **56**(5): p. 221-7.

282. Pelosi, E., et al., *Expression of transferrin receptors in phytohemagglutinin-stimulated human T-lymphocytes. Evidence for a three-step model.* J Biol Chem, 1986. **261**(7): p. 3036-42.

283. Seligman, P.A., et al., *Transferrin-independent iron uptake supports B lymphocyte growth.* Blood, 1991. **78**(6): p. 1526-31.

284. Djeha, A. and J.H. Brock, *Effect of transferrin, lactoferrin and chelated iron on human T-lymphocytes.* Br J Haematol, 1992. **80**(2): p. 235-41.

285. Chitambar, C.R. and J.P. Wereley, *Iron transport in a lymphoid cell line with the hemochromatosis C282Y mutation.* Blood, 2001. **97**(9): p. 2734-40.

286. Lentner, C., *Geigy Scientific Tables, Vol. 3: Physical Chemistry Composition of Blood, Hematology Somatometric Data*, ed. C. Lentner. 1985.

287. Dorner, M.H., et al., *Ferritin synthesis by human T lymphocytes.* Science, 1980. **209**(4460): p. 1019-1021.

288. Reuben, A., et al., *T lymphocyte-derived TNF and IFN-gamma repress HFE expression in cancer cells.* Mol Immunol, 2015. **65**(2): p. 259-66.

289. Layoun, A., et al., *Toll-like receptor signal adaptor protein MyD88 is required for sustained endotoxin-induced acute hypoferremic response in mice.* Am J Pathol, 2012. **180**(6): p. 2340-50.

290. Gumireddy, K., et al., *ID1 promotes breast cancer metastasis by S100A9 regulation.* Mol Cancer Res, 2014. **12**(9): p. 1334-43.